Fall 12-14-2011

L-Lysine Decarboxylase and Cadaverine Gamma-Glutamylation Pathways in Pseudomonas Aeruginosa PAO1

Han Ting Chou

L-LYSINE DECARBOXYLASE AND CADAVERINE γ-GLUTAMYLATION PATHWAYS IN *PSEUDOMONAS AERUGINOSA* PAO1

by

HAN TING CHOU

Under the Direction of Dr. Chung-Dar Lu

ABSTRACT

In comparison to other *Pseudomonas*, *P. aeruginosa* grows poorly in L-lysine as a sole source of nutrient while fast growth mutants can be obtained. The proposed catabolic pathway involves lysine decarboxylation to cadaverine and its subsequent degradation through γ-glutamylation pathway to δ-aminovalerate and glutarate. The *l*ysine *de*carboxylase *A* (*ldcA*) gene, previously identified as a member of the ArgR regulon of L-arginine metabolism, was found essential for L-lysine catabolism. The *ldcA* gene encodes a decarboxylase which takes L-lysine but not L-arginine as substrate. Contrarily, the *ldcA* expression was inducible by L-arginine but not by L-lysine. This peculiar arginine control on lysine utilization was also noted from uptake experiments. The lack of lysine-responsive control on lysine catabolism and its tight connection to arginine regulatory network provided an explanation of lysine as poor nutrient for *P. aeruginosa*. Catabolism of cadaverine, a product from lysine decarboxylation, was investigated and compared to that of putrescine, another diamine of similar biochemical properties that is derived from arginine and ornithine. While the γ-glutamylation pathway was first reported in *E. coli* for putrescine utilization, an expanded version of this pathway was found in *P. aeruginosa* with redundant enzymes for polyamine degradation. The PauR protein was identified as a

transcriptional repressor of genes for the catabolism of putrescine and cadaverine, as well as their corresponding downstream metabolites, γ-aminobutyrate (GABA) and δ-aminovalerate (AMV). PauR shows distinct dimer configuration after glutaraldehyde crosslinkage, and possible conformational changes could be triggered by the presence of putrescine and cadaverine, but not GABA. A newly identified ABC transport system, encoded by the *agtABCD* operon, was found important for the uptake of GABA and AMV; and expression of which is controlled by the AgtSR two-component system. The CbrAB two-component system was proposed to regulate the catabolite repression control protein Crc through a small RNA CrcZ. A consensus CbrB recognition sequence was proposed based on the conserved palindromic nucleotide sequence in the upstream activating sequence of the *crcZ* promoter. Genetic studies indicated utilization of arginine, lysine and diamines (but not histidine, GABA and AMV) might be under CbrAB regulation through the CbrAB/CrcZ/Crc system in *P. aeruginosa.*

INDEX WORDS: Pseudomonas, Lysine, Arginine, Cadaverine, Putrescine, GABA, AMV, Catabolism, Decarboxylation, γ-Glutamylation, Uptake, Regulation, Catabolite Repression, Two-Component System.

L-LYSINE DECARBOXYLASE AND CADAVERINE γ-GLUTAMYLATION PATHWAYS IN *PSEUDOMONAS AERUGINOSA* PAO1

by

HAN TING CHOU

A Dissertation Submitted in Partial Fulfillment of the Requirements for the Degree of

Doctor of Philosophy

in the College of Arts and Sciences

Georgia State University

2011

L-LYSINE DECARBOXYLASE AND CADAVERINE γ-GLUTAMYLATION PATHWAYS IN *PSEUDOMONAS AERUGINOSA* PAO1

by

HAN TING CHOU

Committee Chair: Dr. Chung-Dar Lu

Committee: Dr. Phang-Cheng Tai

Dr. John Edgar Houghton

Electronic Version Approved:

Office of Graduate Studies

College of Arts and Sciences

Georgia State University

December 2011

DEDICATION

To my parents Mei-Chu Lin and Tjuen-Wuu Chou with love

ACKNOWLEDGEMENTS

I would like to express my deepest gratitude to my advisor Dr. Chung-Dar Lu, Director of the Molecular Genetics and Biochemistry Program, for his guidance and friendship. He taught me how to think scientifically and gave me suggestions and directions for my career. I have special thanks to Dr. Phang-Cheng Tai, Chair of the Department of Biology, for giving me this opportunity to develop my career in science and for the continuous encouragement and positive attitude towards life. I am also very thankful to my committee member Dr. John Edgar Houghton for his knowledge, appreciation and critical advices.

My special thanks to Dr. Sheng Chung Lee for his influence in my life to choose science as my career. I certainly owe him for encouragement and help to join the Ph. D. program at the Georgia State University.

I would also like to acknowledge Dr. Dong-Hyeon Kwon and Dr. Wei-Qing He for helping me with mutant strains construction and for their friendships and support. I also thank Dr. Bob Hancock for *agt* mutant strains from his mini-Tn*5* *lux* transposon mutant library, and Dr. Siming Wang for ESI-MS analysis.

I want to extend my gratitude to all my lab mates especially Dr. Hsiuchin Yang, Dr. Congran Li, Dr. Chun-Ko Ko, Dr. Zhe Yang, Dr. Hassan Wally, Dr. Hosam Ewis, Ying-Ju Huang, Ying-Hsin Hsieh, Jinshan Jin, Xiaozhou Zhang, Hao Zhang, Chun-Kai Yang, Xiang-Yu

Yao, Jeng-Yi Li, Yu-Chih Peng, Pallavi Batu and Ronald Nettey, for their valuable suggestions, assistance and friendship. I am also very grateful to all faculty, staff and friends in the Department of Biology and the Department of Chemistry at the Georgia State University for their help, support and encouragement.

I am deeply indebted to my parents, my little sister Dr. Han-Yi Chou, and my husband Chen-Hsiang Shen, for their unconditional love, great understanding, endless patience and support. Without them, this dissertation would have never been possible.

This dissertation is dedicated to my parents, Mei-Chu Lin and Tjuen- Wuu Chou, who raise me up and took care of my lovely daughter Felicitas Shen in Taiwan.

TABLE OF CONTENT

LIST OF TABLES

LIST OF FIGURES

LIST OF ABBREVIATIONS

2YT	2 x tryptone-yeast extract media
ADC	arginine decarboxylase
ADI	arginine deiminase
ADP	adenosine diphosphate
Agm	agmatine
Ala	alanine
Amp	ampicillin
AMV	δ-aminovalerate
Arg	arginine
AST	arginine succinyl-transferase
ATA	arginine transaminase
ATP	adenosine triphosphate
BLAST	Basic Local Alignment Search Tool
Cad	cadaverine
Cam	chloramphenicol
CB7	cucurbit[7]uril
CCR	carbon catabolite repression
cDNA	complementary deoxyribonucleic acid
DNA	deoxyribonucleic acid
dSAM	decarboxylated S-adenosylmethionine
DTT	dithiothreitol

EDTA	ethylene diamine tetra acetic acid
ESI-Q-TOF	electrospray ionization-quadrupole time of flight
FAD	flavin adenine dinucleotide
FMN	flavin mononucleotide
GABA	γ-aminobutyrate
GEO	Gene Expression Omnibus
Glc	glucose
Glu	glutamate
Gm	gentamicin
GSA	glutarate semialdehyde
His	histidine
HTH	helix-turn-helix motif
IPTG	isopropylthiogalactopyranoside
Km	kanamycin
LB	Luria-Bertani
LDC	L-lysine decarboxylase
LTA	L-lysine transaminase
Lys	lysine
MMP	minimal medium P
MS	mass spectrometry
NADH	β-nicotinamide adenine dinucleotide
NADPH	β-nicotinamide adenine dinucleotide phosphate
NCBI	National Center for Biotechnology Information

Ni-NTA	nickel-nitrilotriacetic acid
NO	nitric oxide
ONPG	*o*-nitrophenyl-β-D-galactopyranoside
ORF	open reading frame
PAGE	Poly Acrylamide Gel Electrophoresis
PBP	periplasmic binding protein
PCR	polymerase chain reaction
Pi	inorganic phosphate
PLP	pyridoxal 5'-phosphate
PMSF	phenylmethanesulfonylfluoride
Put	putrescine
Pyr	pyruvate
RNA	ribonucleic acid
SSA	succinate semialdehyde
SDS	sodium dodecyl sulfate
Sm	streptomycin
TBE	Tris/Borate/EDTA
Tc	tetracycline
TCA	tricarboxylic acid
TNBS	2,4,6-trinitrobenzenesulfonic acid
UAS	upstream activating sequence
WT	wild type
X-Gal	5-bromo-4-chloro-3-indolyl-*β*-D-galactopyranoside

GENERAL INTRODUCTION

Pseudomonas aeruginosa, an opportunistic human pathogen, is the leading source for pneumonia in immunosuppressed, cystic fibrosis, cancer and burn patients. This Gram-negative rod-shaped bacterium resides ubiquitously in a wide variety of environments. Exploration of catabolic pathways is of particular interest in such a nutritionally versatile organism. With the sequenced genome coupled with an impressive array of genetic and functional genomics tools, this organism is relatively amenable to investigation.

P. aeruginosa cannot use L-lysine efficiently as sole source of nutrient for growth (19, 85). However, mutants with improved growth on L-lysine can be isolated by repeated subcultures in L-lysine suggesting existence of catabolic genes on the chromosome (19). In this study, a peculiar arginine control on lysine utilization was unraveled in *P. aeruginosa*. The proposed pathway consists of lysine decarboxylation with formation of cadaverine and its subsequent degradation through the γ-glutamylation pathway (Figure 0.1). Catabolic enzymes, uptake and regulatory systems involved were analyzed in detail using genetic and biochemical approaches.

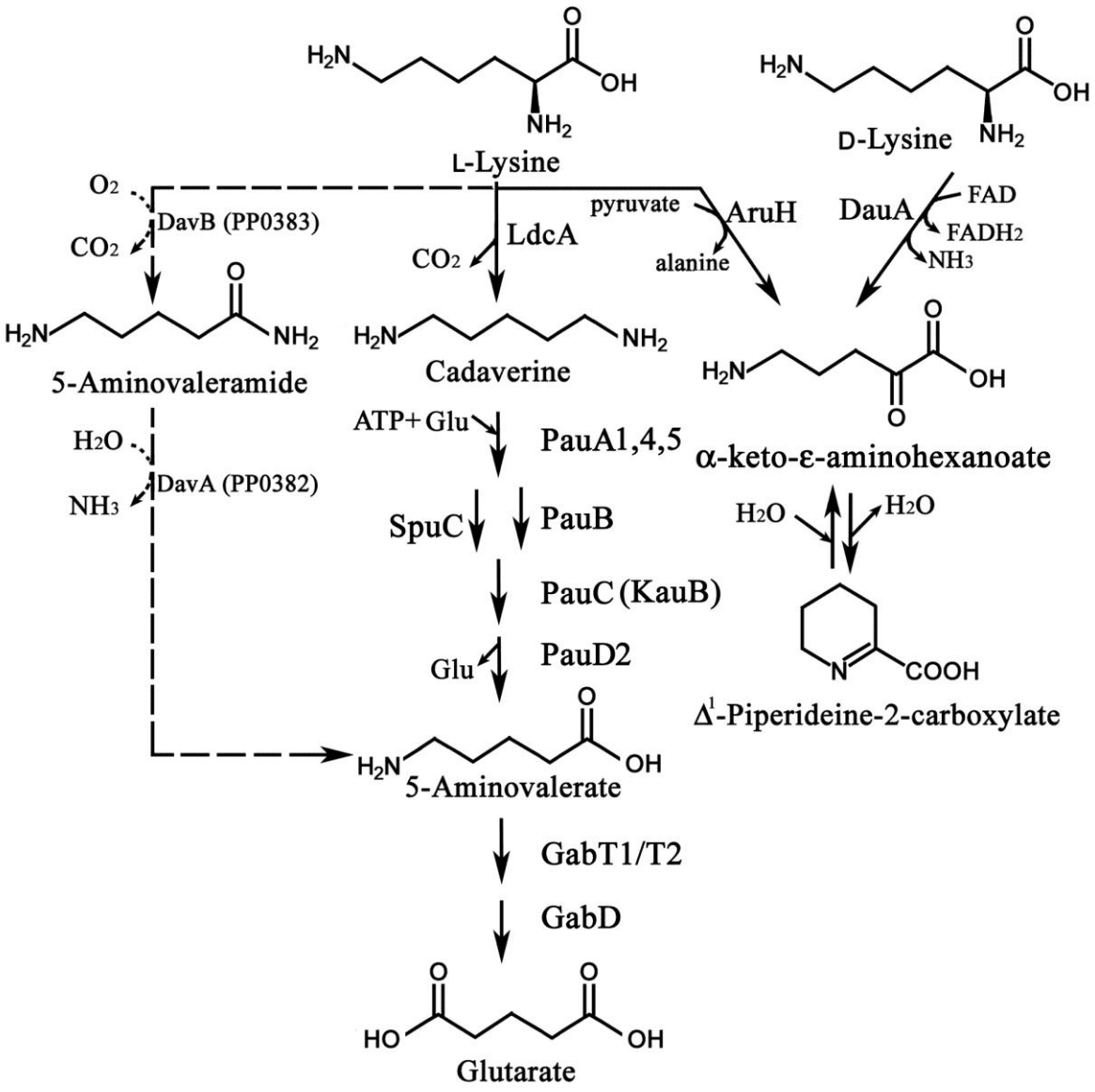

Figure 0.1. Lysine catabolic pathways.

L-lysine decarboxylase pathway leading to cadaverine degradation into 5-aminovalerate and glutarate is shown in the center as the main route for L-lysine catabolism in *P. aeruginosa*. L-lysine transaminase and D-lysine dehydrogenase pathways are shown in the right. Broken arrows represent L-lysine monooxygenase pathway from *P. putida* which is not present in *P. aeruginosa*. Cadaverine degradation through the γ-glutamylation pathway merges with the monooxygenase pathway of *P. putida* at aminovalerate which is further degraded into glutarate.

0.1 LYSINE CATABOLISM IN *PSEUDOMONAS AERUGINOSA*

Possible pathways for L-lysine catabolism in bacteria. In microbes, lysine catabolism can be initiated either through monooxygenase, decarboxylase or transaminase activities (Figure 0.1). While L-lysine is mainly degraded by 2-monooxygenase in *P. putida*, counterparts for this pathway are not present in *P. aeruginosa* (pseudomonas.com). On the other hand, pioneer biochemical studies using fast-growth mutants suggest lysine decarboxylation as the main catabolic route in *P. aeruginosa* (19, 81). Among the several amino acid decarboxylases, those that attack the basic amino acids, arginine, ornithine and lysine with subsequent polyamine formation, are the most significant physiologically (23, 29, 65). However, even the enzymology of this pathway has been established decades ago, lysine decarboxylation and regulatory mechanism involved were mostly unexplored at the genetic level in *P. aeruginosa*.

Lysine deaminase activity can be detected in different species of the genus *Pseudomonas*. The AruH protein from *P. aeruginosa* has been studied and characterized as a transaminase able to remove the 2-amino group from arginine and other amino acids including lysine *in vitro* (103). In this study, the role of L-lysine transaminase pathway in *P. aeruginosa* metabolism will be investigated using genetics approach.

D-lysine Catabolism. Our laboratory reported a novel racemase system formed by DauA and DauB to convert D-arginine into L-arginine through two step reactions with 2-keto-arginine as intermediate compound (52, 53). In these studies, DauA shows high deamination activity with

D-lysine resulting in ketolysine and ammonia (53). Growth on D-lysine as nitrogen source is also abolished in *dauA* mutant strain supporting the *in vitro* activity of DauA on D-lysine (53).

On the other hand, the product from DauA dehydrogenase, 2-keto-lysine, is supposed to turn into the more stable cyclic form, Δ^1-piperideine-2-carboxylate (36). Studies from *P. putida* suggest D-lysine catabolism with further degradation of this compound into L-pipecolate by the reductase DpkA (84). However, this pathway is still undefined in *P. aeruginosa* since no *dpkA* orthologue can be found on the chromosome and the corresponding enzymatic activity was not detectable (19).

0.2 THE ARGININE EFFECT ON LYSINE UTILIZATION

Inducible lysine utilization by arginine. *P. aeruginosa* has been considered unable to grow on L-lysine as sole carbon source and grows poorly on this compound as a nitrogen source. However, initial observations in this study indicate that in fact *P. aeruginosa* can grow on L-lysine as sole carbon and nitrogen source; however, it needs to pass an extensively long lag phase of approximately 44 hrs before entering the exponential phase with an estimated generation time of 122 minutes. In addition, this long lag phase can be shortened significantly by supplementing the media with a small amount of arginine (~100 μM). This phenomenon intrigued me to conduct a series of studies to understand how arginine triggers lysine utilization in this organism.

The ArgR regulon contains candidate transport and catabolic genes for lysine. The ArgR protein was initially identified as the major arginine-responsive transcriptional regulator of the AraC/XylS family. Using Affymetrix GeneChip® DNA microarray, a group of genes for basic amino acids uptake and catabolism emerge from the ArgR transcriptome analysis (60). Interestingly, orthologues of a subset of these genes have been reported as key transport systems and enzymes for lysine utilization in other bacteria. The transport systems *PA5152-PA5155* and *aotJQMP* encoding two ABC transporters are the counterparts of *PP0283-PP0280* and the *PP4486-PP4482* in *P. putida* which have been reported to contribute in lysine utilization (82). These orthologues show high similarities in gene organization as well as in amino acids sequences (82-84).

Because of its high induction level by arginine, PA1818 was initially proposed as a catabolic arginine decarboxylase under ArgR control. However, no enzyme activity is detectable using arginine as substrate in biochemical studies from our laboratory (29). Based on sequence analysis, PA1818 also possesses potentials to catalyze lysine decarboxylation. Up to date, there are two lysine decarboxylases identified from *E. coli*: the *l*ysine *dec*arboxylase *C* (LdcC) of low expression level with no response to exogenous lysine; and a well-studied inducible lysine decarboxylase CadA for acid stress responses (29, 39, 50). LdcC shows higher optimal pH and lower tolerance to heat than CadA (39, 50). Since PA1818 showed no response to acid stress (29), this result suggests PA1818 might be the counterpart of the non-inducible decarboxylase LdcC. And since *P. aeruginosa* has only one candidate for lysine decarboxylase, other amino acids decarboxylase systems such as glutamate or arginine decarboxylases might be responsible for acid stress responses in this organism.

In this study, ArgR is proposed to regulate lysine utilization which is inducible by arginine but not by lysine. This hypothesis may give an explanation to the long lag phase for growth in lysine as sole source of nutrient in *P. aeruginosa*.

0.3 POLYAMINE CATABOLISM IN MICROORGANISMS

L-lysine catabolism through the decarboxylase pathway leads to formation of cadaverine (Figure 0.1). On the other hand, ornithine decarboxylation yields putrescine, and L-arginine decarboxylation, with agmatine as intermediate product, which also leads to putrescine (13, 58). Many bacteria including *Pseudomonas* can use cadaverine and putrescine as sole source of nutrient for growth (12, 13, 93). As a continuation of my study on lysine catabolic pathway, cadaverine degradation was investigated and compared to putrescine in *P. aeruginosa*.

Physiological significance of polyamines. Although their functions have not yet been fully understood, biogenic polyamines (diamines: diaminopropane, putrescine, cadaverine; and triamines: spermidine, norspermidine and spermine) are natural polycations involved in a wide range of biological reactions (8, 14, 102). In higher organisms, polyamines are involved in cell proliferation and differentiation (7). Decades of polyamine biology has been focusing in cell cycle control since impaired polyamine metabolism can be found in abnormal eukaryotic cells with high proliferation rates such as cancer cells (6, 62). In microbes, different sets of polyamines are present in each species which are controlled through uptake, biosynthesis and catabolism (49, 97). It is believed to bind nucleic acid-containing macromolecules through

charge interactions *in vivo* and are thought to play significant roles in the structural and functional organization of the chromosome and protect DNA from oxidative damage as free radical scavengers (26, 33, 38, 97). Exogenous polyamines also exert a significant effect on antibiotic susceptibility in bacteria (46-48). Other interesting studies link polyamines to microbial carcinogenesis, escape from phagolysosomes, biofilm formation, bacteriocin production, toxin activity and protection from oxidative and acid stress, showing the multifaceted roles of these intriguing molecules in nature (45, 90, 97). While intracellular polyamines play pivotal roles in ensuring optimal growth, accumulation of these compounds inside the cells may cause excess binding to DNA forming condensed complexes leading to protein synthesis inhibition and decrease in cell viability (11, 20, 55). Thus, balanced polyamine biosynthesis/catabolism and uptake/export appear to be required to adjust the optimal homeostasis of these compounds in accord with the growth environment.

Cadaverine and putrescine metabolism in bacteria. Cadaverine and putrescine are diamines with a central methylene chain of similar length: 1,5-diaminopentane, and 1,4-diaminobutane, respectively. It was first reported in *E. coli* that putrescine is degraded into γ-aminobutyrate (GABA) through the γ-glutamylation pathway (42, 44). This pathway is initiated by γ-glutamylputrescine synthetase PuuA, followed by three reactions catalyzed by PuuB, PuuC, and PuuD.

Recent studies from our laboratory found an expanded version of the γ-glutamylation pathway in *P. aeruginosa* for polyamine catabolism including cadaverine and putrescine. Different from *E. coli*, that the *puu* genes are clustered in a single locus of several transcriptional

units under negative control of PuuR (44, 70), *puu* orthologues are scattered on the chromosome of *P. aeruginosa* (www.pseudomonas.com). These genes are designated as *p*oly*a*mine *u*tilization genes *pauA*, *pauB*, *pauC* and *pauD* (Figure 0.1). Interestingly, there are seven γ-glutamylpolyamine synthetases (PauA1-7) for the first step of the pathway (105). Many of these enzymes are able to catalyze the glutamylation of different polyamines. Following the glutamylation, the free amino group is subjected to deamination either by oxidation or transamination. Four PauB candidates for oxidative deamination can be found in *P. aeruginosa* which are supposed to function only under aerobic conditions. On the other hand, SpuC was proposed to catalyze transamination between glutamylpolyamine and alanine regardless of the oxygen level (105). Following deamination, the aldehyde compounds were suggested to be degraded into carboxylates by the dehydrogenase PauC (KauB) (13), This enzyme was initially identified as a NAD(P)-dependent dehydrogenase for ketoarginine utilization (104). Since *pauC* mutant cannot grow on putrescine, this is the only step without redundant enzymes. And finally, the glutamyl group is released by PauD in the last step of the pathway. Two γ-glutamyl hydrolases were proposed for *P. aeruginosa*: PauD1 (SpuA) which affects spermidine utilization but not to putrescine (59); and PauD2 (PA1742) which requires further studies to confirm its involvement in the pathway.

Regulation on γ-glutamylation pathway. Based on studies in *E. coli*, putrescine γ-glutamylation and deglutamylation are negatively regulated by PuuR (Gene ID 945886) in the first and last steps of the Puu pathway (44). By BLAST search, there is only one candidate for PuuR orthologue in *P. aeruginosa*, PA5301, showing 45% identities and 64% similarities to *E. coli* PuuR. In the second part of this study, this regulatory protein was shown involved not only

in the γ-glutamylation pathway but also in catabolism of their corresponding downstream metabolites, γ-aminobutyrate (GABA) and δ-aminovalerate (AMV).

GABA/AMV catabolism in *P. aeruginosa*. Like putrescine and cadaverine, it is possible that the downstream GABA and AMV share similar pathways with common enzymes for the degradation (12, 42). The *gabDT* operon encodes for a dehydrogenase GabD and a transaminase GabT which along with the transaminase GabT2 (PA5313) contribute to GABA degradation into succinate (13). Besides, it has been reported in *P. putida* that *davDT* are the essential genes for AMV catabolism (82); the DavD and DavT exhibit 92% and 82% sequence similarity to *P. aeruginosa* GabD and GabT, respectively. In this study, the roles of *gabDT* and *gabT2* were investigated for AMV degradation into glutarate.

This study will provide valuable information on the intriguing connection between lysine catabolism to arginine through arginine-responsive regulatory gene ArgR in *P. aeruginosa*. This catabolic pathway became even more complex by redundant enzymes for cadaverine and putrescine degradation through the γ-glutamylation pathway. This will be a first complete report on enzymatic, genetic and regulatory aspects of lysine-cadaverine-aminovalerate degradation in this organism.

0.4 CARBON CATABOLITE REPRESSION IN PSEUDOMONAS AERUGINOSA

Pseudomonas aeruginosa is noted for its ability to use a wide range of carbon and nitrogen sources. Different from *E. coli* and *B. subtilis* where glucose is the preferential carbon

source, *P. aeruginosa* prefers carboxylates of the tricarboxylic acid (TCA) cycle such as succinate which can exert carbon catabolite repression (CCR) over sugars (including glucose), amino acids and other nutrients (15, 57, 92). Hallmarks of catabolic regulatory mechanisms like inducer exclusion and cAMP-dependent transcriptional activation play minor role in CCR control of this organism. Instead, complex regulatory networks with different regulatory mechanisms are used to optimize metabolism to achieve efficient growth and cellular carbon-nitrogen balance in *P. aeruginosa*.

While the CbrAB two-component system is essential for growth on several carbon and nitrogen sources for *Pseudomonas* (54, 74), the *crc* (*c*atabolite *r*epression *c*ontrol) gene encoding a RNA-binding protein has been reported to participate in control of several catabolic operons of less-preferred nutrients (94). It had been a puzzle to understand how CbrAB and Crc work together to regulate different catabolic pathways until recent discovery of the small RNA CrcZ (94). On the other hand, CbrA and CbrB exhibit moderate sequence similarity to the well-studied NtrB and NtrC two-component system for nitrogen assimilation controls in Gram-negative bacteria (31, 74). Combined regulation of CbrAB with NtrBC has been reported for arginine and histidine utilization in *pseudomonas* (54, 107). The last chapter of this study demonstrates how CbrAB regulates *crcZ* to release CCR by the Crc protein. Possible cross talk between CbrAB and NtrBC two-component systems was also investigated.

CHAPTER ONE

L-LYSINE CATABOLISM IS CONTROLLED BY L-ARGININE AND ARGR IN *PSEUDOMONAS AERUGINOSA* PAO1

This work was partially published by Han-Ting Chou, Mohamed Hegazy and Chung-Dar Lu in "L-lysine Catabolism is Controlled by Arginine/ArgR in *Pseudomonas aeruginosa* PAO1". J. Bacteriol. 2010 Nov; 192(22):5874-80.

1.1 INTRODUCTION

Decarboxylation of amino acids, including lysine, arginine, and glutamate, is important for bacterial survival under low pH (9, 23, 65). Lysine is abundant in rhizosphere where fluorescent *Pseudomonas* preferentially reside, and serves as nitrogen and carbon source by these organisms (85). In microbes, lysine catabolism can be initiated either through monooxygenase, decarboxylase or transaminase activities. The monooxygenase pathway has been considered as the major route for L-lysine utilization in *Pseudomonas putida*, and *davBATD* encoding enzymes for the first four steps of the pathway have been characterized (82, 83). In contrast, *P. aeruginosa* cannot use exogenous L-lysine efficiently for growth (19, 81). It has been reported that enzymatic activities for the first two steps of the monooxygenase pathway are not detectable in *P. aeruginosa*, and no *davBA* orthologs can be identified from this organism (81, 82).

Mutants of *P. aeruginosa* with improved growth on L-lysine and a high level of lysine decarboxylase activity can be isolated by repeated subcultures in L-lysine (19). This suggests that in *P. aeruginosa*, L-lysine utilization might be mediated by lysine decarboxylase pathway with cadaverine and 5-aminovalerate as intermediates. Alternatively, conversion of L-lysine into 5-aminovalerate may also be accomplished by a coupled reaction catalyzed by AruH and AruI. The AruH and AruI enzymes were reported as arginine:pyruvate transaminase and 2-ketoarginine decarboxylase, respectively (104). Interestingly, transamination by AruH using L-lysine as amino group donor can also be detected *in vitro* (103). The reaction product α-keto-ε-aminohexanoate can potentially be decarboxylated into 5-aminovalerate by AruI providing an alternative route for lysine degradation.

In this study, the lysine decarboxylase pathway was shown to be the main route for lysine utilization under arginine control. Expression of the *ldcAB* operon encoding L-lysine decarboxylase and a putative lysine/cadaverine antiporter was analyzed regarding its response to L-lysine, L-arginine, and the arginine-responsive regulator ArgR. Enzyme characterization was performed to verify the function of LdcA as L-lysine decarboxylase. Arginine control on lysine incorporation was also investigated by genetic studies and uptake experiments. The peculiar role of ArgR controlling arginine and lysine uptake and catabolism provides the explanation for poor growth in lysine, and it implies a higher level of complexity in metabolic networks of pseudomonads.

Table 1.1. Strains and Plasmids

Strain or plasmid	Genotype or description[a]	Source
***E.coli* strains**		
DH5α	F$^-$Φ80d*lac* ΔM15 Δ(*lacZYA-argF*)U169 *deoR recA1 endA1 hsdR17* (r_K^- m_K^-) *supE44* λ$^-$ *thi-1gyrA96 relA*	Bethesda Research Laboratories
TOP10	F- *mcr*A Δ(*mrr-hsd*RMS-*mcr*BC) Φ80*lac*ZΔM15 D*lac*X74 *rec*A1 *ara*D139 Δ(*ara-leu*)7697 *gal*U *gal*K *rps*L (Str^R) *end*A1 *nup*G	Invitrogen
SM10	*thi-1 thr leu tonA lacY supE recA*::RP4-2-Tc::Mu (Km^r)	(91)
***P. aeruginosa* strains**		
PAO1	Wild type	(27)
PAO1-Sm^r	Spontaneous Sm^r mutant strain of PAO1	(35)
PAO501	*argR*::Gm^r	(76)
PAO1214	*aotJ*::Tn*5-751* insertion mutant of PAO1	(76)
PAO5715	Δ*aruC~aruE*::Gm^r	This study
PAO5716	*ldcA*::Tc^r	This study
PAO5717	*ldcB*::Tc^r	This study
PAO5602	*aruH::*Tc^r Δ*aruF*	(104)
PAO5718	Δ*aruC~aruE*::Gm^r, *ldcA*::Tc^r	This study
PAO5720	*aruH*::Tc^r	This study
PAO5721	*aruI*::Tc^r	This study
PAO5802	*dauA*::Tc^r	(27, 53)

Plasmids

pRTP1	Amp^r Sm^s conjugation vector	(95)
pRTP2	pRTP1 derivative EcoRI site deleted	(52)
pGMΩ1	*Bla gen*; gentamicin resistance gene cassette with omega loop on both ends	(88)
pUCP18	*Escherichia-Pseudomonas* shuttle vector.	(89)
pHC5306	pUCP18 derivative carrying *ldcA* gene	This study
pHC5307	pUCP18 derivative carrying *aruH* gene	This study
pBAD-His6	Modified protein expression vector derived from pBAD-HisA	(52)
pBAD-ldcA	6 x His-tagged LdcA protein expression vector	This study
pQF50	*bla lacZ* transcriptional fusion vector	(18)
pQF52	*bla lacZ* translational fusion vector derived from pQF50	(76)
pST500	*aotJ*::*lacZ* translational fusion of pQF52	(75)
pZY5	*PA4980*::*lacZ* translational fusion of pQF52	(104)
pHT1818	*ldcA*::*lacZ* transcriptional fusion of pQF50	This study

[a] Cam^r, chloramphenical resistance; Km^r, kanamycin resistance; Sm^r, streptomycin resistance; Sm^s, streptomycin sensitive; Tc^r, tetracycline resistance; Gm^r, gentamicin resistance; Amp^r, ampicillin resistance.

1.2 MATERIALS AND METHODS

Bacterial strains, plasmids, media, and growth conditions. Bacterial strains and plasmids used in this study are listed in Table 1.1. *E. coli* and *P. aeruginosa* strains were grown in Luria-Bertani (LB) medium supplemented with or without antibiotics at conventional concentrations (104). Minimal medium P containing the indicated carbon sources at 20 mM and nitrogen sources at 5 mM was used for the growth of *P. aeruginosa* (27).

Construction of *ldcA::lacZ* fusion. The upstream regulatory region of the *ldcAB* operon covering 635-bp upstream from of the start codon and the first 24-bp of the structural gene was PCR amplified from the genomic DNA of *P. aeruginosa* PAO1 using the following primers: 5'-TCA CTC TGG GCG CAA GCT TAG GCG CCG GTC GGC-3' and 5'-GGG AAA TTT GAG GTC TTT-3'. PCR product was cloned into pQF50 and confirmed by DNA sequencing.

Construction of mutant strains. For tetracycline resistant mutants, DNA fragments covering the genes of interest were PCR amplified from PAO1 genomic DNA using the following primers: for *ldcAB* mutants, 5'-ATG TAT AAA GAC CTC AAA TTT CCC GTC CTC-3' and 5'-TCA GTC ATT GGC TTT GAG CGT CGG CAC TCC-3'; for *aruHI* mutants, 5'-GTC TAA GCT TGA CTG GCC TGG CGC GCG TCG-3' and 5'-CGC AAG CTT CGG GCA GTC CGG CGT GAC CCT-3'. PCR products were cloned into a conjugation vector pRTP1 (95) and the tetracycline resistance cassette was introduced by using EZ-Tn5 <TET-1> insertion system (Epicentre). For gentamicin deletion mutants, two flanking regions of a targeted gene were amplified by PCR with following primers: 5'- GAG GGA TCA CTC GGG TGC ATA CTT CTT

CTA CG -3', 5'-GAG GAA TTC AGC GCT TCC AGG TCG TTG TAG -3', 5'-GAG GAA TTC GAG CGC TAC GTC GAA CAG GAC ATG A -3' and 5'- GAG AAG CTT CAA TCC GAG CAG GTT GCT CAT GGT C -3'. The PCR products were cloned into pRTP1. A cassette carrying gentamicin-resistance gene from pGMΩ1 was inserted into the conjunction of the two DNA fragments (88). For gene replacement, *E. coli* SM10 was served as the donors in biparental mating with PAO1-Sm^r (21). The desired knockout mutants were selected on LB plates containing streptomycin and either gentamicin or tetracycline, and the mutation was confirmed by PCR.

Constitutive expression from pUCP18. Full length *ldcA (PA1818)* and *aruIH (PA4976~PA4977)* genes were successfully PCR amplified and subcloned into pUCP18 to construct pHC5306 and pHC5307 using the following primers: PA1818F 5'-TGA AGA TCT GAG GAG TCA ACA ATG TAT AAA GAC CTC-3', PA1818R 5'-CCC AAG CTT TCA TTC CTT TAT GCA TTC AAC GGT-3', PA4976F 5'-CAC GGA TCC GCT TGT GGG AAT GGG AGC AAG AGC-3' and PA4976R 5'-CAC AAG CTT CAT CGT GGT TTC CGA ATC GTG GTG AC-3'. These plasmids can reach 10 to 25 copy numbers per cell with constitutive expression in *P. aeruginosa* (89).

Measurements of β-galactosidase activity. The cells were grown in the minimal medium P containing the carbon and nitrogen sources as indicated. Cells in the mid-log phase were harvested by centrifugation, and then passed through a French press cell at 8500 lb/in^2 The cell debris were removed by centrifugation at 20,000 *g* for 15 min, at 4 °C, and protein concentrations in the crude extracts were determined by the Bradford method (5). The levels of

β-galactosidase activity were measured using Miller's method (64).

Overexpression and purification of LdcA. Full-length *ldcA* was amplified from the genomic DNA of *P. aeruginosa* using designed primers: 1818F 5'-TAT AAA GAC CTC AAA TTT CCC GTC-3' and 1818R 5'-TCA TTC CTT TAT GCA TTC AAC GGT -3'. The PCR product was sub-cloned into pBAD-HisD, a modified pBAD expression vector (52, 103). Recombinant 6xHis-LdcA was expressed in *Escherichia coli* TOP10 (Invitrogen life technologies) by arabinose induction. Cell extract was obtained by passing through a French pressure cell at 8,500 lb/in^2 followed by centrifugation at 25,000 *g* for 30 minutes at 4 °C. Soluble His-LdcA protein was purified from HisTrap HP column (GE Healthcare) at the concentration of 100 mM imidazole. Eluted fractions detected by UV were analyzed by SDS PAGE, pooled together and concentrated by Amicon Ultra-15 centrifugal filter unit (Millipore). Active fractions were determined by lysine decarboxylase assay as described below. Protein concentration was determined by the method of Bradford (5).

Measurements of lysine decarboxylase activity. Purified His-LdcA was used to test L-lysine decarboxylation *in vitro.* Enzyme-catalyzed decarboxylation was assayed by measuring the liberated $^{14}CO_2$ at 37 ºC as previously described with slight modification (101). The assay was carried out in a standard scintillation vial and the liberated $^{14}CO_2$ was trapped by a filter paper pre-impregnated with 0.1 ml barium hydroxide in the cap. One milliliter of standard reaction mixture contains 125 μM pyridoxal 5'-phosphate, 100 μg/ml acetylated bovine serum albumin, 0.2 μCi [^{14}C]-L-lysine and 3 mM of cold L-lysine in 100 mM Tris buffer at pH 8.5. The mixture was incubated at 37 ºC in water bath and the reaction was started by adding 1.5 μg of

purified LdcA. Reaction was stopped by adding seven drops of 1N H_2SO_4, and continued the incubation for 30 min more for complete absorption of CO_2. Labeled CO_2 was measured in a liquid scintillation counter. Apparent kinetics parameters were determined using non-linear regression equations of the kinetics module of SigmaPlot 9.0 software.

L-lysine uptake experiments. Radiolabeled L-lysine was used for uptake assays as previously described with slight modification (59). Cultures were grown in glutamate-MMP in the absence or presence of 20 mM L-arginine or L-lysine. Cells were harvested during logarithmic growth (OD_{600} = 0.5~0.8), washed twice and resuspended at a concentration of ca. 10^8 cells/ml (OD_{600} = 0.1) using MMP containing chloramphenicol (250 μg/ml). After incubation of the cell suspension for 5 min in 37°C water bath, ^{14}C-labeled L-lysine was added to a final concentration of 20 μM (10 mCi/mmole), and samples (0.5 ml) were withdrawn at various time intervals. Cells were collected on a cellulose membrane filter (0.22 μm pore size, type GS, Millipore) and washed with 10 ml of MMP. Membranes were air dried in clean scintillation vials overnight. Incorporated radioactivity was measured using adequate scintillation liquid and spectrometer (Beckman).

DNA microarray. GeneChip® *P. aeruginosa* Genome Array from Affymetrix was used for transcriptome analysis of physiological responses to different nutrients in *P. aeruginosa*. All cells were grown aerobically in minimal medium P with 350 rpm shaking at 37 °C supplemented with 20 mM L-glutamate as background nutrient until optical density at 600nm reaches 0.55 ± 0.05. Cells were harvested by centrifugation for 5 minutes at 4 °C. Total RNA samples were isolated by RNeasy purification kit following instructions of the manufacturer (Qiagen). Reverse

transcription for cDNA synthesis, fragmentation by DNase I treatment, cDNA probe labeling and hybridization were performed according to the instructions of GeneChip® manufacturer (Affymetrix). Data were processed by Microarray Suite 5.0 software normalizing absolute expression signal values to a target intensity of 500. GeneSpring GX software (Silicon Genetics) was used for expression pattern analysis and comparison. Genes showing consistent expression profiles in duplicates were selected for further analysis. All data were deposited in the Gene Expression Omnibus (GEO) database (GSE9926).

1.3 RESULTS

ArgR dependent induction of the *ldcA* promoter by arginine but not by lysine. The putative *ldcAB* operon was initially identified as a member of the ArgR regulon from transcriptome analysis (60). ArgR is autoinducible from the *aot-argR* operon and is initially identified as the major regulator of aerobic arginine catabolism and biosynthesis in response to arginine (76). The *ldcA* promoter in response to exogenous L-arginine and L-lysine was tested by measurements of β-galactosidase activities in PAO1 harboring pHT1818, a $P_{ldcA::lacZ}$ fusion. As shown in Table 1.2, exogenous arginine but not lysine exerted strong induction effect (12 folds) on the *ldcA* promoter.

The *ldcA* gene was shown essential for lysine utilization. The results of *ldcA* expression in response to arginine from above experiments led me to propose *ldcA* encodes an arginine-inducible arginine decarboxylase (ADC), the first enzyme of the ADC pathway (69). Arginine succinyltransferase (AST) and arginine transaminase (ATA) pathways were reported to sustain for aerobic growth in *P. aeruginosa* (104). In order to test for ADC pathway as an alternative route for arginine utilization, I used a double mutant strain PAO5602 devoid of the AST (by *aruF* deletion) and ATA (by *aruH*::Tc^r) pathways while the putative ADC pathway remained intact (Table 1.3). However, growth on L-arginine as sole source of carbon and nitrogen was completely abolished in PAO5602 and growth on L-arginine can be restored when the mutant strain was complemented by pHC5307, which expressed *aruH* from the *lac* promoter on the pUCP18 vector (Table 1.4). Contrarily, PAO5602 harboring pHC5306 (*ldcA* in pUCP18) still

Table 1.2. Promoter activities of *aotJ*, and *ldcA* in response to arginine and lysine

Strain	Genotype	Nutrients	Sp act (μmole/mg/min)[a] for:	
			$P_{ldcA::lacZ}$	$P_{aotJ::lacZ}$
PAO1	Wild type	G	0.8 (1)	14 (1)
		A+G	9.5 (12)	61 (4)
		L+G	1.2 (1.5)	18 (1.2)
PAO5715	Δ*aruC~aruE*::Gm^r	G	4.1 (1)	58 (1)
		A+G	16.0 (4)	105 (2)
		L+G	4.0 (1)	26 (0.5)

[a] Cells were grown in minimal medium P supplemented with 20 mM of : L, lysine, A, arginine or G, glutamate. Specific activities represent the averages from three measurements with standard errors below 5%. Fold changes are in parenthesis.

Table 1.3. Lysine decarboxylase pathway is the main route for lysine catabolism

Strain	Genotype	Affected Pathway	Supplements[a]				
			Lc	Ln	Ac	An	GN
PAO1	WT	none	+	++	+++	+++	+++
PAO5716	*ldcA::Tc*^{r}	LDC	−	−	+++	+++	+++
PAO5717	*ldcB::Tc*^{r}	LDC	+/−	++	+++	+++	+++
PAO5720	*aruH::Tc*^{r}	ATA	+	++	+++	+++	+++
PAO 501	*argR::Gm*^{r}	AST/LDC	−	+	+	++	+++
PAO5602	*aruH::Tc*^{r}*/ΔaruF*	AST/ATA	++	+++	−	−	+++
PAO5715	*ΔaruC~aruE::Gm*^{r}	AST	++	+++	+	++	+++
PAO5718	*ΔaruC~aruE::Gm*^{r} *ldcA::Tc*^{r}	LDC/AST	M	M	+	++	+++

[a] Logarithmically growing cells were plated on MMP solid agar media supplemented with: Lc, 20 mM lysine + 5 mM ammonia; Ln, 5 mM lysine + 20 mM glucose; Ac, 20 mM arginine + 5 mM ammonia; An, 5 mM arginine + 20 mM glucose; GN, 20 mM glucose + 5 mM ammonia; Growth at 37°C were recorded daily during 3 days of incubation period: +++, growth in one day; ++, growth in 2 days; +, growth in 3 days; +/−, faint growth in 3 days; −: no growth in 3 days; M: growth under stress with high mutation rate.

showed no growth on L-arginine. From these results I concluded that *ldcA* is not involved in arginine utilization in *P. aeruginosa* PAO1.

Surprisingly, the *ldcA* mutant strain, PAO5716, lost the ability to grow on lysine while arginine utilization remained unaffected (Table 1.3). Introducing pHC5306 to PAO5716 complemented the growth defect on lysine. Even growth of the wild type strain PAO1 on lysine can be enhanced by the presence of pHC5306. These data support that *ldcA* may encode a lysine decarboxylase that is essential for L-lysine catabolism via the decarboxylase pathway (19).

LdcA as lysine-specific PLP-dependent decarboxylase. To further confirm the enzymatic function of LdcA in lysine degradation, initial characterization of a purified His-tagged LdcA was performed with radioactive-labeled L-lysine to determine the reaction rate by measuring the liberated $^{14}CO_2$. As shown in Figure 1.1A, LdcA possesses calculated K_m and V_{max} values of 0.73mM and 2.2 μmole/mg/min, respectively. An estimated Hill slope of 2.0 indicated cooperative substrate activation by L-lysine. The decarboxylase activity of LdcA was also checked with ^{14}C-labeled L-arginine as substrate, and no activity on L-arginine can be detected.

A pyridoxal 5'-phosphate (PLP) binding site of LdcA was predicted in A_{387}THSTHKMLAAF$_{398}$, which shows 90% and 91 % similarities to the PLP binding sites of *E. coli* lysine decarboxylase (CadA ; ETESTHKLLAAF) and arginine decarboxylase (AdiA; ATHSTHKLLNAF), respectively (68). Indeed, when PLP was removed from the reaction mixture, enzyme activity was abolished for LdcA (data not shown).

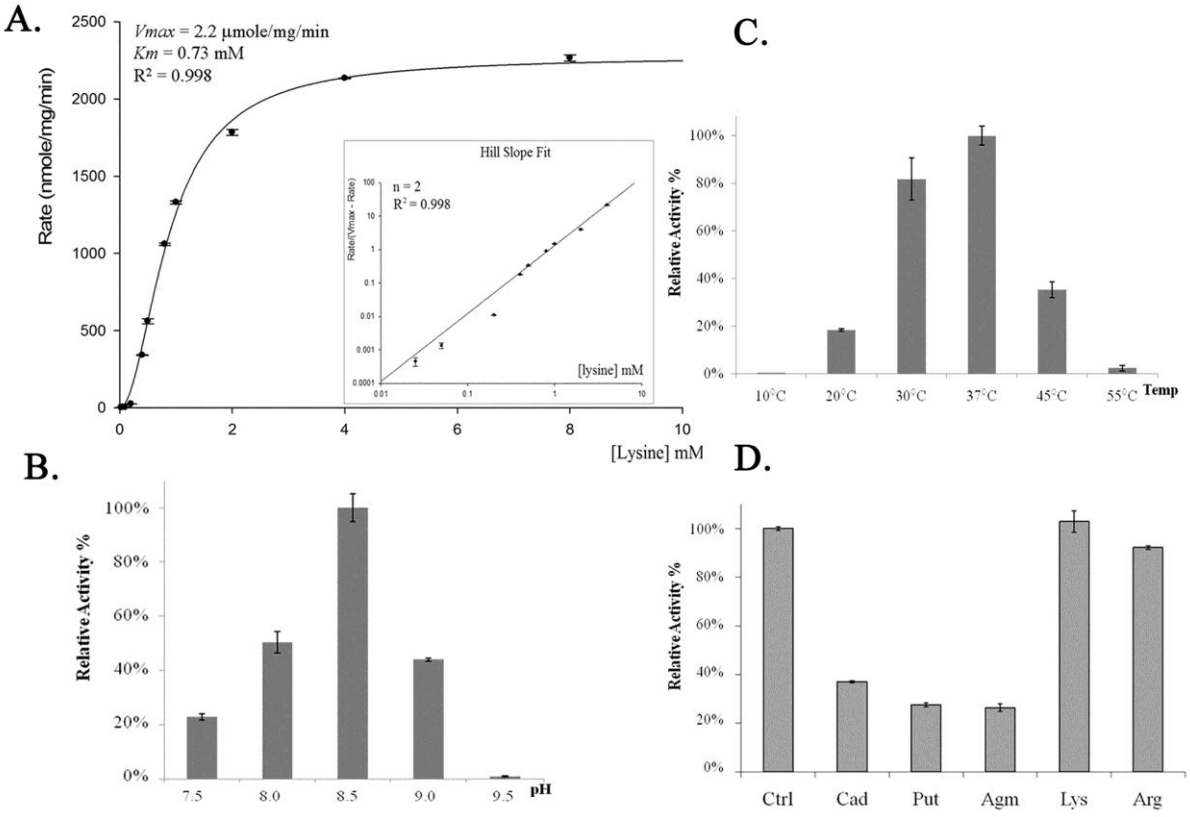

Figure 1.1. Lysine decarboxylase enzyme characterization.

His-tagged LdcA protein was purified from *E. coli*. Enzyme-catalyzed lysine decarboxylation was assayed by measuring the liberated $^{14}CO_2$ as previously described in methods. **A**, Kinetics studies exhibiting cooperative substrate activation pattern with the corresponding Hill slope plot. Assays with increasing lysine concentrations were performed at pH 8.5, 37°C. **B** and **C**, Optimal conditions for lysine decarboxylation were tested as described in methods. **D**, Cold polyamines or amino acids (5 mM) were added into the standard reaction mixture to test for allosteric effects.

The optimal pH and temperature for LdcA were also determined. As shown in Figure 1.1C and 1.1D, LdcA exhibited a maximum activity around 37ºC, pH 8.5 with L-lysine as substrate. At pH 6, almost no activity was detectable for LdcA in this acidic environment (data not shown). These results strongly suggest that LdcA may not be involved in acid stress as *E. coli* CadA and AdiA do (9, 63, 100) but rather is suitable for lysine catabolism under alkaline conditions.

The potential effects of L-arginine and compounds derived from L-arginine/ornithine/lysine decarboxylation (agmatine, putrescine, and cadaverine) on LdcA were tested. An inhibition effect was detected by the last three compounds but not by L-arginine (Figure 1.1B). These results imply that arginine intervention on lysine utilization is exerted only at the transcriptional level, and that lysine decarboxylation is subjected to product inhibition by cadaverine and other polyamines.

Lysine uptake was enhanced by exogenous arginine but not lysine. Arginine effect on lysine utilization may range from uptake to degradation. In order to investigate this hypothesis, lysine uptake was examined in a pair of isogenic strains of *P. aeruginosa*, PAO1 (wild type) and PAO501 (*argR::Gm-R*). Cells were grown in minimal medium P with L-glutamate as the background nutrient with or without addition of exogenous L-arginine or L-lysine. The uptake of lysine in cell suspensions was examined. As shown in Figure 1.2, uptake of lysine was significantly induced by the presence of exogenous arginine but not by lysine. Interestingly, this arginine inducible lysine uptake was also ArgR dependent.

A.

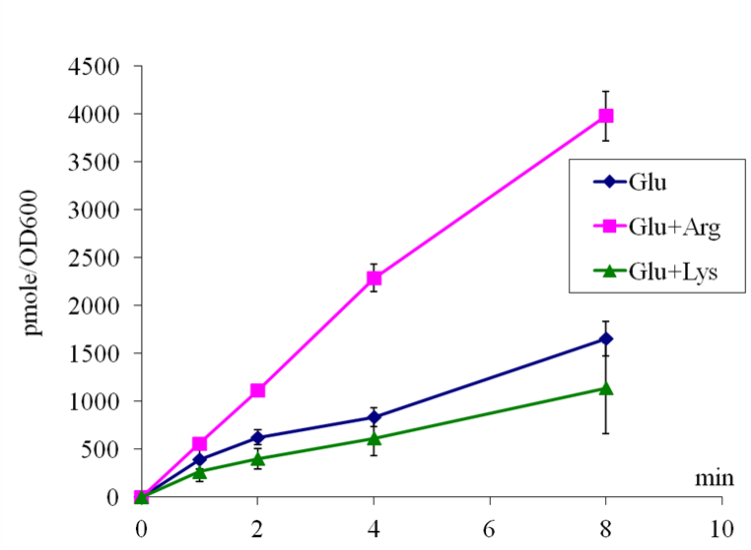

B.

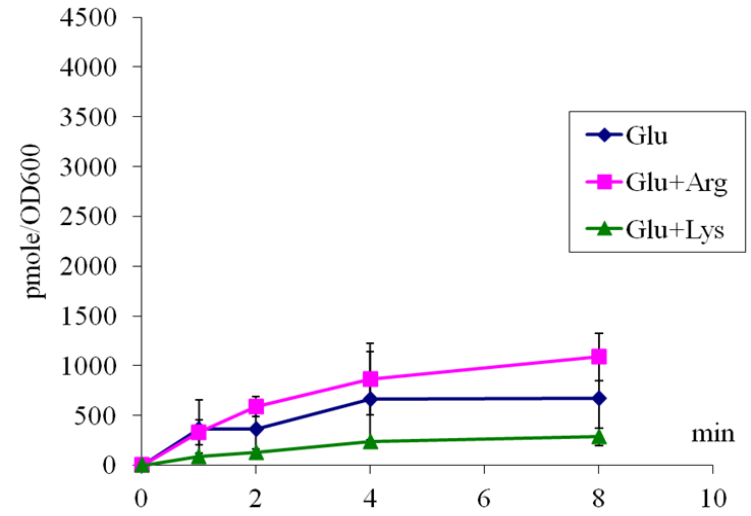

Figure 1.2. Enhanced lysine uptake by arginine.

Induction of L-lysine uptake by exogenous arginine in **A,** *P. aeruginosa* PAO1 and **B,** its *argR* mutant. Cultures grown in glutamate-MMP in the absence (diamond) or in the presence of L-arginine (square) or L-lysine (triangle) were harvested during exponential growth and used for L-lysine transport assays as described in Materials and Methods.

Improved growth on lysine by exogenous arginine in PAO1. All my data indicated that expression of *ldcA*, the essential gene for lysine catabolism, is controlled by ArgR in response to L-arginine but not to L-lysine. In the wild type strain PAO1, the estimated generation time was about 122 minutes when grown on L-lysine; however, it experienced a long lag phase of 44±2 h. I reasoned this growth curve as lack of *ldcA* induction by exogenous lysine, and hypothesized that growth of PAO1 on lysine can be improved by a trace amount of L-arginine to kick off *ldcA* expression. Indeed, addition of 0.15 mM L-arginine removed completely the otherwise long lag phase while the generation time remained unchanged (data not shown).

The basal level of *ldcA* expression is elevated in the mutant devoid of the major arginine catabolic pathway. In analysis of the growth phenotype of PAO5602 (an arginine no-grower), I observed significant improvement of this strain on lysine in comparison to PAO1 (Table 1.3). Similar growth behavior on lysine was also detected in PAO5717, an *aruC-E* deletion mutant devoid of the major pathway (AST) for arginine catabolism (35). One hypothesis was that the intracellular level of arginine may be elevated when the major catabolic pathway is blocked, which in turn activates ArgR to induce the ArgR regulon (60) including the *aotJQMOP-argR* operon for uptake and regulation, *ldcAB*, and many others. To test this hypothesis, I compared the activities of *aotJ* and *ldcA* promoters from *lacZ* fusions in PAO1 and PAO5717. As shown in Table 1.2, the basal level of these two promoters was increased 4-5 fold in PAO5717, and they were still responsive to the presence of arginine but not lysine in both strains. These results support the hypothesis of an activated ArgR regulon and hence high lysine uptake and catabolism in AST mutant strains.

Potential lysine catabolism by transamination. While the LdcA-catalyzed decarboxylation appeared to be the major route for lysine catabolism, L-lysine can potentially be degraded by other approaches, e.g. transamination. One possible candidate was AruH, which has been studied and characterized *in vitro* as a transaminase able to remove the α-amino group from arginine and lysine (103). Although the *ldcA* mutant lost completely the capability to grow on L-lysine as sole source of carbon and/or nitrogen (Table 1.3), introducing *aruH* carried on pHC5306 to this mutant indeed restored growth on lysine as sole source of nitrogen but not carbon (Table 1.4).

Transcriptome analysis reveals lysine-inducible genes. DNA microarray experiments were performed to understand genome-wide responses of *P. aeruginosa* PAO1 to exogenous L-lysine and L-arginine at exponential growth phase. The results showed no response to exogenous lysine of the uptake and catabolic genes for lysine utilization identified in this chapter (Tables 1.5). This reinforces the model of lysine utilization under arginine control.

Table 1.4. Effects of constitutive expression of *ldcA* or *aruH*

Strain	Affected Pathway	Plasmid	Genotype	Supplements[a]			
				Lc	Ln	Arg	Agm
PAO1	none	pUCP18	WT, pUCP18	+	++	+++	+++
		pHC5307	WT, pUCP18/aruH	+	+++	+++	+++
		pHC5306	WT, pUCP18/ldcA	+++	+++	+++	+++
PAO5716	LDC	pUCP18	*ldcA::Tc*^{r}, pUCP18	−	−	+++	+++
		pHC5307	*ldcA::Tc*^{r}, pUCP18/aruH	−	+++	+++	+++
		pHC5306	*ldcA::Tc*^{r}, pUCP18/ldcA	+++	+++	+++	+++
PAO5602	ATA/AST	pUCP18	*aruH::Tc*^{r}*/ΔaruF*, pUCP18	+++	+++	−	+++
		pHC5307	*aruH::Tc*^{r}*/ΔaruF*, pUCP18/*aruH*	+++	+++	+++	+++
		pHC5306	*aruH::Tc*^{r}*/ΔaruF*, pUCP18/*ldcA*	+++	+++	−	+++

[a] Logarithmically growing cells were subjected to growth phenotype test in MMP media supplemented with: Lc, 20 mM lysine + 5 mM ammonia; Ln, 5mM lysine + 20 mM glucose; Arg, 20 mM arginine; Agm, 20 mM agmatine; and GN, 20mM glucose + 5 mM ammonia. Aerobic growth at 37°C was monitored during 3 days: +++, prominent growth in 1 day; ++, growth in 2 days; +, growth in 3 days; −, no growth in 3 days.

Table 1.5. L-arginine inducible genes for lysine utilization selected from DNA microarray analysis

PA ID[a]	Gene	Signal Value[b]							Annotations
		Glu	Glu Arg	Glu Put	Glu GABA	Glu Lys	Glu Cad	Glu AMV	
PA0888	***aotJ***	1911	**7331 (4)**	1567 (1)	1228 (1)	**1067 (1)**	1369 (1)	1262 (1)	arginine/ornithine binding protein
PA0889	***aotQ***	432	**2157 (5)**	318 (1)	399 (1)	**453 (1)**	470 (1)	303 (1)	arginine/ornithine transport protein
PA0890	***aotM***	700	**2962 (4)**	516 (1)	781 (1)	**806 (1)**	807 (1)	822 (1)	arginine/ornithine transport protein
PA0892	***aotP***	1461	**4401 (3)**	1051 (1)	1500 (1)	**1959 (1)**	2167 (1)	2039 (1)	arginine/ornithine transport protein
PA0893	***argR***	671	**2090 (3)**	526 (1)	606 (1)	**1050 (2)**	1114 (2)	1135 (2)	transcriptional regulator
PA5152		1918	**4617 (2)**	1377 (1)	935 (0)	**1786 (1)**	1210 (1)	1185 (1)	ATP-binding component of ABC transporter
PA5153		4771	**14117 (3)**	2954 (1)	1298 (0)	**4147 (1)**	2141 (0)	2160 (0)	periplasmic binding protein
PA5154		912	**2371 (3)**	383 (0)	271 (0)	**1410 (2)**	750 (1)	694 (1)	permease of ABC transporter
PA5155		607	**2105 (3)**	327 (1)	194 (0)	**372 (1)**	319 (1)	270 (0)	permease of ABC transporter
PA1818	***ldcA***	581	**3070 (5)**	531 (1)	379 (1)	**997 (2)**	712 (1)	603 (1)	lysine decarboxylase
PA1819	***ldcB***	190	**796 (4)**	152 (1)	134 (1)	**445 (2)**	579 (3)	500 (3)	probable lysine/cadaverine antiporter
PA4975		83	**225 (3)**	70 (1)	71 (1)	**345 (4)**	55 (1)	93 (1)	NAD(P)H quinone oxidoreductase
PA4976	***aruH***	98	**192 (2)**	80 (1)	83 (1)	**630 (6)**	133 (1)	53 (1)	Arginine:Pyruvate Transaminas
PA4977	***aruI***	68	**149 (2)**	80 (1)	130 (2)	**424 (6)**	119 (2)	121 (2)	2-ketoarginine decarboxylase
PA4978		108	**177 (2)**	81 (1)	80 (1)	**940 (9)**	292 (3)	171 (2)	hypothetical acetyl-CoA C-acetyltransferase
PA4979		83	**17 (0)**	44 (1)	27 (0)	**887 (11)**	168 (2)	69 (1)	probable acyl-CoA dehydrogenase
PA4980		122	**687 (6)**	232 (2)	149 (1)	**2241 (18)**	66 (1)	95 (1)	putative enoyl-CoA hydratase/isomerase
PA4981		54	**573 (11)**	54 (1)	43 (1)	**5855 (108)**	189 (4)	39 (1)	probable amino acid permease

[a] The PA ID numbers were taken from the PAO1 genome annotation project (www.pseudomonas.com).

[b] GeneChip raw data are mean values from two independent sets of cultures. Cells were grown in minimal medium P supplemented with 20 mM of the following supplements as indicated: Glu, glutamate; Arg, L-arginine; Put, putrescine; GABA, γ-aminobutyrate; Lys, L-lysine; Cad, cadaverine; AMV, δ-aminovalerate. Fold changes are in parenthesis.

Table 1.6. L-lysine inducible genes selected from DNA microarray analysis

PA ID[a]	Gene	Signal Value[b]							Annotations
		Glu	Glu Arg	Glu Put	Glu GABA	Glu Lys	Glu Cad	Glu AMV	
PA0446		169	45(0)	127(1)	66(0)	**1263(7)**	**1699(10)**	**2294(14)**	Predicted acyl-CoA transferase
PA0447	***gcdH***	167	134(1)	141(1)	189(1)	**9747(58)**	**7201(43)**	**9184(55)**	glutaryl-CoA dehydrogenase
PA2662		64	144(2)	107(2)	60(1)	**600(9)**	**525(8)**	**617(10)**	conserved hypothetical protein
PA2663	***ppyR***	49	140(3)	96(2)	54(1)	**923(19)**	**614(13)**	**939(19)**	*psl* and pyoverdine operon regulator
PA2664	***fhp***	14	6(0)	15(1)	6(0)	**1602(114)**	**618(44)**	**1490(106)**	flavohemoprotein
PA1027	***amaA***	100	20(0)	124(1)	76(1)	**1230(12)**	197(2)	238(2)	α-aminoadipate δ-semialdehyde dehydrogenase
PA1028	***amaB***	87	243(3)	109(1)	98(1)	**483(6)**	231(3)	144(2)	L-Pipecolate oxidase
PA4181		171	323(2)	174(1)	164(1)	**5721(33)**	432(3)	385(2)	hypothetical protein of unknown function
PA4182		189	306(2)	252(1)	179(1)	**8959(47)**	423(2)	457(2)	hypothetical transcriptional factor
PA4364		56	58(1)	38(1)	58(1)	**2448(44)**	125(2)	30(1)	hypothetical protein of unknown function
PA4365		54	70(1)	52(1)	26(0)	**2304(43)**	181(3)	111(2)	probable lysine exporter

[a] The PA ID numbers were taken from the PAO1 genome annotation project (www.pseudomonas.com).
[b] GeneChip raw data are mean values from two independent sets of cultures. Cells were grown in minimal medium P supplemented with 20 mM of the following supplements as indicated: Glu, glutamate; Arg, L-arginine; Put, putrescine; GABA, γ-aminobutyrate; Lys, L-lysine; Cad, cadaverine; AMV, δ-aminovalerate. Fold changes are in parenthesis.

In contrast, a group of 11 genes in five putative operons was subjected to specific induction by L-lysine but not L-arginine (Table 1.6). Among them, the PA0446-PA0447 and PA2662-PA2664 operons were inducible either by L-lysine, cadaverine or AMV. PA0446 encodes a putative acyl-CoA transferase, and PA0447 (*gcdH*) a glutaryl-CoA dehydrogenase. This *locus* might be involved in lipid and amino acid catabolism (96). On the other hand, PA2662-PA2664 operon seems related to nitric oxide (NO) detoxification. PA2664 (*fhp*) encodes a flavohemoglobin with NO reductase activity under anaerobic conditions and NO dioxygenase activity under aerobic conditions (2, 80). PA2663 (*ppyR*) encodes a membrane sensor protein. Upon *ppyR* inactivation, defective biofilm formation and quorum sensing were reported in *P. aeruginosa* (3). And PA2662 encodes a membrane protein predicted for response to NO.

Among the lysine inducible genes, six genes in three operons were specifically inducible by L-lysine but not by its downstream metabolites cadaverine or AMV (Table 1.6). The first operon, PA1027-PA1028, is the counterpart of *amaA-amaB*, encoding important enzymes of the D-lysine catabolic pathway in *P. putida* (82, 84). 2-ketolysine derived from lysine deamination is spontaneously converted into Δ^1-piperidine-2-carboxylate, a cyclic form of higher stability (36). In *P. putida,* Δ^1-piperidine-2-carboxylate derived from D-lysine deamination leads to L-pipecolate biosynthesis by DpkA which in turn is channeled to aminoadipate by AmaB and AmaA (82, 84). AmaB, a FAD-dependent oxidoreductase, converts L-pipecolate into Δ^1-piperidine-6-carboxylate, and AmaA, an aldehyde dehydrogenase, synthesizes 2-aminoadipate from Δ^1-piperidine-6-carboxylate. The existence of the *ama locus* in *P. aeruginosa* is intriguing since the *dpkA* gene for L-pipecolate synthesis is absent on the chromosome. Possible explanation might be a cross reaction of AmaA with Δ^1-piperidine-2-carboxylate. However, no

growth on lysine in lysine decarboxylase *ldcA* deficient strain suggested limited role of AmaA and AmaB in lysine utilization. The second operon, PA4181-PA4182, encodes hypothetical proteins of unknown function. PA4182 might be a transcriptional regulator with a FMN-binding domain. More studies are required to investigate the functions of these genes. The third and last operon of this group, PA4364-PA4365, encodes a hypothetical protein of unknown function and a putative lysine exporter with six transmembrane helices. This LysE type transporter is predicted to excrete excess lysine from the cell as in *C. glutamicum* (99). Induction of this exporter may suggest that L-lysine were taken up but needed to be pumped out due to intracellular accumulation.

1.4 DISCUSSION

The bottleneck of lysine catabolism. The most intriguing finding in this study was that both lysine uptake and degradation are inducible by L-arginine and show no response to L-lysine. The arginine dependent *ldcA* expression was revealed from its promoter activities; and electro-mobility shift assays also revealed interactions of the arginine-responsive regulator ArgR to its putative binding site in the promoter region. The lack of lysine-responsive induction on *ldcA* is likely the major limiting factor of growth on L-lysine. Growth of *P. aeruginosa* on L-lysine exhibited a long lag phase of 44±2 hours. In comparison, growth on cadaverine, the decarboxylation product of L-lysine by LdcA, has normal lag phase. Indeed putting *ldcA* under control of the constitutive *lac* promoter in a plasmid improved growth significantly.

Conditions that increase the level of intracellular arginine and ArgR could also induce *ldcA* expression, and hence promote a better growth on L-lysine. While *ldcA* was induced under these conditions, at least two ABC transporter systems for L-arginine were also increased (*aotJQMP* and *PA5152-PA5155*). Interestingly, counterparts of these two systems in *P. putida* KT2440 have been reported as candidate L-lysine transport systems in recent studies (83). *PP0283-PP0280* and the *PP4486-PP4482* show high similarities in gene organization as well as in amino acids sequences (82% and 76% respectively) with *P. aeruginosa, PA5152-5155* and *aotJQMP-argR* loci. Together with LdcB, a candidate lysine/cadaverine antiporter, all three candidate transport systems in *P. aeruginosa* are regulated by ArgR in response to L-arginine but not to L-lysine. This may explain the lack of lysine-inducible uptake as another limiting factor for growth on L-lysine in *P. aeruginosa* PAO1.

The lysine decarboxylase LdcA is conserved among pseudomonads. In the Pseudomonas Genome Database (www.pseudomonas.com), orthologs of LdcA can be found in strains of *P. entomophila*, *P. fluorescens*, *P. mendocina*, *P. putida*, and *P. stutzeri*, but not in *P. syringae*. For *P. putida* KT2440, the corresponding gene (PP4140) contains an authentic mutation that causes a frame shift of the translated product. While gene organization of *ldcA* and its upstream *dnaQ* encoding the epsilon subunit of DNA polymerase III is conserved among these strains, the downstream *ldcB* can only be found in strains of *P. aeruginosa*. In conclusion, it is reasonable to predict that most species of pseudomonads possess the L-lysine decarboxylase.

Other pathways of lysine catabolism. The *aruH* gene encodes for an L-arginine and L-lysine:pyruvate transaminase (104). Contribution of this enzyme in lysine utilization as the sole nitrogen source can only be detected when constitutively expressed from a plasmid. However, AruH may not have any physiological implication on lysine catabolism in PAO1 as the *ldcA* mutant showed no growth on L-lysine as the sole source of carbon or nitrogen. Perhaps it was because of low L-lysine uptake and low affinity of AruH on L-lysine.

The *aruH* and *aruI* genes encode the first two enzymes of the arginine transaminase pathway in *P. aeruginosa* (104). While *aruHI* are conserved in *P. putida*, an extra gene encoding an amino acid racemase is located between *aruH* and *aruI* of this organism. The amino acid sequence of this racemase contains a predicted signal peptide at the N-terminus, suggesting its secretion to the periplasm. This implies the role of this additional gene as the racemase to convert

L-lysine into D-lysine before channeled into the D-lysine catabolic pathway in *P. putida* (10, 34, 82).

P. aeruginosa can only utilize D-lysine as nitrogen source but not carbon source by the FAD-dependent dehydrogenase DauA (52). Transamination of L-lysine by AruH or D-lysine by DauA leads to α-keto-ε-aminohexanoate which is spontaneously converted into its cyclic form Δ^1-piperideine-2-carboxylate at physiological pH (40). Recent studies in *P. putida* suggests further degradation of this molecule into L-pipecolate by the reductase DpkA (PP3591) (84). However, viability of this pathway is still undefined in *P. aeruginosa* since *dpkA* orthologue is not present on the chromosome, corresponding biochemical reaction cannot be detected, and no growth is detectable using D-lysine as carbon source (19).

Lysine decarboxylation is the main route of L-lysine catabolism in *P. aeruginosa*. With the purified enzyme, I demonstrated that LdcA is an L-lysine decarboxylase with no activity toward L-arginine. Genetic studies also indicated that *ldcA* is essential for L-lysine utilization in *P. aeruginosa*. Therefore, I concluded that the lysine decarboxylase LdcA is the enzyme responsible of the pivotal step of L-lysine catabolism in this organism.

Transcriptome analysis of arginine and putrescine unraveled lysine and cadaverine catabolic pathways. It had been very confusing the initial studies of the lysine decarboxylase pathway gene *ldcA* since it is highly induced by arginine in the DNA microarray data. And none of the genes for lysine utilization identified in this study were inducible by lysine. Without the strong arginine background of our laboratory, it would not be possible to discover the arginine

control on lysine utilization through ArgR. Similarly, I also encountered difficulties analyzing genome-wide responses to exogenous cadaverine. No obvious hints of catabolic genes for cadaverine were able to be picked up from this set of DNA microarrays. Fortunately, I performed transcriptome analysis using putrescine, a similar compound derived from ornithine and/or arginine, where candidate genes for polyamine γ-glutamylation were noticed (13). This motivated me to propose putrescine and cadaverine degradation through γ-glutamylation pathway in *P. aeruginosa* which will be described in Chapter Two of this thesis.

CHAPTER TWO

CADAVERINE AND PUTRESCINE CATABOLISM THROUGH γ-GLUTAMYLATION IN *PSEUDOMONAS AERUGINOSA* PAO1

2.1 INTRODUCTION

Cadaverine and putrescine are diamines involved in a wide spectrum of physiological functions from prokaryotic to eukaryotic cells (45, 90), and intracellular concentrations of these compounds are finely tuned through biosynthesis, degradation and transport (14). In microbes, putrescine and cadaverine are synthesized directly from decarboxylation of ornithine (*speC*) and lysine (*ldcA*) respectively (12, 72). Alternatively, endogenous putrescine can also be generated through arginine and agmatine degradation (13, 73). On the other hand, exogenous putrescine and cadaverine can be taken as carbon and nitrogen sources by many bacteria including *P. aeruginosa* (12, 13, 93). It was first reported in *E. coli* that putrescine is degraded through the γ-glutamylation pathway (43, 44). This pathway consists of four consecutive reactions with consumption of ATP in the first step for γ-Glu-putrescine biosynthesis (Figure 2.1).

In order to understand how *P. aeruginosa* responds to exogenous polyamines, DNA microarray experiments had been conducted to get snapshots of gene expression at the exponential phase of growth (13). A group of redundant genes were identified for γ-glutamylation and were shown essential for polyamine utilization in *P. aeruginosa* (13, 105). Different from *E. coli*, the γ-glutamylation pathway is more complex by the existence of multiple homologous enzymes with redundant specificity toward different polyamines for a larger metabolic capacity in *P. aeruginosa* (105).

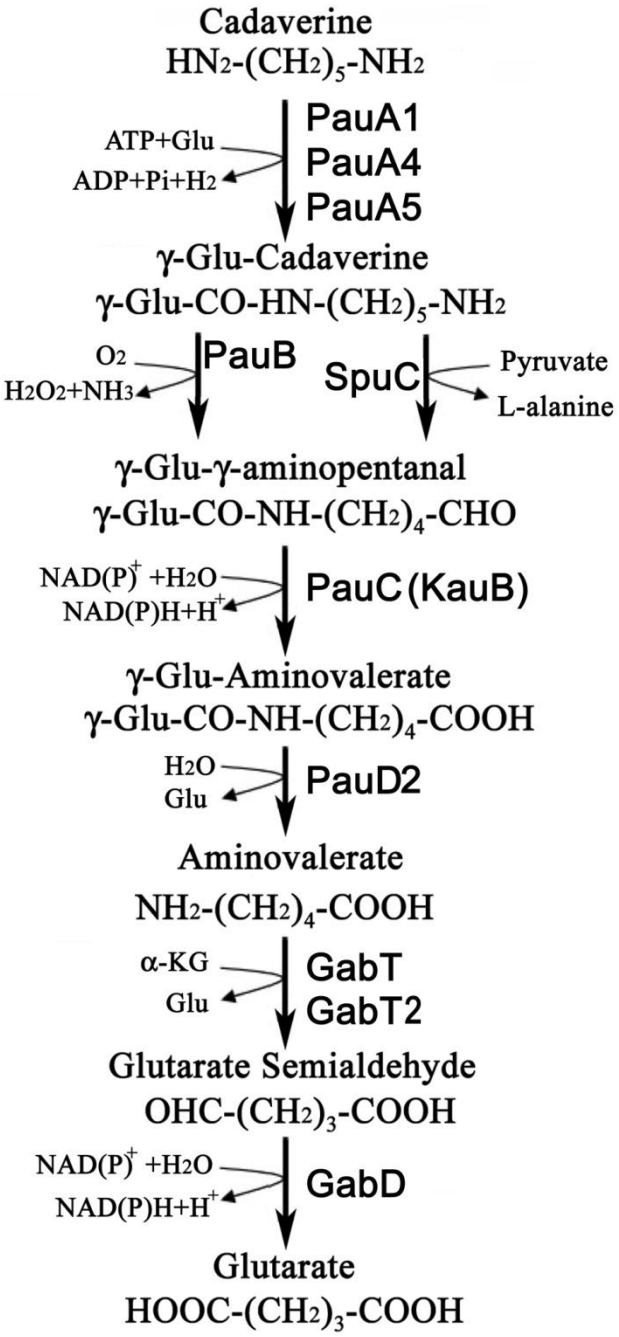

Figure 2.1. Proposed cadaverine catabolic pathway in *P. aeruginosa*

Proposed cadaverine catabolism by the γ-glutamylation pathway was shown above. The Pau proteins for polyamine utilization were marked. For putrescine glutamylation, PauA1, PauA2 and PauA5 catalyze the first step of the pathway. Also shown were the enzymes GabT, GabT2, and GabD, for AMV and GABA degradation.

Alternatively, putrescine was proposed to be degraded without γ-glutamylation through a traditional transaminase-dehydrogenase pathway (13). PA0299 (SpuC) and PA5312 (PauC/KauB) were proposed as putrescine:alanine transaminase and aldehyde dehydrogenase for direct degradation of putrescine into γ-aminobutyrate (GABA) due to the growth deficiency on putrescine of the corresponding mutant strains (13, 59). However, deletion mutants devoid of the glutamylation pathway cannot grow on polyamines (105). Therefore the direct transaminase-dehydrogenase pathway has limited contribution in polyamine utilization, and PA0299 and PA5312 were proposed to play their roles after polyamine glutamylation.

Putrescine and cadaverine were proposed to be degraded into γ-aminobutyrate (GABA) and δ-aminovalerate (AMV), respectively. To serve as carbon sources, subsequent reactions are required to degrade GABA into succinate and AMV into glutarate. Based on similarities in chemistry, pathways with common enzymes for the utilization of GABA and AMV were proposed (12, 42).

This study was undertaken to investigate the importance of the γ-glutamylation pathway for putrescine and cadaverine utilization in *P. aeruginosa*. Essential Glu-putrescine and Glu-cadaverine synthetases were identified by genetics approach. Different from putrescine, carbon catabolite repression was detected for cadaverine utilization. A regulatory protein of the cupin family, PauR, was identified revealing regulation on putrescine/cadaverine glutamylation and GABA/AMV degradation through conformational changes. The *gabD*, *gabT* and *gabT2* genes for GABA degradation were investigated for AMV degradation into glutarate. In addition to common catabolic pathways, a newly identified ABC transport system *agtABCD* under

regulation of a two-component system *agtSR* were proven to contribute in both GABA and AMV utilization. The genetics and regulatory aspects of the γ-glutamylation pathway for putrescine and cadaverine utilization in this organism were investigated in this study.

Table 2.1. Strains and plasmids

Strain or plasmid	Genotype or description[a]	Source
***E. coli* strains**		
DH5α	F$^-$Φ80d*lac* ΔM15 Δ(*lacZYA-argF*)U169 *deoR recA1 endA1 hsdR17* (r_K^- m_K^-) *supE44* λ$^-$ *thi-1gyrA96 relA*	Bethesda Research Laboratories
TOP10	F- *mcr*A Δ(*mrr-hsd*RMS-*mcr*BC) Φ80*lac*ZΔM15 D*lac*X74 *rec*A1 *ara*D139 Δ(*ara-leu*)7697 *gal*U *gal*K *rps*L (Sm^r) *end*A1 *nup*G	Invitrogen
SM10	*thi-1 thr leu tonA lacY supE recA*::RP4-2-Tc::Mu (Km^r)	(91)
***P. aeruginosa* strains**		
PAO1	Wild type	(27)
PAO1-Sm^r	Spontaneous Sm^r mutant strain of PAO1	(35)
PAO5725	Δ*pauA1-A6* (Δ*PA0296*; Δ*PA0298*; Δ*PA1566*; Δ*PA2040*::*Gm^r*; Δ*PA3356*; Δ*PA5522*)	This study
PAO5722	*pauR*::*Gm^r*	This study
PAO5701	*gabD*::*Tc^r*	(13)
PAO5703	*gabT*::*Tc^r*	(13)
PAO5708	*gabT2*::*Gm^r*	(13)
PAO5704	*gabT/T2 (gabT*::*Tc^r; gabT2*::*Gm^r)*	(13)
H103	Wild type	(51)
PAO5723	*agtS*::*lux*, ID:PAO1_lux_23_C9	(51)
PAO5724	*agtA*::*lux*, ID: PAO1_lux_25_F4	(51)

Plasmids

pRTP1	Amp^r Sm^s conjugation vector	(95)
pGMΩ1	Amp^r Gm^r; gentamicin resistance gene cassette with omega loop on both ends	(88)
pQF50	*bla; lacZ* transcriptional fusion vector	(18)
pQF52	*bla; lacZ* translational fusion vector derived from pQF50	(76)
pGU101	*spuA*::*lacZ* (for *pauA2*) translational fusion of pQF52	(59)
pGU102	*pauA1(spuI)*::*lacZ* translational fusion of pQF52	(59)
pHT2040	*pauA4*::*lacZ* transcriptional fusion of pQF50	This study
pHT3356	*pauA5*::*lacZ* transcriptional fusion of pQF50	This study
pHT0603	*agtA*::*lacZ* transcriptional fusion of pQF50	This study
pMH105	*gabD*::*lacZ* translational fusion of pQF52	(29)
pHT0265-1	palindrome-*gabD*::*lacZ* transcriptional fusion of pQF50	This study
pHT0265-2	No palindrome-*gabD*::*lacZ* transcriptional fusion of pQF50	This study
pHT5313	*gabT2*::*lacZ* transcriptional fusion of pQF50	(13)
pBAD-His6	Modified protein expression vector derived from pBAD-HisA	(52)
pBAD-PauR	6 x His-tagged PauR protein expression vector	This study
pBAD-GabD	6 x His-tagged GabD protein expression vector	This study
pBAD-AgtR	6 x His-tagged AgtR protein expression vector	This study

[a] Sm^r, streptomycin resistance; Km^r, kanamycin resistance; Gm^r, gentamicin resistance; Tc^r, tetracycline resistance; Amp^r, ampicillin resistance; Sm^s, streptomycin sensitive.

2.2 MATERIALS AND METHODS

Bacterial strains, plasmids, media, and growth conditions. Mutant strains of the *agt* locus are from the *lux* transposon mutant library courtesy of Dr Hancock at University of British Columbia, Vancouver, B.C., Canada (pseudomutant.pseudomonas.com). Luria-Bertani (LB) medium was used with the following supplements as required: ampicillin at 100 µg ml^{-1}, tetracycline at 12.5 µg ml^{-1}, gentamicin at 10 µg ml^{-1}, 5-bromo-4-chloro-3-indolyl-*β*-D-galactopyranoside (X-Gal) at 0.03 % (wt/vol) for *E. coli*; and carbenicillin at 100 µg ml^{-1}, streptomycin at 500 µg ml^{-1}, tetracycline at 100 µg ml^{-1} and gentamicin at 100 µg ml^{-1} for *P. aeruginosa*. Minimal medium P (27) containing the indicated carbon sources at 20 mM and nitrogen sources at 5 mM was used for the growth of *P. aeruginosa*.

DNA Microarray. DNA microarray experiment was conducted as described in Chapter One. Data was deposited in the Gene Expression Omnibus (GEO) database (GSE9926).

Construction of a *pauR* knockout mutant. For deletion mutants, two flanking regions of the targeted gene were PCR amplified and cloned into pRTP1 using primers: pauR1F 5'-CGG GAT CCC GAT CAG AAA TTT GCG GGC GTG G-3'; pauR1R 5'- CGG AAT TCC GGC GCG GTG TCC ATG CGC CTG-3'; pauR2F 5'- CGG AAT TCC GGT CGA TCA GTT CGT CTG CCT -3'; pauR2R 5'- CCA AGC TTG GGG TGC TCG TCT GCA AAC CAT -3'. The PCR products were cloned into pRTP1. A cassette carrying gentamicin-resistance gene from pGMΩ1 was inserted into the conjunction of the two DNA fragments (88). For gene replacement, *E. coli* SM10 was served as the donors in biparental mating with PAO1-Sm^r (21). The desired

knockout mutants were selected on LB plates containing streptomycin and either gentamicin or tetracycline, and the mutation was confirmed by PCR.

Construction of *lacZ* fusions. Plasmids pGU101, pGU102 and pHT5313 were used to measure *pauA2, pauA1 and gabT2* promoters activities, respectively (13, 59). Regulatory regions of *gabDT, pauA5 (PA3356), pauA4 (PA2040)* and *agtA (PA0603)* were amplified by PCR from the genomic DNA of *P. aeruginosa* PAO1 using the following primers: Pgab_F, 5'-GGA TTC GTT TGA GAT TTC AAA CGC CCC-3'; Pgab_palindrome_R, 5'-GGG GCG TTT GAA ATC TCA AAC GAA TCC-3'; Pgab_no palindrome_R, 5'-TCT CAA ACG AAT CCT AGG GCC-3'; P pauA5_F, 5'-GGT GG A TCC GAG AAT CAA CGG CAG TAC TC-3'; PpauA5_R, 5'-GGT AAG CTT GAT GCA TTG CAG CAG CAC GCCA-3'; PpauA4_F, 5'-GGT GGA TCC TTG AAC GAT CTT GCT CTT CGT ATC-3'; PpauA4_R, 5'-GGT AAG CTT GAA GGA ACA GGC TCG GCT CAG-3'; PagtA_F, 5'-GGT GGA T CC GCA AGC TCG ACG AGC TGA AGC CCT ATA TC-3'; PagtA_R, 5'- GGT AAG CTT GAG TCT CGG CCA TAA CCG CAC CTT TGT TC-3'. PCR products were cloned into pQF50 and confirmed by DNA sequencing.

Measurements of LacZ enzyme activity. The cells were grown in the minimal medium P containing carbon and nitrogen sources as indicated. Cells in the mid-log phase when the optical density at 600 nm reached 0.7 were harvested by centrifugation, and then passed through a French press cell at 8500 lb/in^2 The cell debris were removed by centrifugation at 20,000 *g* for 10 min, at 4°C, and protein concentrations in the crude extracts were determined by the Bradford method (5), using bovine serum albumin as standard. The levels of *β*-galactosidase activity were

measured at 37˚C using *o*-nitrophenyl-*β*-galactopyranoside as the reaction substrate, and the formation of *o*-nitrophenol was determined by spectrophotometry at 420 nm (64).

Overexpression and purification of the histidine-tagged PauR and AgtR proteins. Full-length *pauR* and *agtR* were amplified from the genomic DNA of *P. aeruginosa* using the following primers: agtR F 5'- GTG ATC CGA GTC CTG GTC GCT GAA G -3', agtR R 5'- GAG GAA TTC TGT CAG AGC AGG CGG TGC TCC ATC-3', pauR F 5'- GAC GTC GGT GCT CGT CTG CAA ACC -3', pauR R 5'- GAG GAA TTC TTG TGC TTC AGG TCA GAA ATT TGC-3'. The PCR products were digested with *Eco*RI restriction endonuclease and assembled onto the *Sma*I and *Eco*RI sites of pBAD-His6, a modified pBAD expression vector (52, 103). Recombinant proteins were expressed by arabinose induction in *Escherichia coli* TOP10 (Invitrogen life technologies). Cell extract was obtained by passing through a French pressure cell at 8,500 lb/in^2. Soluble fraction was subjected to protein purification using HisTrap HP column (GE Healthcare) following manufacturer's instructions. Protein purity was analyzed by SDS PAGE and concentration was determined by the method of Bradford (5).

Glutaraldehyde crosslinking. Purified His-PauR was subjected to glutaraldehyde treatment in 20mM HEPES buffers at pH 7.5. Reaction mixtures with 25µg of purified His-PauR in a total volume of 100 µl were treated with 5 µl of 2.3% freshly prepared solution of glutaraldehyde for 2 minutes at 25^{o}C followed by 3 minutes at 37^{o}C. The reaction is terminated by addition of 10 µl of 1 M Tris-HCl (pH 8.0). Diamines, GABA or AMV are incorporated into the reaction mixture at 1mM concentration either prior glutaraldehyde treatment or after quenching with Tris buffer.

Cross-linked proteins were analyzed by SDS-polyacrylamide gels electrophoresis and visualized by ProtoBlue Safe staining (National Diagnostics).

Electrophoretic mobility shift assays. DNA fragments covering regulatory regions were PCR amplified from the genome using the same primers as for the construction of the cognate promoter-*lacZ* fusions. For *pauA1/spuA* divergent promoters, the following primers were used: Pspu F 5'-GTA CCG ACA TGA TGC AAC AC -3' and Pspu R 5'- CAG GCG AGA CAT GAG ACA C -3'. For radioactively labeled DNA probes, [γ-^{32}P] dATP were incorporated by polynucleotide kinase. DNA probes (0.2 ng) were allowed to interact with different concentrations of purified proteins in a 20 μl reaction mixture containing 50 mM Tris-HCl (pH 8), 50 mM KCl, 1mM EDTA, 5% (v/v) glycerol, and 150 μg/ml acetylated bovine serum albumin. A smaller DNA fragment amplified from the *lipA* promoter region was used as negative control for non-specific binding. The reaction mixtures were incubated for 30 min at room temperature before applying to a 4% native polyacrylamide gel in 0.5X TBE (pH7.5) buffer. After being dried, the gel was auto-radiographed by exposure to a phosphorimager plate, scanned using FLA-7000 version 1.1, and analyzed by Multi Gauge version 3.0 (FUJIFILM). For non-radioactive DNA probes, 1 ng of DNA was used in the reaction mixture and visualized from the polyacrylamide gel by SYBR green I staining (Invitrogen) followed by Omega UltraLum imaging system with 473 nm excitation and 520 nm emission wave lengths.

2.3 RESULTS AND DISCUSSION

Putrescine and cadaverine are the inducer molecules of the γ-glutamylation pathway. For the first step of the γ-glutamylation pathway, seven glutamyl-polyamine synthetases (PauA1~PauA7) were identified in *P. aeruginosa* based on sequence homology to *E. coli* glutamyl-putrescine synthetase PuuA. Parallelly, DNA microarray experiment showed PauA1~PauA6 (not PauA7) were inducible by either putrescine or spermidine (Table 2.2). To confirm involvement of these enzymes in polyamine utilization, a series of deletion knockouts with different combinations of *pauA*(s) was performed. Based on these genetics studies, the γ-Glu-polyamine synthetases PauA1, PauA2 and PauA4 were proven essential for growth on putrescine, and PauA1, PauA4 and PauA5 for cadaverine (Figure 2.1, Table 2.3).

To determine the inducer molecule of the γ-glutamylation pathway, the *pauA* promoter activities in response to exogenous putrescine and cadaverine were measured in the wild type PAO1 harboring pGU101 (P*pauA2*::*lacZ*), pGU102 (P*pauA1*::*lacZ*), pHT2040 (P*pauA4*::*lacZ*) or pHT3356 (P*pauA5*::*lacZ*). As shown in Figure 2.2, tested *pauA(s)* promoters were inducible by either putrescine (>5 folds) or cadaverine (>2.5 folds) in glucose/ammonia minimal medium. Then I compared the expression profile in the PAO5725 mutant strain where all six γ-Glu-polyamine synthetase genes (*pauA1-pauA6)* were deleted. As shown in the same graphs, while the basal expression levels of these four *pauA* promoters were similar in PAO1 and PAO5725 induction by putrescine and cadaverine were further enhanced (except *pauA5* promoter) in PAO5725 due to internal accumulation of polyamines in this mutant. These data indicate that putrescine and cadaverine are the inducer molecules of the γ-glutamylation pathway.

Table 2.2. Genes for polyamine γ-glutamylation pathway

PA ID[a]	Gene Name	Signal Value[b]						Descriptions
		Glu	Glu Put	Glu GABA	Glu Cad	Glu AMV	Glu Spd	
PA0296	***pauA1/spuI***	1113	**7613 (7)**	**4045 (4)**	1055 (1)	1211 (1)	**5044 (5)**	glutamylpolyamine synthetase, *pauA4* (PA2040) homolog
PA0297	***pauD1/spuA***	275	**1663 (6)**	**1260 (5)**	341 (1)	214 (1)	**1926 (7)**	putative γ-glutamyl hydrolase
PA0298	***pauA2/spuB***	582	**2625 (5)**	**1892 (3)**	459 (1)	502 (1)	**4244 (7)**	glutamylpolyamine synthetase
PA0299	***spuC***	1203	**6179 (5)**	**4112 (3)**	2331 (2)	2893 (2)	**7115 (6)**	aminotransferase
PA0534	***pauB1***	26	**398 (15)**	**555 (21)**	**883 (34)**	**250 (10)**	**42 (2)**	FAD-dependent oxidoreductase
PA1565	***pauB2***	58	42 (1)	62 (1)	140 (2)	175 (3)	**2111 (36)**	FAD-dependent oxidoreductase
PA1566	***pauA3***	23	13 (1)	46 (2)	22 (1)	19 (1)	**2057 (89)**	glutamylpolyamine synthetase
PA1742	***pauD2***	366	**1605 (4)**	**2292 (6)**	606 (2)	685 (2)	762 (2)	putative γ-glutamyl hydrolase
PA2776	***pauB3***	194	**2555 (13)**	**5078 (26)**	186 (1)	327 (2)	460 (2)	FAD-dependent oxidoreductase
PA3356	***pauA5***	591	**3232 (5)**	1687 (3)	1635 (3)	1960 (3)	**3240 (5)**	glutamylpolyamine synthetase
PA5309	***pauB4***	398	**1007 (3)**	**1316 (3)**	690 (2)	703 (2)	477 (1)	FAD-dependent oxidoreductase
PA5508	***pauA7***	128	119 (1)	155 (1)	156 (1)	272 (2)	79 (1)	glutamylpolyamine synthetase
PA5522	***pauA6***	116	591 (5)	411 (4)	265 (2)	282 (2)	566 (5)	glutamylpolyamine synthetase
PA5312	***pauC/kauB***	922	**7744 (8)**	**5130 (6)**	1392 (2)	1256 (1)	**5540 (6)**	aldehyde dehydrogenase
PA5302	***dadX***	53	**2770 (52)**	359 (7)	468 (9)	297 (6)	**1947 (37)**	alanine racemase
PA5303		105	**3934 (37)**	493 (5)	438 (4)	359 (3)	**2826 (27)**	
PA5304	***dadA***	165	**5682 (34)**	755 (5)	793 (5)	685 (4)	**3842 (23)**	D-alanine dehydrogenase
PA0265	***gabD***	448	**6923 (15)**	**6247 (14)**	**1889 (4)**	**2161 (5)**	**4434 (10)**	succinate-semialdehyde dehydrogenase
PA0266	***gabT***	721	**9244 (13)**	**7800 (11)**	**3199 (4)**	**3617 (5)**	**6136 (9)**	4-aminobutyrate aminotransferase
PA5313	***gabT2***	144	**4226 (29)**	**1426 (10)**	107 (1)	146 (1)	**2095 (15)**	pyridoxal-dependent aminotransferase
PA5314		91	**2298 (25)**	**666 (7)**	104 (1)	88 (1)	**1385 (15)**	hypothetical protein

[a] The PA ID numbers were taken from the PAO1 genome annotation project (www.pseudomonas.com).

[b] GeneChip raw data are mean values from two independent sets of cultures. Cells were grown in minimal medium P supplemented with 20 mM of the following supplements as indicated: Glu, glutamate; Put, putrescine; GABA, γ-aminobutyrate; Lys, L-lysine; Cad, cadaverine; AMV, δ-aminovalerate; Spd, spermidine. Fold changes are in parenthesis.

Table 2.3. Growth phenotypes of *pauA* mutants on polyamines, GABA, and AMV

Strain	Carbon Sources*				
	Cad	AMV	Put	GABA	Spd
WT	+	++	++	++	++
ΔpauA2	+	++	++	++	-
ΔpauA1	++	++	++	++	++
ΔpauA4	++	++	++	++	++
ΔpauA5	++	++	++	++	++
ΔpauA1/4	++	++	+	++	++
ΔpauA1/5	+	++	++	++	++
ΔpauA4/5	++	++	++	++	++
ΔpauA1/2/4	++	++	-	++	++
ΔpauA1/4/5	-	++	+	++	++
ΔpauA1-6	-	++	-	++	-

* Cells were grown on MMP media agar plates with the indicated supplements as the sole source of carbon: Cad, cadaverine; AMV, δ-aminovalerate; Put, putrescine; GABA, γ-aminobutyrate; Glc, glucose. All supplements were added to 10mM. Ammonia was added to 5 mM as the sole source of nitrogen. Growth was recorded in 3 days at 37°C. ++, growth after 1 day; +, growth after 2 days; -, no detectable growth after 3 days. All unmarked deletion mutants were derived from PAO1.

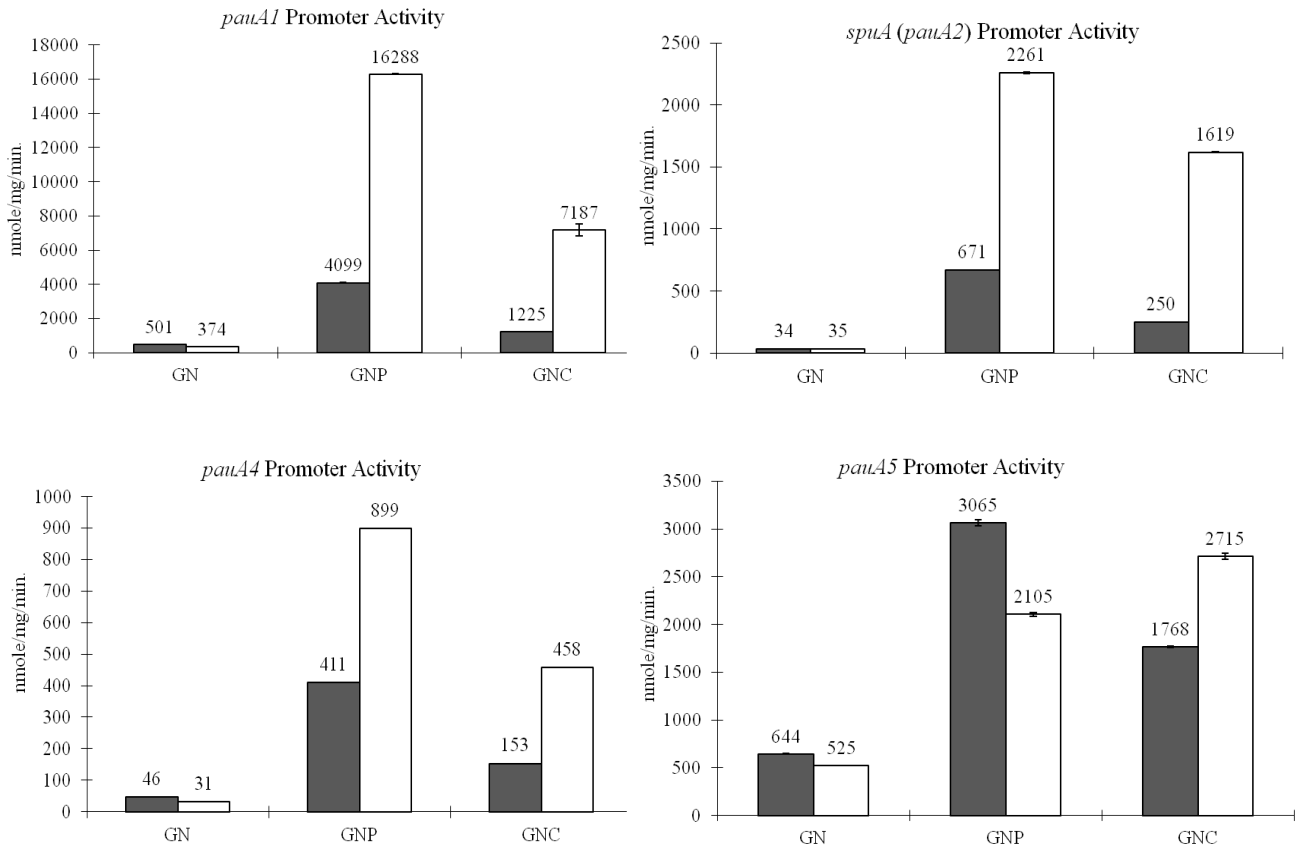

Figure 2.2. Expression profile of *pauA* promoters in *P. aeruginosa* PAO1.
Specific activities of β-galactosidase expressed from pGU102 for the *pauA1* promoter, pGU101 for the *pauA2* promoter, pHT2040 for the *pauA4* promoter, or pHT3356 for the *pauA5* promoter, were measured from the host strains wild type PAO1 (solid bars) and Δ*pauA1-6* mutant PAO5725 (empty bars) devoid of six glutamyl-polyamine synthetase genes. The cells were grown in glucose/ammonia (GN) minimal medium in the presence or absence of putrescine (P) and cadaverine (C).

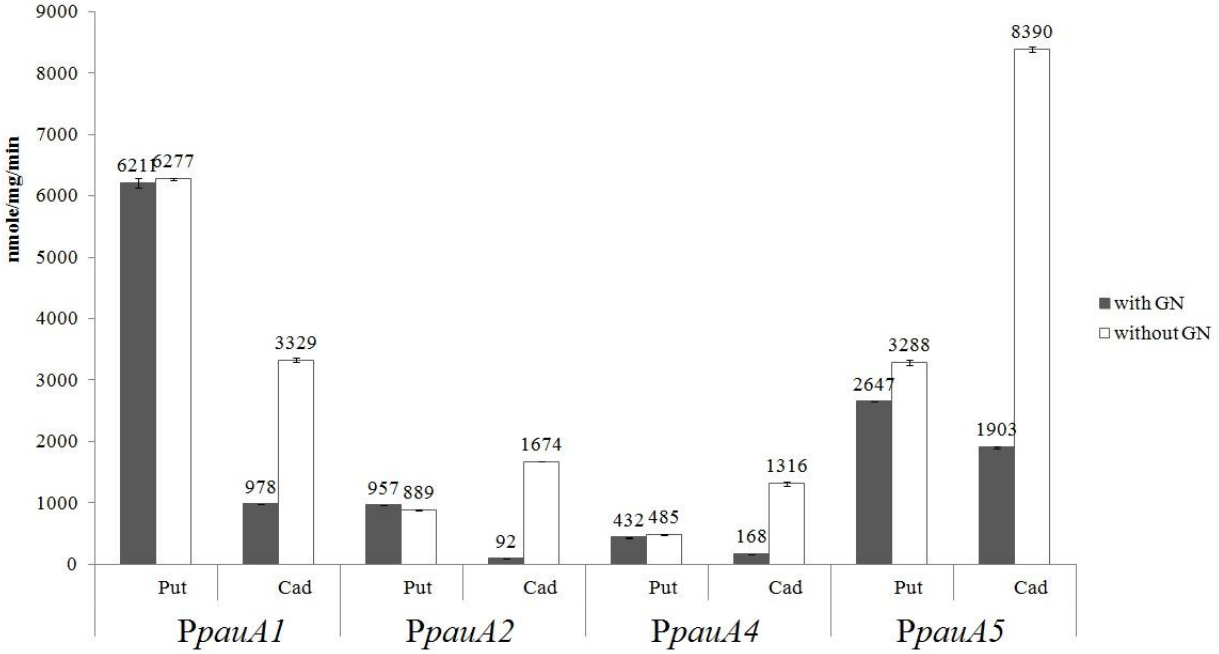

Figure 2.3. Glucose/ammonia effect on expression profile of *pauA* promoters

Specific activities of β-galactosidase expressed from *pauA* promoter-*lacZ* fusions (same constructs as in Figure 2.2) were measured from the host strain wild type PAO1. The cells were grown in minimal medium P in the presence of putrescine (P) or cadaverine (C). Empty bars represent expression levels when 10 mM putrescine or cadaverine was used as sole source of nutrient for growth. Solid bars show repression on cadaverine utilization by 10 mM glucose and 5 mM ammonia (GN) as background nutrients while PauA expression with putrescine remained unaffected.

Catabolite repression on cadaverine utilization. Cadaverine and putrescine are diamines of similar chemical structure and molecular weight. However, there was a longer lag phase (1 day) for growth on cadaverine compared to putrescine. Additionally, it was noted that even *pauA1*, *pauA4* and *pauA5* are essential for cadaverine utilization (Table 2.3), *pauA5* was only slightly induced (3 folds) and *pauA1* and *pauA4* were not induced by exogenous cadaverine in the DNA microarray data where the cells were grown in glutamate minimal media (Table 2.2). To understand the possible effect of glutamate and other nutrient sources on these expression patterns, *pauAs* expressions at the exponential growth phase were monitored in wild type PAO1 using the same promoter-*lacZ* fusions as in the previous section. As shown in Figure 2.3, while all *pauA* promoter activities with putrescine remained unaffected by background nutrients, expression levels with cadaverine were significantly reduced when glucose and ammonia were added into the media. Among these four *pauA* promoters, *pauA1* and *pauA5* promoters showed higher specific activities from the β-galactosidase assays with approximately 4 folds of difference when cadaverine was used as sole source of carbon and nitrogen. On the other hand, *pauA2* and *pauA4* promoters showed lower specific activities but with high fold changes (18 and 8 folds respectively) when compared to expression levels in glucose and ammonia minimal media. Similar phenomenon of repression was observed using glutamate minimal media (data not shown) suggesting strong catabolite repression for cadaverine utilization in this organism.

Regulation of the γ-glutamylation pathway. Based on studies in *E. coli*, γ-glutamylation pathway is negatively regulated by PuuR (44). The *puuR* counterpart in *P. aeruginosa*, PA5301, was replaced by a gentamicin resistance cassette in the mutant strain PAO5722. While there is no significant effect on growth in either LB or glutamate (data not shown), the four *pauA* promoters

(from previous sections) showed constitutive expression levels in PAO5722 (Figure 2.4). This strongly suggests a regulatory role of *PA5301* in the pathway thus I designated this gene as *p*oly*a*mine *u*tilization *r*egulator, *pauR*.

Binding of PauR on *pauA* promoters were successfully proven *in vitro*. PauR was purified to homogeneity as described in Methods and subjected to electrophoretic mobility shift experiments using the same regulatory regions of the four *pauA* genes as in expression measurements. As shown in Figure 2.5A, clear binding on *pauA1-2* (divergent promoters), *pauA4* and *pauA5* were detected with high affinity. However, when I tested for effect of polyamines by adding 1 mM of putrescine or cadaverine in the reaction, no apparent effect on the binding was detectable (Figures 2.5B and 2.5C). This intrigued me, so I performed PauR (24 KDa) glutaraldehyde crosslinking analysis to see changes in PauR in response to polyamines. As shown in Figure 2.5D, distinct PauR homo-dimmer formation was detected after crosslinking. When putrescine or cadaverine was added into the reaction, the monomeric and dimeric bands became diffused with a slight increase in molecular weight on SDS PAGE. This change is specific to putrescine and cadaverine but not to diaminopropane, a diamine with shorter methylene chain. As controls, polyamines were added after the crosslinking reaction and no change was detectable in these samples indicating that band diffusion was not due to the presence of polyamines during electrophoresis. This data suggests that PauR regulates the γ-glutamylation pathway through conformational changes in response to putrescine/cadaverine.

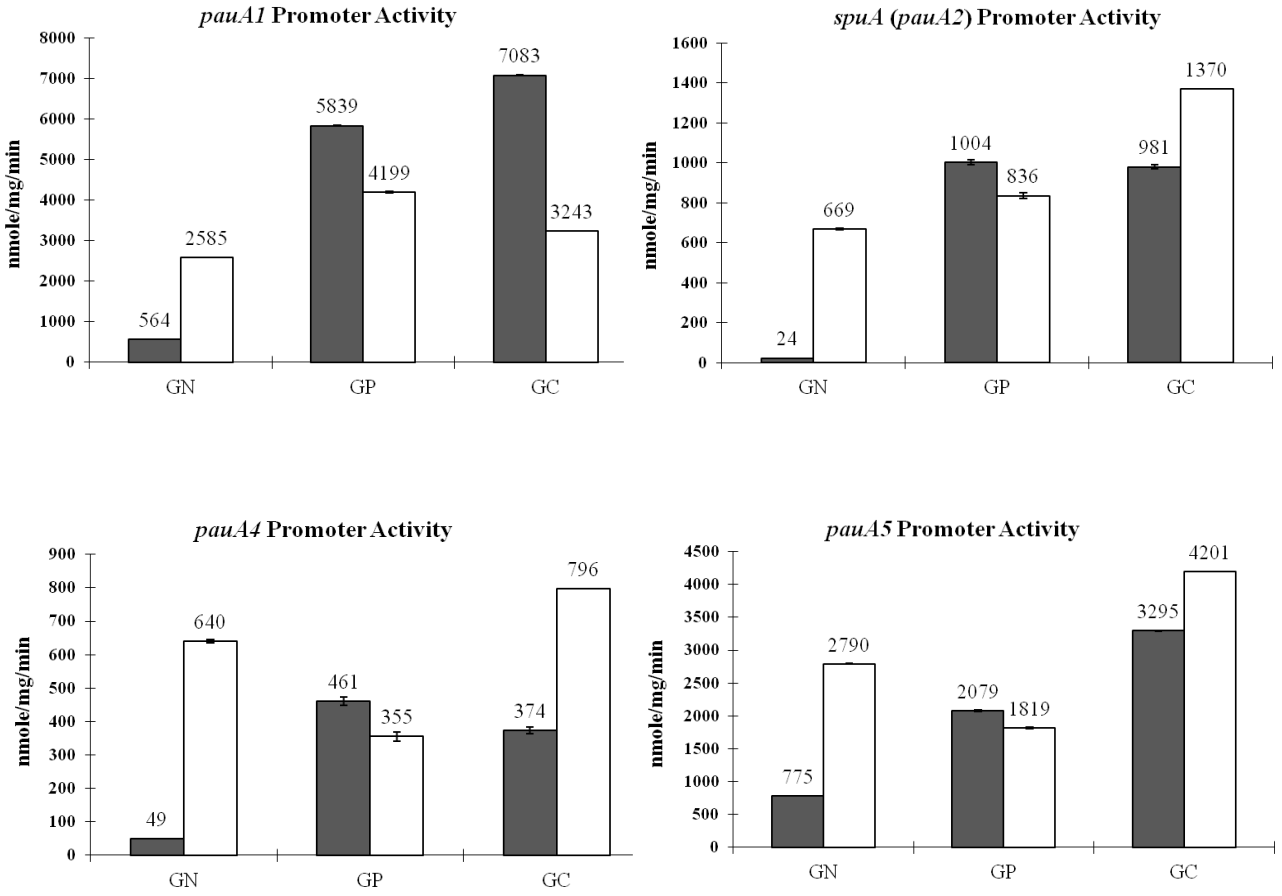

Figure 2.4. Effects of *pauR* on expression profiles of the *pauA* promoters

Specific activities of β-galactosidase expressed from *pauA* promoter-*lacZ* fusions (same constructs as in Figure 2.2) were measured from the host strains wild type PAO1 (solid bars) and *pauR* mutant PAO5722 (empty bars). The cells were grown in minimal medium P supplemented with glucose (G) as the sole source of carbon, and putrescine (P), cadaverine (C), or ammonia (N), as the sole source of nitrogen.

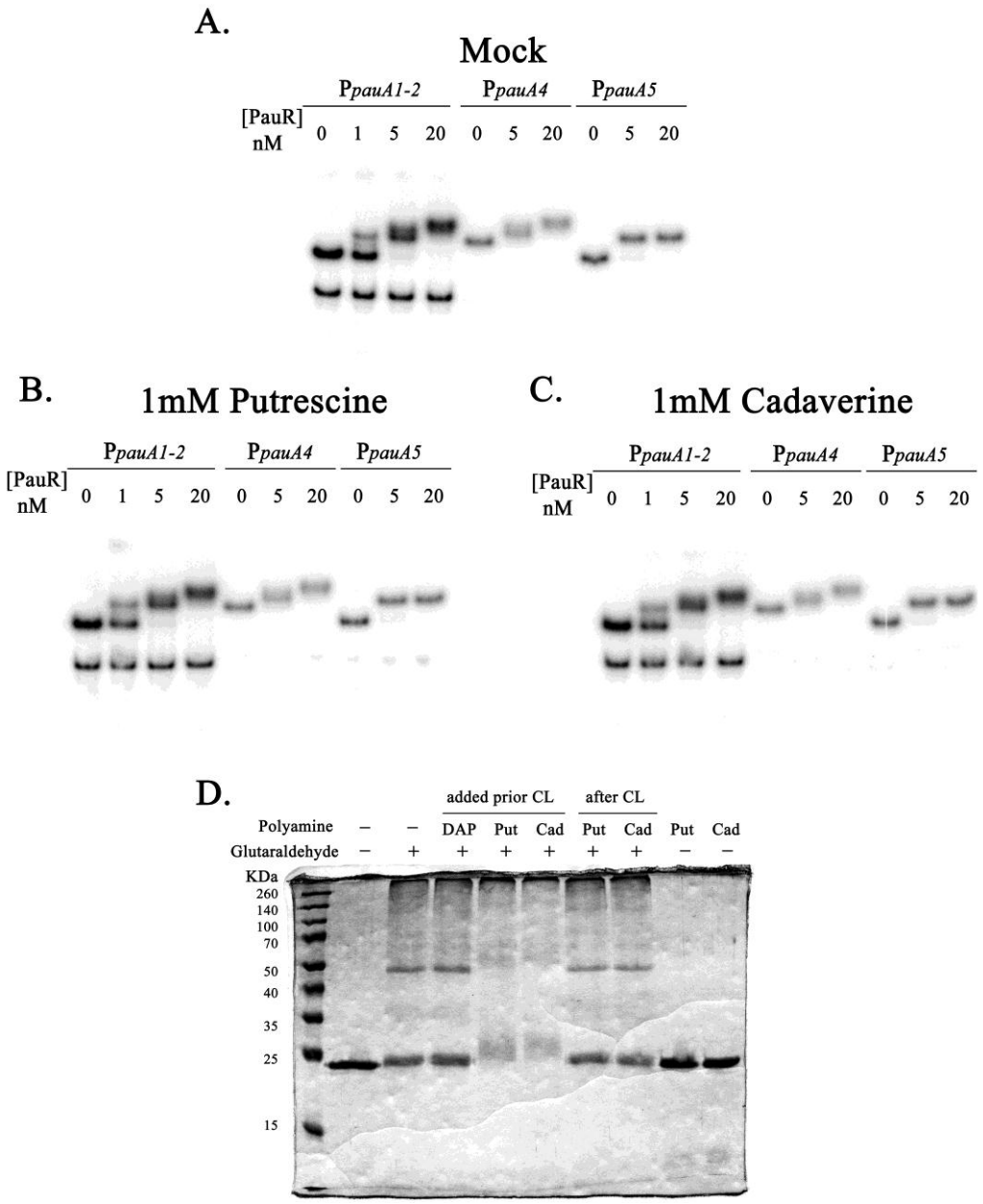

Figure 2.5. PauR binding on *pauA* promoters.

A, B and C. PauR binding on *pauA1-2, pauA4* and *pauA5* promoters. Interactions of purified His-PauR with radioactively labeled *pauA* promoter regions were demonstrated by the electrophoretic mobility shift assays. No evident effects of polyamines on PauR binding were detectable by adding 1mM of putrescine or cadaverine in the reaction mixture, gel, and running buffer (B and C). **D. PauR conformation change in response to putrescine and cadaverine.** PauR showed distinct dimmer formation after glutaraldehyde crosslinkage (lane 3). Putrescine and cadaverine, but not diaminopropane, seemed to induce conformational changes (lanes 4 to 6). As negative controls, polyamines were added after the termination of crosslinking reaction (lanes 7 and 8). No glutaraldehyde was added in the reactions of lanes 9 and 10.

Common enzymes for GABA and AMV catabolism. GABA and AMV are the corresponding downstream metabolites of putrescine and cadaverine in the γ-glutamylation pathway (Figure 2.1) (12, 13, 42). Based on previous reports of our laboratory, *gabDT* and *gabT2* code for two transaminases and a succinic semialdehyde dehydrogenase essential for the two-step degradation of GABA into succinate (13). Due to similarities in chemistry, overlaps in putrescine/cadaverine catabolic pathways may extend to GABA/AMV degradation. To prove this hypothesis, I tested the GABA catabolic genes for AMV. As expected, growth on AMV was completely depleted in *gabT/T2* double mutant PAO5704 suggesting essential roles of these transaminases in both GABA and AMV utilization (Table 2.4). In contrast, leaky growth of *gabD* mutant PAO5701 on AMV suggests alternative route for glutarate semialdehyde degradation.

Two promoter-*lacZ* fusions pMH105 (covering 718 base pairs upstream from the *gabDT* coding region) and pHT5313 (covering the entire intergenic region upstream the *gabT2* coding region) were transformed into wild type PAO1 to see how these candidate genes respond to exogenous GABA and AMV. While these loci were highly induced (6 folds) by exogenous GABA, expression patterns with exogenous AMV showed no response of the *gabDT* promoter, and only two-fold induction of the *gabT2* promoter was detected in tested conditions (Figures 2.6 and 2.7).

Table 2.4. Growth phenotypes of mutants with compromised GABA/AMV utilization.

Strain	Genotype	Nutrients*				
		Cad	AMV	Put	GABA	Glc
PAO1	**wild type**	++	++	+++	+++	+++
PAO5701	***gabD***	+	+	+	+	+++
PAO5703	***gabT***	+	+	+++	+++	+++
PAO5708	***gabT2***	++	++	+++	+++	+++
PAO5704	***gabT/T2***	-	-	+++	+	+++
H103	**wild type**	++	++	+++	+++	+++
PAO5723	***agtS***	++	-	+++	++	+++
PAO5724	***agtA***	+	-	+++	+	+++

* Cells were grown on MMP media agar plates with the indicated supplements as the sole source of carbon: Cad, cadaverine; AMV, δ-aminovalerate; Put, putrescine; GABA, γ-aminobutyrate; Glc, glucose. Ammonia was added as the sole source of nitrogen. Growth was recorded in 3 days at 37°C. +++, growth after 1 day; ++, growth after 2 days; +, growth after 3 days; -, no detectable growth after 3 days. The *gab* mutants were derived from PAO1, and the *agt* mutants were derived from H103.

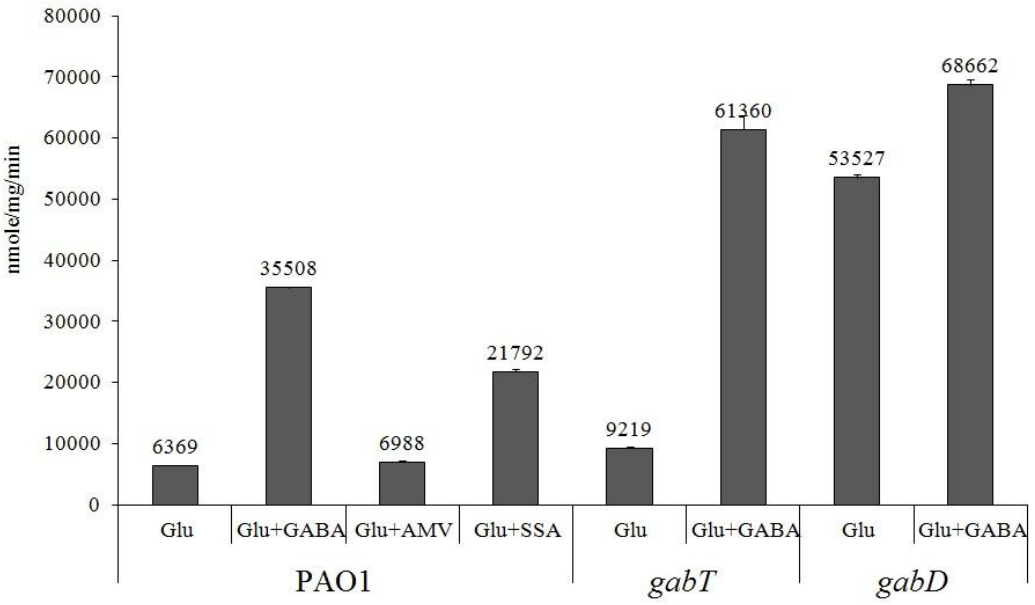

Figure 2.6. Expression profile of the *gabDT* promoter

Specific activities of β-galactosidase expressed from pMH105 for the *gabD* promoter covering 740 base pairs upstream from the coding region were measured from the host strains wild type PAO1, *gabT* mutant PAO5703 and *gabD* mutant PAO5701. Constitutive activation was detected in *gabD* mutant suggesting succinate semialdehyde as the inducer molecule of the operon. The cells were grown in glutamate (Glu) minimal medium in the presence or absence of γ-aminobutyrate (GABA), δ-aminovalerate (AMV), or succinate semialdehyde (SSA).

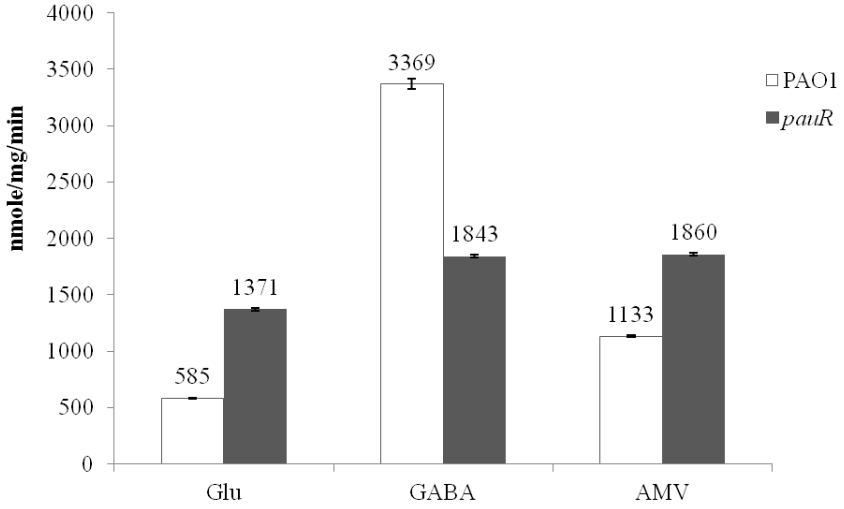

Figure 2.7. Expression profile of *gabT2* promoter.

Specific activities of β-galactosidase expressed from pHT5313 for the *gabT2* promoter were measured from the wild type strain PAO1. The cells were grown in glutamate (Glu) minimal medium in the presence or absence of γ-aminobutyrate (GABA), or δ-aminovalerate (AMV).

SSA might be the activating signal of the *gabD* promoter. Deamination of GABA and AMV by GabT/T2 leads to succinate semialdehyde (SSA) and glutarate semialdehyde (GSA), which are further degraded by GabD into succinate and glutarate, respectively (13, 83). To investigate the regulatory aspects of this catabolic pathway, the *gabDT* expression levels in response to GABA or its downstream metabolite SSA were measured using the promoter-*lacZ* fusion pMH105 in the wild type PAO1 strain. As shown in Figure 2.6, although *gabDT* was inducible by both compounds, induction by GABA (5.6 folds) was stronger than SSA (3.4 folds). This data suggested that SSA might be the inducer molecule of the *gabDT* operon. To test this hypothesis, the *gabD* promoter activities were measured in the *gabD* (PAO5701) and *gabT* (PAO5703) mutant strains using pMH105. Curiously, *gabDT* expression became constitutive in *gabD* but not in *gabT* (Figure 2.6). Since GabD is responsible for the degradation of SSA and GSA, the high expression levels detected in the *gabD* mutant could be caused by internal accumulation of either of these aldehyde compounds. However, since AMV has only marginal effects on the *gabD* promoter, its downstream metabolite GSA may not play as an activating signal in this pathway.

Mutational analysis of the *gabD* promoter region. A study using serial deletions on the 5' end of the *gabD* promoter indicated essential elements for full activation reside within -290 base pairs upstream from the transcriptional starting site (29). As shown in Figure 2.8A, this region contains putative σ^{-70} recognition sites -10 (5'-TAGGAT-3') and -35 (5'-TTGCCC-3') with 17 base pairs of distance between these two boxes. The +1 position was suggested based on published data from *P. putida* (83). At the transcription starting site, a 18 base-pairs-long sequence with dyad symmetry (5'-CGTTT**G**AGATTTCAAACG-3') was found highly

conserved among different *Pseudomonas* suggesting a regulatory role involved. Two *gabDT* promoter-*lacZ* (transcriptional) fusions, pHT0265-1 and pHT0265-2, differing in this palindrome were constructed in order to test for differences in response to GABA and AMV. As shown in Figure 2.8B, *gabDT* exhibit high background expression levels when this palindrome was removed from the promoter region. This suggests existence of a repressor protein for *gabDT* induction.

Effects of PauR on the *gabD* promoter. Direct interaction between GabD and its own promoter may serve as an alternative explanation of the high expression levels of pMH105 in the *gabD* mutant strain PAO5701. I tested for *in vitro* binding of purified His-GabD to the full length promoter region amplified from pMH105. No apparent interaction was detected using electrophoretic mobility shift experiments (data not shown). Therefore, the possibility of a direct regulation by GabD on its own promoter was excluded. On the other hand, the general repressor form the γ-glutamylation pathway, PauR, may extend its regulation to the utilization of these downstream metabolites. Indeed, higher levels of *gabDT* and *gabT2* expression were detected in the *pauR* mutant (Figure 2.7 and 2.8B). While the background levels of the *gabD* promoter in the *pauR* mutant were elevated to the induced level in PAO1 by GABA, the background expression levels of the *gabT2* promoter were lower than the induced level in PAO1 by GABA. Additionally, removal of the palindrome at the +1 site caused further induction of the *gabD* promoter in the *pauR* mutant strain (Figure 2.8). These data suggested a more complex regulatory system for GABA and AMV utilization other than a single repressor protein in this organism.

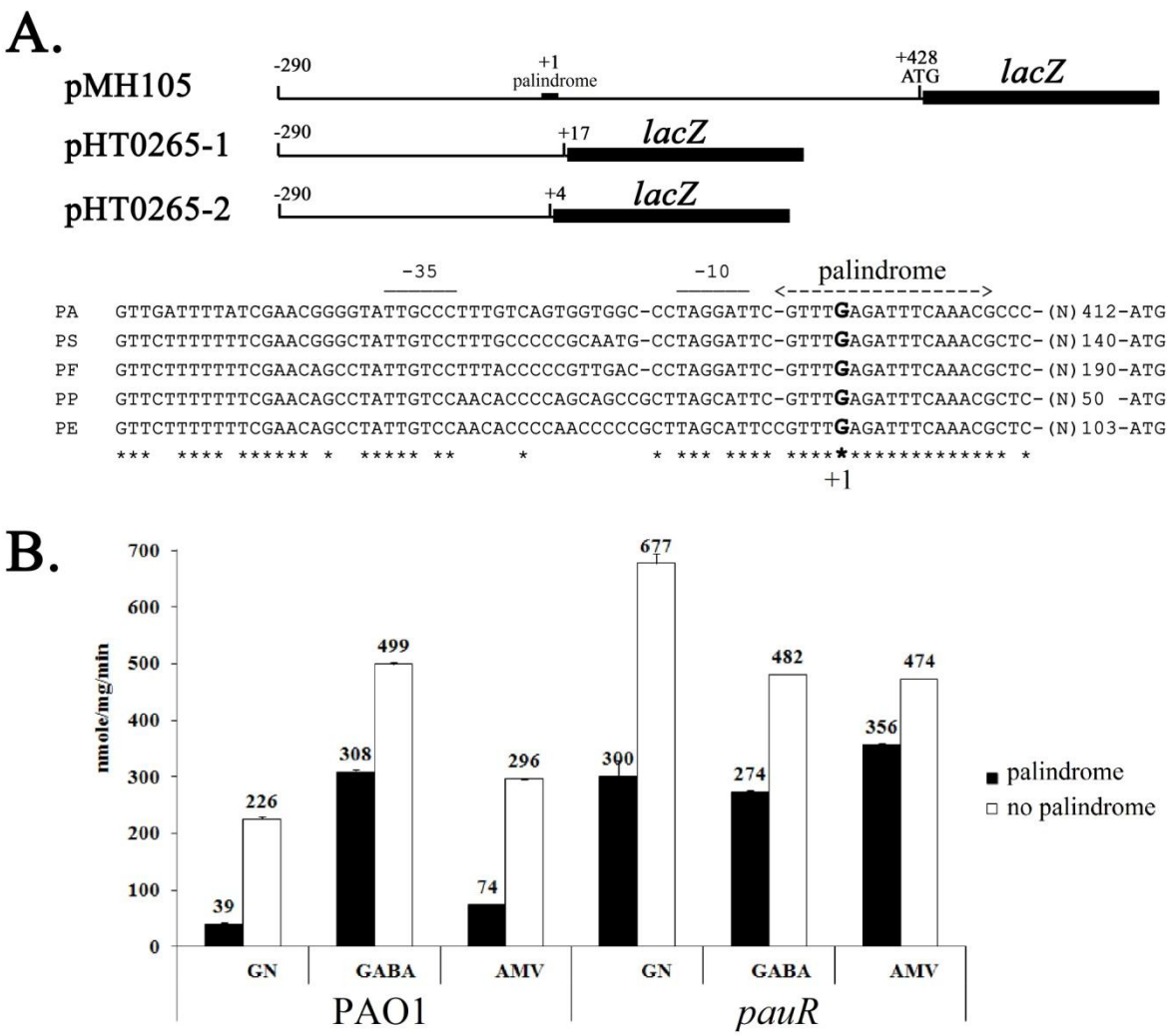

Figure 2.8. PauR regulation on the *gabD* promoter.

A. Schematic presentation of three *PgabD::lacZ* promoter fusions used in this study. Also shown is the sequence comparison of the *gabDT* promoters from indicated species of pseudomonads. Well-conserved palindromic sequence downstream the -10 and -35 motifs is marked with dashed arrow. The transcriptional starting site is in larger font. PA, *P. aeruginosa*; PS, *P. syringae*; PF, *P. fluorescens*; PP, *P.putida*; PE, *P. entomophila*.
B. Effects of the palindrome on the expression profiles of the *gabD* promoter. Expression of the *gabD* promoter-*lacZ* fusions pHT265-1 (with palindrome, solid bars) and pHT265-2 (no palindrome, empty bars) were monitored by measurements of β-galactosidase activity in the host strains wild type PAO1 and *pauR* mutant PAO5722. The cells were grown in glucose/ammonia (GN) minimal medium in the presence or absence of γ-aminobutyrate (GABA), or δ-aminovalerate (AMV).

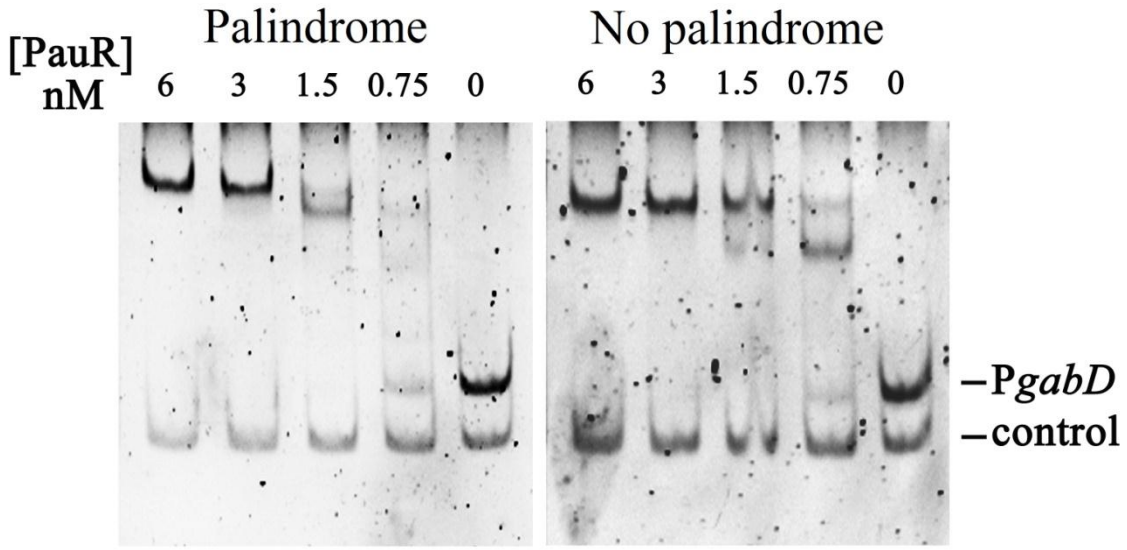

Figure 2.9. PauR binding on *gabDT* promoter.

PauR binding on *gabDT* regulatory region was demonstrated using electrophoretic mobility shift assays as described in Methods. Highest PauR concentration used was 6 nM followed by 2 fold serial dilutions. Promoter regions from pHT0265-1 and pHT0265-2 *gabD* promoter-*lacZ* fusions differing in the palindromic sequence at the +1 site (as shown in Figure 2.8A) were used as probes in the left and right panels, respectively. Free probes were in the last lane.

Binding of PauR on the *gabD* promoter. To further confirm the role of *pauR* as a repressor, binding of PauR to the *gabDT* promoter region was demonstrated by electrophoretic mobility shift experiments (Figure 2.9). No apparent difference in binding was detectable when the promoter lacking the highly conserved sequence as described above (Figure 2.8A) was used as probe, which indicated that this palindromic sequence is not a PauR operator site. Conformational change in PauR was also tested using the glutaraldehyde crosslinking experiment as described in previous section, and no change was detectable when GABA or AMV was added in the reaction (data not shown). These data support PauR as a repressor protein on *gabD* and *gabT2* promoter.

These data confirmed that like putrescine/cadaverine, significant overlaps were found for GABA/AMV catabolism. The role of PauR was expanded to a general regulatory protein of the pathways from putrescine/cadaverine glutamylation to GABA/AMV degradation. However, possibilities of additional regulatory system(s) are not excluded since interacting mechanisms on the palindromic sequence of the *gabD* promoter still await identification.

Table 2.5. Expression profiling of the *agt* locus by DNA microarray

PA ID[a]	Gene Name	Signal Value[b]							Descriptions
		Glu	Glu Arg	Glu Put	Glu GABA	Glu Lys	Glu Cad	Glu AMV	
PA0600	***agtS***	169	78 (0)	157 (1)	101 (1)	156 (1)	57 (0)	103 (1)	two-component sensor
PA0601	***agtR***	266	225 (1)	326 (1)	220 (1)	262 (1)	305 (1)	262 (1)	two-component response regulator
PA0602		158	174 (1)	100 (1)	90 (1)	268 (2)	300 (2)	255 (2)	putative periplasmic binding protein
PA0603	***agtA***	432	497 (1)	1007 (2)	**8165**	1904 (4)	4269 (10)	**7581 (18)**	ATP-binding component of ABC transporter
PA0604	***agtB***	341	481 (1)	514 (2)	**4520**	1102 (3)	1998 (6)	**3127 (9)**	binding protein of ABC transporter
PA0605	***agtC***	201	21 (0)	340 (2)	**4767**	693 (3)	2118 (11)	**2259 (11)**	permease of ABC transporter
PA0606	***agtD***	131	230 (2)	224 (2)	**3136**	448 (3)	927 (7)	**1341 (10)**	permease of ABC transporter

[a] The PA ID numbers were taken from the PAO1 genome annotation project (www.pseudomonas.com).
[b] GeneChip raw data are mean values from two independent sets of cultures. Cells were grown in minimal medium P supplemented with 20 mM of the following supplements as indicated: Glu, glutamate; Arg, L-arginine; Put, putrescine; GABA, γ-aminobutyrate; Lys, L-lysine; Cad, cadaverine; AMV, δ-aminovalerate. Fold changes are in parenthesis.

Different responses to endogenous and exogenous GABA and AMV. Based on DNA microarray analysis shown in Table 2.5, *PA0603-PA0605* were picked up among the entire transcriptome as the only locus inducible specifically by exogenous GABA (15~24 folds) but not by endogenous GABA produced from putrescine degradation (13). Following the logic that genes for GABA utilization may have relaxed specificity with AMV, I tested the importance of this transport system for both GABA and AMV utilization. As revealed from genetics studies, growth on GABA and AMV were severely affected in *PA0603* (ATPase) mutant strain PAO5724 (Table 2.4). While this transport system seemed essential for AMV uptake, growth on GABA was reduced but not completely depleted in PAO5724. This implies alternative uptake system(s) for GABA in this organism. Based on this information, *PA0603~PA0605* were designated as AMV/GABA transport genes *agtABCD*. The gene organization with predicted functions was shown in Figure 2.10A.

Upstream of the *agtABCD* operon, the PA0602 gene encodes another putative periplasmic solute-binding protein exhibiting 79% sequence similarity to AgtB. Because PA0602 is not present in other *Pseudomonas*, and it was not inducible by GABA based on the DNA microarray analysis, it was excluded from the *agtABCD* operon.

Expression of the *agtABCD* operon responds exclusively to exogenous GABA/AMV. To verify my DNA microarray data, I used PAO1 harboring pHT0603 (*agtA*::*lacZ*) to test for responses of the Agt transport system to exogenous GABA/AMV. As shown in Figure 2.10B, the *agtA* promoter is distinctly induced by exogenous GABA (20 folds) and AMV (27 folds) when compared to the corresponding upstream precursors putrescine (2 folds) and cadaverine (3 folds).

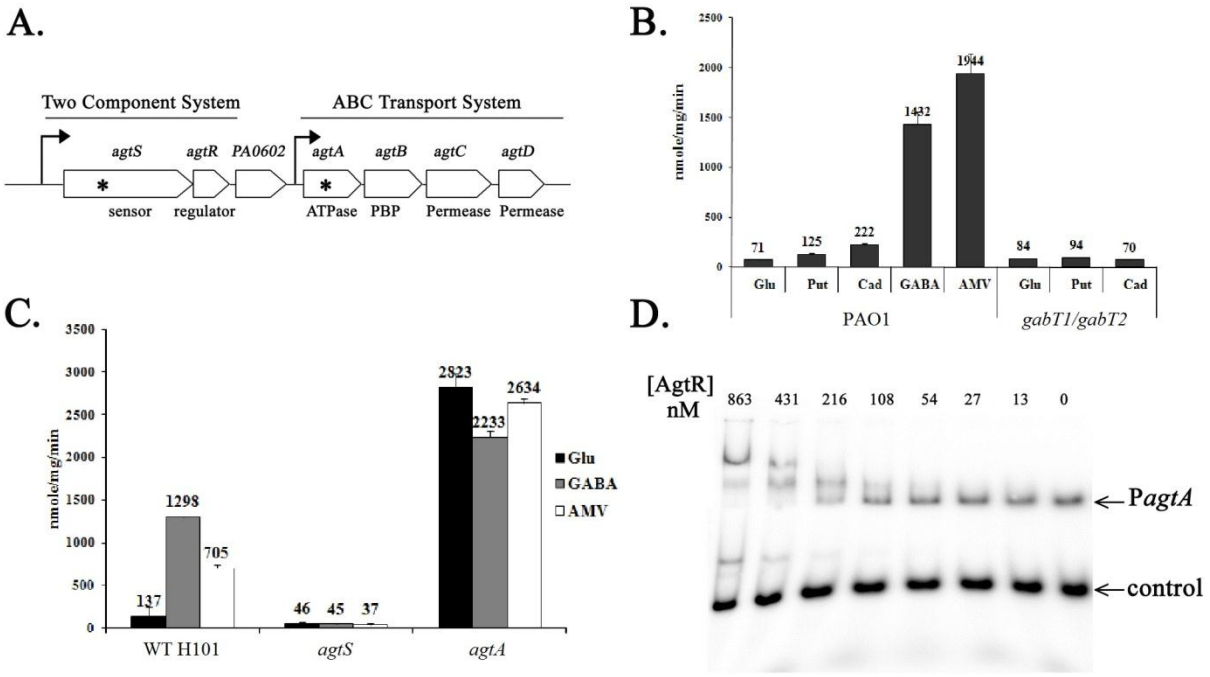

Figure 2.10. The Agt transport system.

A. Schematic presentation of the gene organization of the *agt* locus. The *agtSR* two-component system and the *agtABCD* transport system genes for GABA and AMV uptake are highly conserved among *Pseudomonas*. PA0602 located between these two operons is unique to *P. aeruginosa*. Insertion points of *lux* mutants analyzed in this study were marked with a star: *lux* gene was inserted with reverted orientation at the nucleotides 1091 of the *agtS* coding region and with transcriptional orientation at the nucleotide 288 of the *agtA* coding region. **B. Agt transport system responses exclusively to exogenous GABA and AMV.** Specific activities of β-galactosidase expressed from pHT0603 for the *agtA* promoter were measured from the host strains wild type PAO1 and *gabT1/T2* double mutant (PAO5704) defected in GABA/AMV degradation. The cells were grown in glutamate (Glu) minimal medium in the presence or absence of putrescine (Put), cadaverine (Cad), GABA or AMV. **C and D. AgtABCD transport system is regulated by AgtSR two component system.** Specific activities of β-galactosidase expressed from pHT0603 for the *agtA* promoter were measured from the host strains *agtS* mutant (PAO5723), *agtA* mutant (PAO5724), and the parental H103. Binding of AgtR on the *agtA* promoter was demonstrated using electrophoretic mobility shift assays as described in Methods. AgtR concentrations used started at 863 nM followed by 2-fold dilutions.

Furthermore, I used the *gabT1/T2* double mutant PAO5704 defective in the transaminases essential for the first step of GABA/AMV catabolism to accumulate endogenous GABA and AMV from putrescine and cadaverine degradation. This data showed no evidence of *agtA* induction in PAO5704 by endogenous GABA/AMV, confirming exclusive response of this transport system to exogenous GABA/AMV (Figure 2.10B).

The Agt transport system is under positive regulation of the AgtSR two-component system. A two-component system *PA0600-PA0601* located just upstream the AgtABCD transport system was found as a candidate regulatory system for GABA/AMV uptake. As revealed from genetics studies, growth on AMV was completely depleted in *PA0600* (sensor) mutant strain PAO5723 (Table 2.4), but growth of this mutant on GABA was leaky because of alternative uptake system(s) for GABA (Table 2.4). Therefore, I designated *PA0600~PA0601* as *agtSR* two-component system.

AgtSR regulation on the *agtABCD* operon was further studied by measuring the *agtA* promoter activity in the *agtS* mutant strain PAO5723 and its parental strain H103 harboring pHT0603. As shown in Figure 2.10C, disruption of the sensor AgtS seemed detrimental for the expression of the downstream ABC transport system in PAO5723. On the other hand, in an electrophoretic mobility shift assay, *agtA* promoter (corresponding to pHT0603) interacted with purified His-AgtR, and the formation of protein-DNA complexes was seen (Figure 2.10D).

As shown in previous sections, growth on GABA and AMV is compromised in PAO5724 with a defected ATPase, AgtA (Table 2.4). Curiously, when measuring the expression levels of

pHT0603 in PAO5724, constitutive promoter activation of the *agtABCD* transport system was found in the *agtA* mutant strain (Figure 2.10C). This unusual pattern of promoter activities independent of the presence of exogenous GABA/AMV suggests that the on/off switch of the AgtRS system might be coupled with the AgtABCD transport system on the membrane.

Effect of Agt transport system on GabDT expression. I further studied the role of Agt transport system in GABA/AMV utilization by measuring changes in catabolic enzymes expression levels in defected uptake strain. The *gabDT* promoter-*lacZ* fusion pHT0265-1 was transformed into PAO5723 *agtS* mutant to test for induction by exogenous and endogenous GABA and AMV. As shown in Figure 2.11, induction by exogenous GABA and AMV were significantly reduced with defected transport system. In PAO5723 *agtS* mutant strain, induction by GABA showed 3 folds reduction and only basal expression level was detected for AMV. This data strengthened the contribution of the Agt transport system in GABA and AMV utilization.

Endogenous GABA and AMV were produced as secondary metabolites from putrescine and cadaverine degradation, respectively. In the same set of experiment, induction levels by endogenous GABA and AMV sustained in *agtS* mutant strain suggesting GABA/AMV should enter the cell to trigger *gabDT* expression (Figure 2.11). On the other hand, since there may be more than one regulatory systems (other than PauR) involved in GABA/AMV catabolism, AgtR was subjected to gel electrophoretic mobility shift experiments as candidate positive regulator on *gabDT*. However, no AgtR binding was detectable on *gabDT* promoter region (Figure 2.12). Therefore I concluded that AgtSR senses and responds to exogenous GABA/AMV for uptake by

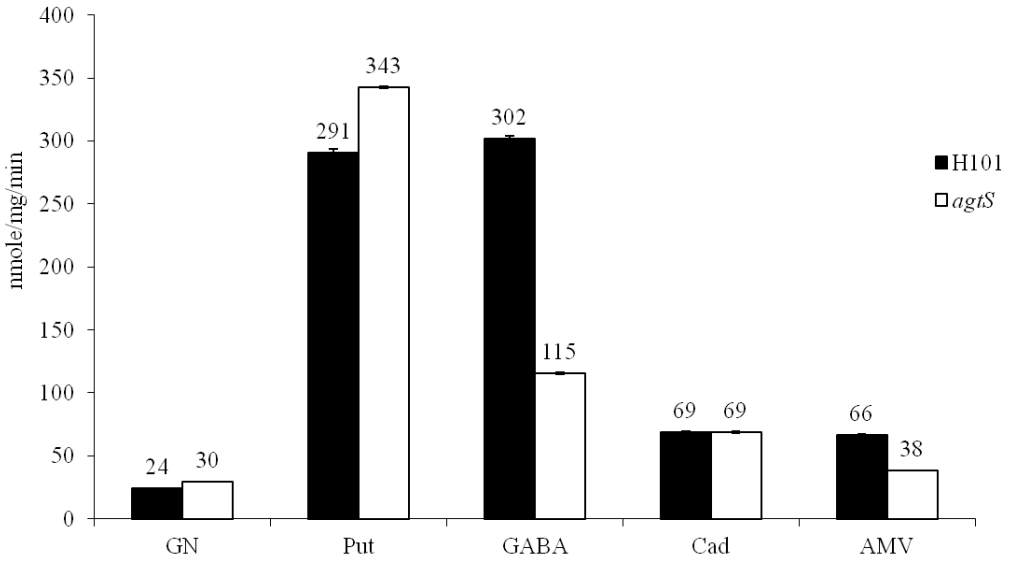

Figure 2.11. GabDT expression in Agt transport system deficient strain.

Specific activities of β-galactosidase expressed from pHT0265-1 for the *gabD* promoter were measured from the host strains wild type H103 and *agtS* mutant (PAO5723) devoid of the sensor component of the *agt* two-component system. The cells were grown in glucose/ammonia (GN) minimal medium in the presence or absence of putrescine (Put), cadaverine (Cad), GABA or AMV.

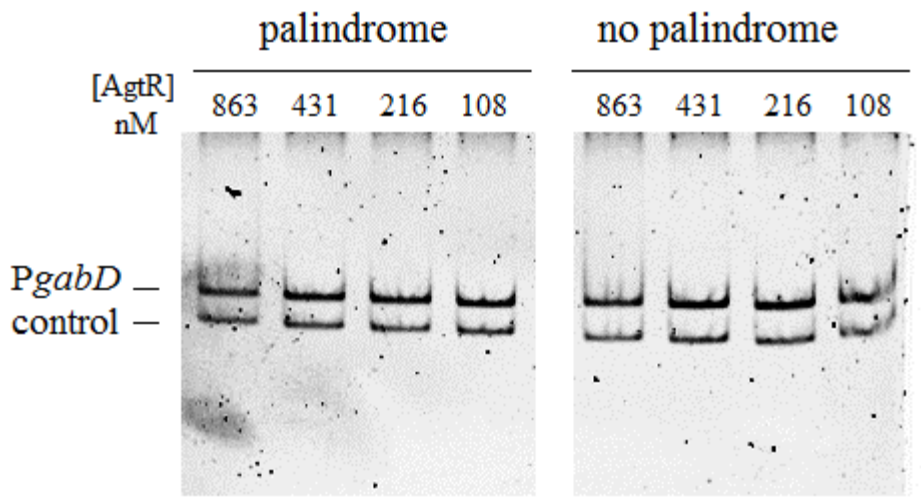

Figure 2.12. AgtR binding on *gabD* promoters was not detected

Interactions of purified His-AgtR with *gabD* promoter regions were tested using the electrophoretic mobility shift assays. Two DNA probes covering the *gabD* regulatory regions with and without the palindromic sequence (corresponding to pHT0265-1 and pHT0265-2, respectively) were used in the experiments in the presence of a non-specific DNA fragment as negative control. Nucleoprotein complex was not detected.

the AgtABCD transport system, but may not be involved in the regulation on *gabDT* operon for GABA/AMV catabolism.

In this report I performed a detailed study of putrescine and cadaverine catabolism via the γ-glutamylation pathway in *P. aeruginosa*. Different combinations of PauA(s) were shown essential for putrescine and cadaverine glutamylation revealing functional redundancy of these enzymes and the importance of the γ-glutamylation pathway in this organism. PauR was identified as a general repressor of this pathway controlling putrescine/cadaverine glutamylation and GABA/AMV degradation. While putrescine and cadaverine seemed to be the inducer molecules of PauA activity, GABA degradation was shown under an unusual regulatory circuit in which an intermediate compound, SSA, served as the activating signal molecule. Additionally, different from putrescine, cadaverine utilization was repressed by the presence of glucose and glutamate as reflected from the expression profiles of the catabolic genes in response to cadaverine. This also implied additional level of repression on lysine utilization since accumulation of polyamines has been reported to inhibit lysine decarboxylase enzyme activity (37, 101).

CHAPTER THREE

CATABOLITE REPRESSION BY CBRA-CBRB TWO-COMPONENT SYSTEM IN *PSEUDOMONAS AERUGINOSA* PAO1

This work was partially published by Laetitia Abdou, Han-Ting Chou, Dieter Haas and Chung-Dar Lu in "Promoter Recognition and Activation by the Global Response Regulator CbrB in *Pseudomonas aeruginosa*". J. Bacteriol. 2011 Jun; 193(11):2784-92.

3.1 INTRODUCTION

The CbrA-CbrB two-component system was first identified to be involved in the global metabolic regulation of carbon and nitrogen utilization in *P. aeruginosa* (54, 74). While the inducer signals for the membrane bound CbrA sensor are unknown, CbrB is a σ^{-54} RNA polymerase dependent transcriptional activator of the NtrC family of response regulators (74). The CbrB/CrcZ/Crc pathway to control CCR through Crc was proposed by the laboratory of Dr. Haas in 2009 (94). The translational regulator Crc binds on mRNAs of uptake and catabolic genes with unpaired A-rich sequences, also termed CA motives (consensus $AA^{c}/_{u}AA^{c}/_{u}AA$), near their ribosome binding sites (66, 67, 94). CCR by Crc has been extensively studied in *P. putida* and *P. aeruginosa* (for review, please refer to Rojo 2010) (86). In the CbrAB/CrcZ/Crc model, CbrAB regulates positively the expression of the 407 nucleotide-long small-RNA CrcZ which contains five CA motives with high affinity for Crc to compete with mRNAs in binding (94). Remarkably, using succinate, glucose and mannitol as different carbon sources, CbrA/CbrB gradually releases catabolite repression by adjusting CrcZ expression level to antagonize Crc to different extends for each nutrient (94).

Other than the CbrAB/CrcZ/Crc pathway, the two-component system CbrAB has other important targets where Crc is not involved. Direct regulation of CbrAB has been reported for the *lipA* (lipase) gene in *P. alcaligenes* (41), and the *hutU* (histidine utilization) operon in *P. aeruginosa* and *P. fluorescens* (54). CbrAB system may play important role in arginine utilization. Promoter scan (PromScan @ Queen's) on *aotJ-argR* (arginine/lysine utilization) regulatory region found conserved -24/-12 boxes $ATGGCTTGN_4TTGCT$ that are typical of σ^{-54}

dependent promoters (consensus TGGCACGN4TTGC$^{T}/_{A}$ scored with 85 out of 100). This sequence motif is located at 273 nucleotides upstream from the start codon of the *aotJ-argR* operon. Direct binding of CbrB to the *aot* and *hutU* promoters was also proven by electrophoretic mobility shift experiments (Wei Li; personal communication). These evidences suggest direct regulation of CbrAB on the *aot* operon independently from Crc.

As mentioned in General Introduction, CbrAB and NtrBC exhibit similar protein sequences and structures and were suggested to be functionally overlap. Suppressor mutants from a *cbrAB* deficient strain PAO5100 grown on arginine can be grouped into two types: mutants with constitutive Ntr system activation (represented by Arg18 with single mutation Asp227Ala on NtrB) and mutants with unknown mechanism to overcome the severe metabolic imbalance (represented by Arg34) (54). Ntr activation restores the ability to use histidine in Arg18, but still handicapped in the utilization of TCA cycle intermediates and most carbon-only sources. In contrast, Arg34 shows almost identical growth phenotype to the wild-type strain PAO1, except in histidine, ornithine and hydroxyl-L-proline utilization (54). Interestingly, the ratio of Arg34 (arginine positive, histidine negative, glucose positive) to Arg18 (arginine positive, histidine positive, glucose negative) is high (85:5). It is possible that the ability of Arg34 to grow on a wide range of compounds is due to mutations on CrcZ to release CCR by Crc.

In this study, direct interaction of CbrB on the *crcZ* promoter was shown by electrophoretic mobility shift experiments. Two putative upstream activating sequences (UASs) on crcZ regulatory region were proven to contribute in CbrB recognition. Participation of

CbrAB, Crc and NtrBC systems were analyzed for arginine, lysine, putrescine and cadaverine catabolism using genetics approach.

Table 3.1. Strains and plasmids

Strain or plasmid	Genotype or description [a]	Source
***E. coli* strains**		
DH5α	F$^-$Φ80d*lac* ΔM15 Δ(*lacZYA-argF*)U169 *deoR recA1 endA1 hsdR17* (r_K^- m_K^-) *supE44* λ^- *thi-1gyrA96 relA*	Bethesda Research Laboratories
TOP10	F- *mcr*A Δ(*mrr-hsd*RMS-*mcr*BC) Φ80*lac*ZΔM15 D*lac*X74 *rec*A1 *ara*D139 Δ(*ara-leu*)7697 *gal*U *gal*K *rps*L (Sm^r) *end*A1 *nup*G	Invitrogen
***P. aeruginosa* strains**		
PAO1	Wild type	(27)
PAO5100	Δ *cbrAB::Gm^r*	(59)
PAO4727	Δ *cbrAB::Gm^r*; Δ *crc*	
PAO5126	Δ *cbrAB::Gm^r*; Δ*ntrBC::Tc^r*	(54)
Plasmids		
pCBRB	Amp^r pUCP18 derivative carrying the wild type *cbrB* fragment of PAO1	This study
pCBRB*	Amp^r pUCP18 derivative carrying K98Q *cbrB*	This study
pME9834	*crcZ-lacZ* with 116-bp promoter region; Tc^r	(1)
pME9842	*crcZ-lacZ* with 138-bp promoter region; Tc^r	(1)
pME9843	*crcZ-lacZ* with 161-bp promoter region and mutated motif 2 (Mut2) in the UAS; Tc^r	(1)
pSU300	pBAD/HisB carrying truncated *cbrB*	This study

[a] Gm^r, gentamicin resistance; Tc^r, tetracycline resistance; Amp^r, ampicillin resistance.

3.2 MATERIALS AND METHODS

Bacterial strains, plasmids, media, and growth conditions. Bacterial strains and plasmids used in this study are listed in Table 3.1. *P. aeruginosa* strains were grown in Luria-Bertani (LB) and 2X tryptone-yeast extract media (2YT) supplemented with or without antibiotics at conventional concentrations (104). Minimal medium P (27) containing the indicated carbon sources at 20 mM and nitrogen sources at 5 mM was used for the growth of *P. aeruginosa*.

Plasmid construction. Full length CbrB was amplified by PCR from the genomic DNA of *P. aeruginosa* PAO1 and subcloned into pUCP18 *EcoRI* and *HindIII* sites to construct pCBRB using the following primers: CbrB_F, 5'-GCT GAA TTC GGC ACA TAT TCT GAT CGT CGA AGA CG-3'and CbrB_R, 5'- GCT AAG CTT CTG TTA CGC GGT ACG TCC GCG GTA AC-3'. The K98Q mutation on CbrB was introduced into pCBRB to construct pCBRB* using the following primers: CbrB*_F, 5'-GTG GAC TAC ATC GCC CAG CCT TTC GAC CAC G-3'and CbrB*_R, 5'-CGT GGT CGA AAG GCT GGG CGA TGT AGT CCA C-3'.

Purification of His-CbrB. His-tagged truncated 'CbrB (His-CbrB) protein was expressed from pSU300 in *E. coli* TOP10 (Invitrogen). The resulting recombinant 'CbrB protein lacks the 13 *N*-terminal amino acid residues of the native CbrB protein and carries an *N*-terminal His_6 tag. After induction by 0.2 % (w/v) arabinose for 3 h, cells were collected by centrifugation and ruptured by passing through a French pressure cell at 8,500 lb/in^2. Cell debris was removed by centrifugation at 25,000×g for 30 min, and the resulting cell-free crude extract was loaded onto a HisTrap HP column (GE Healthcare) in an AKTA FPLC system, following a purification

protocol suggested by the manufacturer. The recombinant His-CbrB protein was eluted by 175 mM imidazole. The purity of His-CbrB in the collected fractions was verified by SDS-PAGE. Protein concentration was determined by the Bradford method with bovine serum albumin as standard.

Electrophoretic mobility shift assays. DNA fragments covering wild-type and mutated regulatory regions were PCR-amplified from the genomic DNA and plasmids as described in Abdou *et al* (2011). DNA probes were prepared by labeling them with [γ-^{32}P]ATP and T4 polynucleotide kinase (34). Radioactively labeled DNA probes were allowed to interact with different concentrations of purified His-CbrB in a 20-µl reaction mixture containing 50 mM Tris-HCl (pH 7.5), 50 mM KCl, 1 mM EDTA, 5 % (v/v) glycerol, 150 µg/ml acetylated bovine serum albumin, and 40 ng cold pUC18 vector as non-specific DNA. The reaction mixtures were incubated at room temperature for 30 min before being applied to a 4 % polyacrylamide gel (bis-acrylamide ratio 1:60) in 0.5× TBE buffer pH 7.5. The gel was dried, auto-radiographed by exposure to a phosphorimager plate, scanned using FLA-7000 version 1.1, and analyzed by Multi Gauge version 3.0 (FUJIFILM).

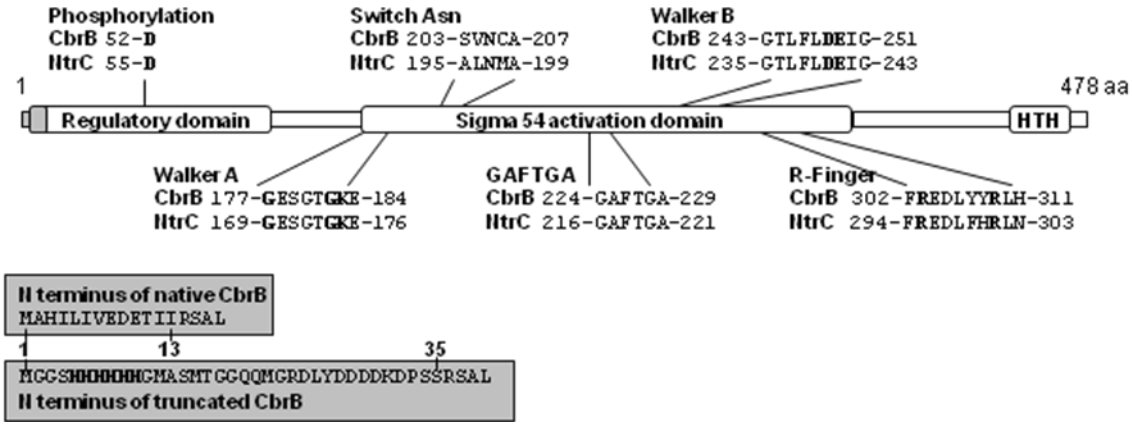

Figure 3.1. Domains of the CbrB protein.

Domain map with conserved sequences in the CbrB and NtrC proteins of *P. aeruginosa* PAO1, based on the domain map of *Salmonella enterica* NtrC (22). CbrB is predicted to contain an *N*-terminal regulatory domain, a central σ^{54} activation domain and a *C*-terminal DNA-binding domain with a helix-turn-helix motif (HTH). The conserved phosphorylation site in the regulatory domain is presumed to enable activation of CbrB by the sensor kinase CbrA (5, 30). Grey boxes below show that the 13 *N*-terminal amino acid residues of the native CbrB protein are replaced by 35 different amino acids including a his_6 tag in the truncated CbrB protein.

3.3 RESULTS AND DISCUSSION

Direct evidence of CbrB regulation on *crcZ* promoter. The regulator CbrB shows similar protein structure to the well known bacterial enhancer binding protein NtrC with 43% identity and 62% similarity in amino acid sequences. As shown in Figure 3.1, this family of regulatory protein exhibits an N-terminal regulatory/receiver domain with a conserved aspartate residue (D52 of CbrB) to be the cognate sensor phosphorylated by CbrA, a central domain to interact with σ^{-54} RNA polymerase, and a C-terminal helix-turn-helix DNA binding domain. It had been reported inhibitory effect of the regulatory domain on the binding activity of some members of the NtrC family and truncation of the N terminus can enhance this activity (25, 77).

Here I study the direct regulation of CbrB on CrcZ promoter as suggested in CbrAB/CrcZ/Crc model. Full length and truncated His-tagged CbrB protein were over-expressed and purified from *E. coli* and subjected to electrophoretic mobility shift experiments as described in methods. In general, optimal conditions for *in vitro* binding activity of CbrB was very hard to find and only the truncated CbrB lacking the 13 N-terminal amino acid residues was able to show binding on *crcZ* promoter in tested conditions (Figure 3.2, full length CbrB was not shown).

The *crcZ* promoter contains conserved -24/-12 boxes typical of σ^{-54} promoters (Figure 3.2). The region -151 to -125 from the transcriptional starting site of *crcZ* contains palindromic sequences (TGTTAC and GTAACA separated by 14 nucleotides) which may function as UAS elements to be recognized by CbrB. Therefore, I PCR amplified these regions containing wild type as well as mutated sequences of these elements using constructs provided by Dr Haas as

template (1), and subjected to electrophoretic mobility shift experiments. As shown in Figure 3.2, deletion of both elements of the palindromic UAS (ΔM1,2) abolished CbrB binding, whereas either deletion of the upstream element (ΔM1) or mutation of the downstream element (Mut2) resulted in diminished CbrB binding. These data indicated that a single element in the UAS was sufficient for CbrB binding. However, both elements might be needed for strong binding and full activation of the *crcZ* promoter.

CbrB interaction on *lipA* promoter. In *P. alcaligenes*, the expression of the *lipA* gene coding for secreted lipase is positively controlled by RpoN and by the LipQ/LipR two-component system, the counterpart of CbrA/CbrB in *P. aeruginosa* (41). A UAS has been proposed as a LipR (CbrB) binding site At -130 to -112 of the *lipA* promoter (16). Here I investigated the molecular details of the *lipA* promoter and its putative UAS in *P. aeruginosa*. In an electrophoretic mobility shift assay, the purified His-CbrB protein interacted with the wild-type *lipA* promoter region at the highest protein concentration used, but caused no band shift of a promoter fragment lacking the UAS (Figure 3.3). The relatively low affinity of His-CbrB for the UAS in the *lipA* promoter reflects a suboptimal recognition sequence, by comparison with the UAS in the *crcZ* promoter.

A.

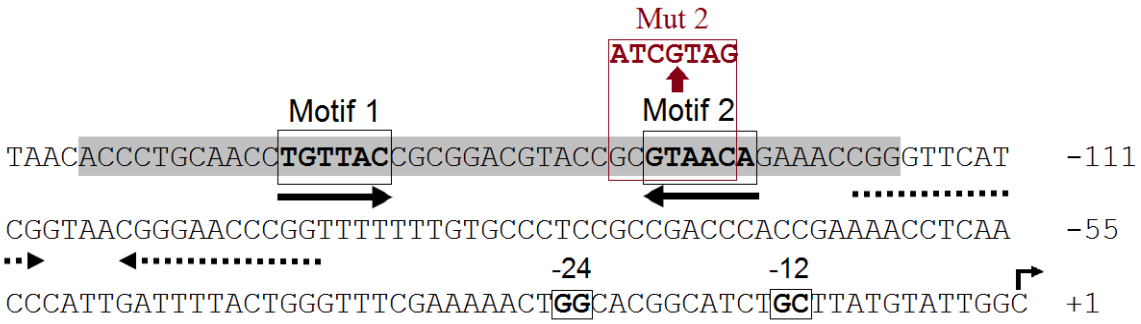

B.

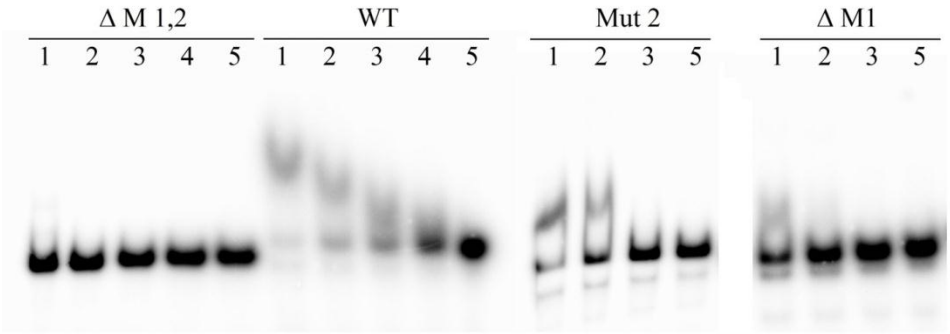

Figure 3.2. His-CbrB binds to the UAS of the *crcZ* promoter *in vitro*

A. Sequence of the *crcZ* promoter region and recognition sites for CbrB. In the nucleotide sequence of the *crcZ* promoter region, the 45-bp UAS region is highlighted in grey. The *cbrB* stop codon, the motif 1 and motif 2 of the UAS, and the -24 and -12 elements of the σ^{54} promoter are all shown in boxes. Inverted arrows show a palindromic sequence in the UAS region; arrows with solid lines below boldface nucleotides indicate the extent of the CbrB consensus binding site. Dashed inverted arrows show a putative ρ-independent terminator of the *cbrB* transcript. An arrow at +1 shows the start of *crcZ* transcription. **B.** Interactions of radioactively labeled wild-type and mutated *crcZ* regulatory regions. Different concentrations of purified His-CbrB were analyzed by electrophoretic mobility shift assays. DNA probes covering *crcZ* promoter from the UAS region (highlighted in A) to +1 transcription starting site were used for probes preparation as described in Methods. WT, wild-type probe, Mut2, mutated motif 2, ΔM1, deletion of motif 1, and ΔM1,2, deletion of motifs 1 and 2, corresponding to pME9834. Concentrations of His-CbrB in lanes 1 to 5 were: 760 nM, 380 nM, 76 nM, 15 nM and 0 nM, respectively.

A.

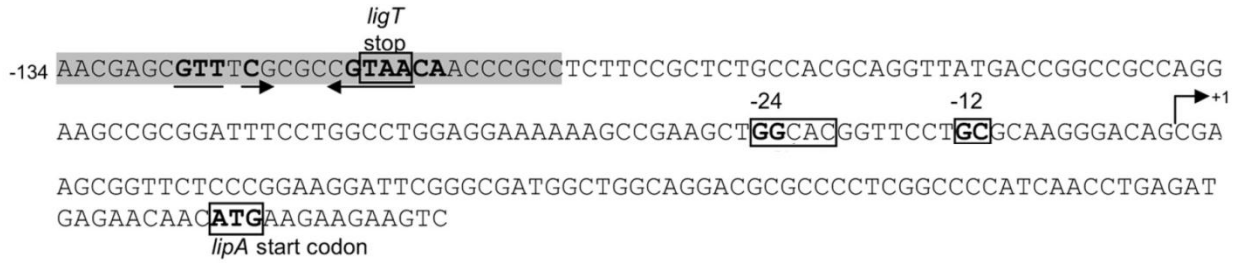

B.

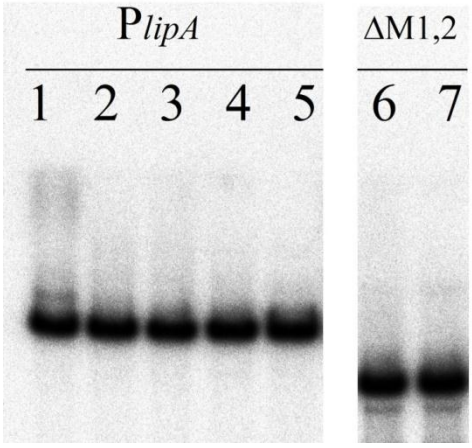

Figure 3.3. Sequence of the *lipA* promoter region, recognition site for CbrB and catabolite repression of the *lipA* promoter.

A. In the nucleotide sequence of the *lipA* promoter, the UAS region is highlighted in grey. The *ligT* stop codon, the -24 and -12 elements of the σ^{54} promoter, and the *lipA* start codon are boxed. Inverted arrows below boldface nucleotides show the palindromic sequence in the UAS region. An arrow at +1 shows the start of *lipA* transcription. **B.** Interactions of the radioactively labeled wild-type *lipA* promoter corresponding to pME9831 (P*lipA*; 0.1 nM) with different concentrations of His-CbrB were tested *in vitro* by electrophoretic mobility shift experiments as described in Methods. Concentrations of His-CbrB in lanes 1 to 5 were: 1520 nM, 760 nM, 380 nM, 190 nM and 0 nM, respectively. The *crcZ* promoter region devoid of motifs 1 and 2 (ΔM1,2) served as negative controls in lane 6 (no His-CbrB) and lane 7 (1520 nM of His-CbrB).

CbrAB/CrcZ/Crc may play partial role in regulation of basic amino acids and polyamines utilization. When CbrAB is deficient, no CrcZ will be expressed to antagonize Crc repression resulting in permanent inactivation of target pathways. Histidine and arginine utilization has been thought to be regulated by CbrAB two-component system independent from CCR by Crc. In this study, as a continuation from previous chapters, I tested for growth of mutant strains *cbrAB* (PAO5100), *cbrAB/ crc* (PAO4727), and *cbrAB/ntrBC* (PAO5126), on positively charged biomolecules such as L-histidine, L-arginine, L-lysine, agmatine, putrescine and cadaverine. Since CbrA-CbrB and Crc are for carbon regulation, and NtrB-NtrC for nitrogen, no growth difference between *cbrAB* and *cbrAB/ntrBC* mutant strains was expected when nutrients were provided as sole source of carbon and nitrogen. In contrast, comparison between *cbrAB* and *cbrAB/ crc* mutants was quite interesting; it can differentiate catabolism that is controlled by *cbrAB* alone or by the coordinated *cbrAB/C*rcZ/Crc system. As shown in Table 3.2, different growth patterns were obtained for L-histidine from L-arginine and polyamines. While histidine utilization seemed independent from Crc repression, growth on L-arginine, agmatine and polyamines were partially restored when *crc* was further mutated in *cbrAB* genetic background to release CCR (PAO4727). This data suggested involvement of the *cbrAB/C*rcZ/Crc system in the utilization of arginine, lysine, agmatine, putrescine and cadaverine. In contrast, growth on GABA and AMV were just slightly affected in CbrAB.

Table 3.2. Growth phenotypes of CbrAB, Crc and NtrBC mutants

Nutrients*	Genotype			
	wild type	***cbrAB***	***cbrAB crc***	***cbrAB ntrBC***
Histidine	++++	-	-	-
Arginine	++++	-	++	-
Agmatine	++++	-	+++	-
Putrescine	++++	-	+++	-
GABA	++++	+++	++++	+++
Lysine	+	-	+	-
Cadaverine	++	-	+	-
AMV	+++	++	+++	+

* Cells (10^4) were grown on MMP media plates supplemented with 10 mM of different energy sources. Growth was recorded during 3 days of incubation period. ++++: prominent growth after 1 day; +++: good growth after 1 day; ++: good growth after 2 days; +: growth after 3 days; -: no detectable growth after 3 days.

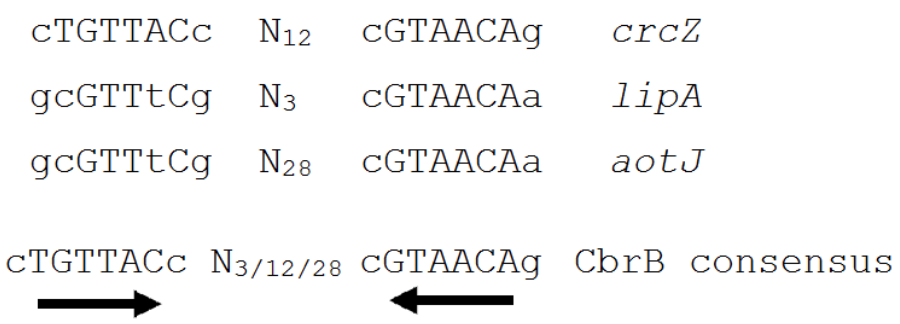

Figure 3.4. Proposed CbrB consensus in *P. aeruginosa*

The CbrB binding sites in the *crcZ* and *lipA* promoters of *P. aeruginosa* were determined in this work. Preliminary data on the *aotJ* promoter of *P. aeruginosa* reveal similar conserved palindromic sequences. Their alignment suggests a consensus CbrB binding site with variable spacer lengths of 3, 12 or 28 nucleotides.

Possible cross-talk between NtrBC and CbrAB was not found. Combined regulation of CbrAB with NtrBC has been reported for arginine and histidine utilization in *pseudomonas* (54, 107). Based on sequence and structure similarities, possible cross-talk may occur between the sensors and regulators of these two-component systems. Based on studies of NtrC regulatory phosphorylation in *E. coli*, replacing the lysine residue 104 by glutamine (K104Q) prevents dephosphorylation of the aspartate residue on NtrC receiver domain (79). Based on amino acid sequence similarity, CbrB K98Q was predicted as the corresponding mutation site of NtrC K104Q. I introduced pCBRB and pCBRB* carrying wild type CbrB and mutated CbrB K98Q, respectively, into wild type PAO1 and *cbrAB* mutant PAO5100. However, no difference in growth was found on minimal media P agar plates where nutrients tested in Table 3.2 were provided as the sole source of carbon and nitrogen (data not shown). These results implied CbrA is necessary for CbrB activation and there may be no cross-talk between NtrB sensor and CbrB regulator.

Comparison of CbrB recognition sites in *P. aeruginosa*. Direct binding of CbrAB were shown for the *crcZ* and *lipA* genes in this study. Based on stronger binding of CbrB and the palindromic symmetry of these elements on the *crcZ* promoter, CbrB consensus was proposed based on the UAS of *crcZ* promoter (Figure 3.4). This allowed me to predict putative UASs on *aotJ* promoter. Putative CbrB recognition sites were found at 455 and 419 nucleotides upstream from the start codon of the *aotJ* promoter (gcGTTtCg N_{28}cGTAACAa). These two elements found on the *aotJ* promoter are almost identical to those in the *lipA* promoter but with a longer spacer sequence (Figure 3.4). More studies are required to verify CbrB regulation on arginine/lysine utilization through these elements.

The *crc* and *crcZ* promoters were intact in Arg34. As mentioned in Introduction, suppressor mutants obtained from *cbrAB* mutant on arginine plates can be classified into two types based on their ability to growth on histidine and glucose. The Arg34 strain represents the phenotype of the majority of these suppressor mutants with positive growth on sugars and TCA intermediates as carbon sources but cannot grow on histidine (54). Since the CbrAB/CrcZ/Crc pathway affects a wide range of metabolic pathways, mutations in genes of this pathway may release from the permanent repression of Crc. To verify this hypothesis, I PCR amplified the regions of the *crc* gene and the *crcZ* gene (covering coding and upstream intergenic regions) for DNA sequencing analysis. However, the results revealed no difference in these regions between Arg34 and the wild type PAO1 strains (data not shown).

GENERAL DISCUSSION

Using DNA microarray to understand microbial metabolic pathways. DNA microarray experiments were conducted to see genome wide response to exogenous L-lysine, L-arginine and polyamines in *P. aeruginosa*. For L-lysine utilization, this approach did not give direct indications since important genes for L-lysine utilization identified so far in this study were under L-arginine/ArgR control (Table 1.2). This also led to misjudge *ldcA* (PA1818) as a candidate of L-arginine decarboxylase gene during the initial studies of our laboratory (29). Fortunately, growth phenotype studies were able to explain the microarray data with the peculiar connection between L-lysine and L-arginine catabolism as reported in this study (Chapter I).

With a relatively large genome of 5,570 open reading frames, traditional genetic approaches such as random mutagenesis may be difficult for the identification of candidate genes, especially when there were several homologous genes with relaxed specificity such as the case of seven γ-glutamyl-polyamine synthetases for polyamine catabolism (Chapter II, Table 2.2). Different from putrescine, cadaverine is under catabolite repression from other energy sources such as glutamate. Since all cells were grown in glutamate minimal media for this set of DNA microarray data, response to cadaverine was severely inhibited. Therefore, candidate genes for the γ-glutamylation pathway (pauA, pauB, pauC and pauD) were selected based on putrescine DNA microarray. Roles of these genes in cadaverine utilization were also confirmed by promoter-*lacZ* fusions and genetics studies. Additionally, it was unusual that almost all genes inducible by putrescine or agmatine were also inducible by GABA (Table 2.2). It is intriguing

that genes responsible for the γ-glutamylation pathway were inducible by the downstream metabolite GABA where feedback inhibition is commonly found.

Besides the proposed oxidative deamination by PauB from *E. coli*, an alternative transamination reaction was suggested for the second step of the γ-glutamylation pathway regardless of the oxygen level (Figure 2.1). The transaminase SpuC was proposed for this alternative route with L-alanine production from pyruvate. Interestingly, an induced *dadAX* operon was found to ensure the recycling of pyruvate for the transamination reaction (Table 2.2) (13, 28). This data implies contribution of this alternative route in polyamine utilization.

Clinical decarboxylase assay could be modified for *P. aeruginosa* detection. *Pseudomonas aeruginosa* causes constant life-threatening infections to hospitalized immunocompromised patients due to its versatile metabolic capacity and quick antibiotic resistance development (17, 87). One of the most common clinical procedures for identification of *Enterobacteriaceae* and other gram-negative enteric bacilli is the biochemical differentiation using decarboxylase media (61). This colorimetric test is based on pH changes first by sugar fermentation followed by activation of arginine dihydrolase and lysine and ornithine decarboxylases as part of acid stress response. Because of its low cost and simplicity, this approach is widely used before more expensive and time-consuming experiments such as PCR or DNA microarray for identification. While I demonstrated that L-lysine decarboxylation is the main route of L-lysine catabolism in *P. aeruginosa*, this test is negative for this organism. It is generally believed that *P. aeruginosa* is not adequate due to its inability to ferment certain sugars under anaerobic conditions. This may be true for the acid stress response through arginine and

ornithine decarboxylation, however, the lysine decarboxylase identified in this study exhibits optimal conditions at physiological pH. Since the bottle neck of lysine decarboxylation is the inducer arginine, it may be useful adding some arginine and adequate pH sensors in the media to identify *P. aeruginosa*. This early identification may be of primordial importance to avoid delayed treatment for immunocompromised patients in intensive care units.

Methods for lysine decarboxylase assay. In the first part of this study, I performed the enzyme characterization of lysine decarboxylase LdcA using radiolabeled [^{14}C]-L-lysine (98). This radiometric method may be one of the most traditional approaches for biochemical enzyme characterization which is generally avoided because of the usage of isotope. Other laborious methods include manometric and multi-step spectrophotometric approaches (4, 78). The most recent advance for this enzymatic reaction uses macrocycle-fluorescent dye complexes to allow continuous monitoring of the product production (30). Actually, our laboratory selected this new method as my first test for LdcA characterization using the macrocyclic cation receptor cucurbit[7]uril (CB7) and Dapoxyl complex. The idea is based on the differential affinity between lysine and cadaverine (product of decarboxylase) to CB7. Ideally, it should be able to monitor the change in fluorescence when Dapoxyl is titrated out throughout cadaverine production. Unfortunately, even this method is successful using lysine decarboxylase from *E. coli* at pH 6.0, I found it impossible for my enzyme because the fluorescence intensity is ten-folds weaker at the optimal pH of my enzyme (data not shown). Therefore I concluded that this approach is not adequate for a complete enzyme characterization.

The second method I tested was the spectrophotometric approach using 2,4,6-trinitrobenzenesulfonic acid (TNBS). This multi-step assay takes the advantage of the water insolubility of the complex formed by cadaverine and TNBS which can be extracted by toluene (78). This method has been widely used for three decades and most reports on lysine decarboxylase consider it as a standard procedure for enzymatic reaction. Curiously, I found a dramatic drop in LdcA enzyme activity once it reaches the maximum velocity around 5 mM lysine concentration suggesting strong substrate inhibition kinetics (Appendix A). Similar pattern was published in the original paper where this method was developed by Phan *at al* in 1981. However, when I tried to analyze the enzyme kinetics with this set of data using GraghPad Prism 5 software, the inhibitory effect is so strong that the values cannot fit into the substrate inhibition equation using non-linear regression curve fit (Figure A.2). This intrigued me, so I used the radiometric approach to double confirm my doubt. Surprisingly, the kinetics obtained from this old-fashioned method was totally different from previous approaches exhibiting cooperative substrate activation pattern (Figure 1.1). Therefore, I decided to perform the complete enzyme characterization using this last method because of the simplicity and stability in chemistry which may cause minimal secondary effects in the reaction.

Instability of the *pauA* mutants. The presence of seven glutamyl-polyamine synthetases in *P. aeruginosa* cause technical difficulties to conduct genetic analysis. The serial cloning conducted by our laboratory for different combination of *pauA*(s) knockouts with markerless gene replacement using the Flp-FRT recombination system was an extensive work (32, 105). This was not only because of the large number of genes and possible combinations; one of the problems that I encountered was the instability between FRT cassettes with proximal locations.

For the case of mutants containing *pauA1* and *pauA2* double mutations, the chromosome fragment between them (which includes *spuA* gene) may be unexpectedly inverted by the FRT cassettes. To avoid this, I had to leave the gentamicin resistant cassette in either *pauA1* or *pauA2*. Additionally, the physiology of the mutant strain M7 devoid of all PauA1-7 is significantly different from the wild type PAO1. This may be due to its inability to use polyamines. And I encounter difficulties to perform chemical transformation experiments with this strain. Therefore, the M6 mutant PAO5725 with gentamicin resistance cassette on *pauA2* was used in Chapter II for experiments involving transformation since this mutant strain has all *pauA*(s) for diamine utilization mutated/deleted and exhibits same growth phenotype than M7 on putrescine and cadaverine.

Difficulties with handling purified His-CbrB protein. In the last part of this thesis, recognition sites for the CbrB response regulator have been identified in the upstream region of the *crcZ and lipA* promoters. This interaction allows CbrB to drive the expression of the small RNA CrcZ which antagonizes the CCR repression by Crc in *P. aeruginosa*. The purification procedure and *in vitro* binding experiments were not easy for CbrB due to the high instability of purified protein and sub-optimal conditions for protein-DNA interaction. Different expression and purification schemes were tested to yield soluble active CbrB protein of high purity. His-CbrB can only be expressed at 37°C and detergent or glycerol was required to avoid immediate precipitation. Furthermore, without the N-terminal truncation, *in vitro* interaction between DNA with native CbrB or full length His-CbrB was not detectable in the electrophoretic mobility shift assay. I also tested for different binding and gel electrophoretic conditions by changing the buffer, pH, temperature, salt, DTT, etc. However, the affinity calculated from the best set of data

still showed poor interaction of CbrB on proposed binding sequences. I also encountered difficulties in performing CbrB footprinting with *crcZ and lipA* promoters. The DNase I digestion worked perfectly. However, there was no footprinting even with the wild type crcZ probe. It turned out that the recombinant His-CbrB was very sensitive to Mg^{2+} ion which was necessary for the DNase I activity.

Different functions of CbrAB/CrcZ/Crc regulation were proposed. Recent reports have extended the functions of the CbrAB/CrcZ/Crc signal transduction pathway beyond the control of catabolic pathways. A proteomic analysis has shown Crc repression on some porins biosynthesis affecting the susceptibility to certain antibiotics (56). Decreased biofilm formation, motility and cytotoxicity were also noted in *cbrB* and *crcZ* mutants (106). However, opposite effects were observed by another group on biofilm formation when rich media was used (71). It has been reported in several bacterial species that CCR systems can influence the expression of genes related to virulence (24). It is possible that with severe defects on the regulation of metabolism as in the *cbrAB* mutants, virulence traits might be directed to facilitate access to new sources of nutrients.

Throughout these series of studies on basic amino acids and polyamine catabolism, I am amazed by the large metabolic capacity and versatility of *Pseudomonas aeruginosa*. How this bacterium develop a connection to the complex arginine network for lysine utilization, the number of redundant enzymes in several steps of the γ-glutamylation pathway, and the sophisticated metabolic regulation by CbrA-CbrB and Crc, deserve our respects for its incredible metabolic flexibility and survival ability in different environments.

APPENDIX A

DIFFERENT LDCA ENZYME KINETICS IN SPECTROPHOTOMETRIC PPROACH

As mentioned in General Discussion, different methods were tested for lysine decarboxylase enzyme kinetics studies. In this section, a widely used spectrophotometric approach was tested for initial enzyme characterization (78). However, the kinetics obtained using this method was significantly different from the data using radiolabeled lysine as in Chapter One.

LdcA protein purification. The construct pHT1818 from Chapter One was used for full length LdcA expression and purification form *E. coli* TOP10 as described before (52, 103). As shown in Figure A1, lowering induction temperature seemed to help dramatically on the correct folding and hence solubility of the enzyme.

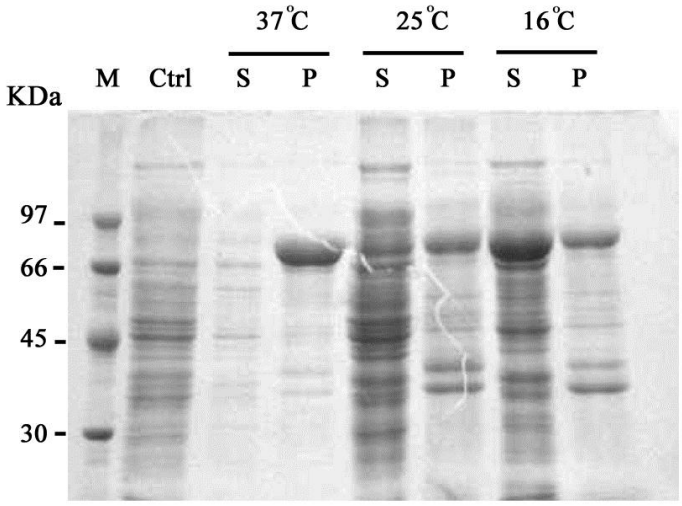

Figure A.1. LdcA solubility depends on expression temperature.

LdcA enzyme assay using spectrophotometric approach. Purified LdcA from above section was used to test L-lysine decarboxylation *in vitro.* The reaction mixture contains 0 mM to 50 mM L-lysine as the substrate and 125 μM pyridoxal-5'-phosphate as the cofactor. Enzyme activity was detected using a spectrophotometric method (78). Cadaverine and lysine can form colorimetric adducts with 1.02 X 10^{-2} M 2,4,6-trinitro-benzenesulfonic acid (TNBS). Base on the differential solubility of the reaction products in toluene, TNP-lysine and TNP-cadaverine, lysine decarboxylation rate was quantified by measuring the concentration of TNP-cadaverine extract from the organic phase by spectrophotometry. A standard curve was determined using cadaverine. Readings were obtained from toluene extracts using OD at 340nm. An average extinction coefficient for TNP-cadaverine was found to be 1.04 x 10^{4} $M^{-1}cm^{-1}$. Enzyme kinetics was analyzed using GraphPad Prism 5.0 and failed to fit into Substrate Inhibition Equation using Non-linear Regression Curve Fit.

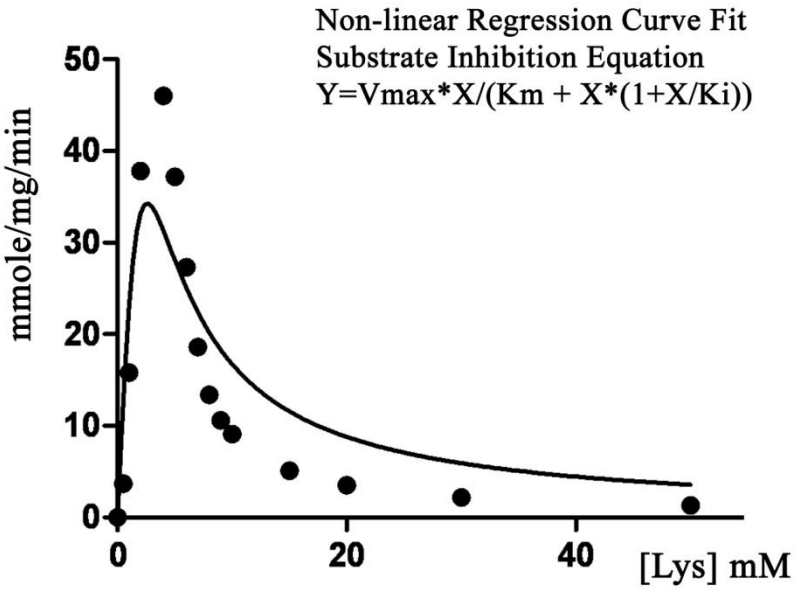

Figure A.2. LdcA kinetics does not fit to non-linear regression curve with substrate inhibition equation. LdcA was purified to homogeneity to perform enzyme characterization using a colorimetric method in Tris buffer pH 8.5 as described above. Enzyme kinetics was analyzed using GraphPad Prism 5.0.

APPENDIX B

TRANSCRIPTOME ANALYSIS OF AGMATINE AND PUTRESCINE CATABOLISM IN *PSEUDOMONAS AERUGINOSA* PAO1

This work was published by Han-Ting Chou, Dong-Hyeon Kwon, Mohamed Hegazy and Chung-Dar Lu in "Transcriptome Analysis of Agmatine and Putrescine Catabolism in *Pseudomonas aeruginosa* PAO1". J. Bacteriol. 2008 Mar; 190(6):1966-75.

JOURNAL OF BACTERIOLOGY, Mar. 2008, p. 1966–1975 Vol. 190, No. 6
0021-9193/08/$08.00+0 doi:10.1128/JB.01804-07

Transcriptome Analysis of Agmatine and Putrescine Catabolism in *Pseudomonas aeruginosa* PAO1▽†

Han Ting Chou, Dong-Hyeon Kwon, Mohamed Hegazy, and Chung-Dar Lu*

Department of Biology, Georgia State University, Atlanta, Georgia

Received 14 November 2007/Accepted 2 January 2008

Polyamines (putrescine, spermidine, and spermine) are major organic polycations essential for a wide spectrum of cellular processes. The cells require mechanisms to maintain homeostasis of intracellular polyamines to prevent otherwise severe adverse effects. We performed a detailed transcriptome profile analysis of *Pseudomonas aeruginosa* in response to agmatine and putrescine with an emphasis in polyamine catabolism. Agmatine serves as the precursor compound for putrescine (and hence spermidine and spermine), which was proposed to convert into 4-aminobutyrate (GABA) and succinate before entering the tricarboxylic acid cycle in support of cell growth, as the sole source of carbon and nitrogen. Two acetylpolyamine amidohydrolases, AphA and AphB, were found to be involved in the conversion of agmatine into putrescine. Enzymatic products of AphA were confirmed by mass spectrometry analysis. Interestingly, the alanine-pyruvate cycle was shown to be indispensable for polyamine utilization. The newly identified *dadRAX* locus encoding the regulator alanine transaminase and racemase coupled with SpuC, the major putrescine-pyruvate transaminase, were key components to maintaining alanine homeostasis. Corresponding mutant strains were severely hampered in polyamine utilization. On the other hand, an alternative γ-glutamylation pathway for the conversion of putrescine into GABA is present in some organisms. Subsequently, GabD, GabT, and PA5313 were identified for GABA utilization. The growth defect of the PA5313 *gabT* double mutant in GABA suggested the importance of these two transaminases. The succinic-semialdehyde dehydrogenase activity of GabD and its induction by GABA were also demonstrated in vitro. Polyamine utilization in general was proven to be independent of the PhoPQ two-component system, even though a modest induction of this operon was induced by polyamines. Multiple potent catabolic pathways, as depicted in this study, could serve pivotal roles in the control of intracellular polyamine levels.

Agmatine, a cationic compound derived from arginine decarboxylation, serves as the precursor of three major polyamines, putrescine, spermidine, and spermine. These polyamines are the major organic polycations found in all living cells. Polyamines have pleiotropic effects on several cellular processes. In more complex organisms, these compounds are required for cell proliferation and differentiation (2). In *Escherichia coli*, these polycations play significant roles in the structural and functional organization of the chromosome (35). They are implicated in RNA synthesis through the stimulation of the activity of RNA polymerase and in protein synthesis through the stabilization of ribosomal structure and modulation of translational fidelity (9). In addition, polyamines are involved in the induction of *recA* in *E. coli* in response to UV or γ irradiation (14). Polyamines are thought to protect DNA from oxidative damage by serving as free radical scavengers (7, 13). Some microorganisms also use polyamines for the synthesis of secondary metabolites (35). Recently, we also reported that exogenous polyamines exert a significant effect on antibiotic susceptibility in bacteria (16–18). While intracellular polyamines play pivotal roles in ensuring optimal growth, their accumulation inhibits protein synthesis and decreases cell viability in the stationary phase and at low temperatures (5, 19). Thus, a balance between polyamine synthesis and catabolism appears to be required to adjust the optimal concentration of these compounds in accordance with the growth environment.

Synthesis of spermidine and spermine requires the addition of an aminopropyl group from decarboxylated *S*-adenosylmethionine (dSAM) to putrescine and spermidine, respectively. These reactions are catalyzed by SAM decarboxylase (*speD*) for the synthesis of the aminopropyl donor and by spermidine synthase (*speE*) for transfer of the aminopropyl group from dSAM to putrescine. Although it is not available in bacteria, a similar reaction catalyzed by spermine synthase is responsible for spermine synthesis in eukaryotes.

Putrescine biosynthesis can occur by three routes (33): route 1, from ornithine by ornithine decarboxylase (*speC*); route 2, from arginine and agmatine, through the actions of arginine decarboxylase (*speA*) and agmatine ureohydrolase (*speB*); and route 3, from arginine, agmatine, and *N*-carbamoylputrescine (*N*-CP) via arginine decarboxylase, agmatine deiminase (*aguA*), and *N*-carbamoylputrescine amidohydrolase (*aguB*). While it is assumed that *E. coli* and many other microorganisms utilize both routes 1 and 2 (35), both routes 1 and 3 are used by *Pseudomonas aeruginosa* (24).

Agmatine and putrescine also serve as good sources of carbon and nitrogen for *P. aeruginosa*. As shown in Fig. 1, exogenous agmatine was first converted into putrescine by AguA and AguB, and the carbon skeleton of putrescine was preserved as succinate via two sets of transamination and dehydrogenation reactions before being channeled into the tricar-

* Corresponding author. Mailing address: Department of Biology, Georgia State University, 24 Peachtree Center Avenue, Atlanta, GA 30303. Phone: (404) 413-5395. Fax: (404) 413-5301. E-mail: biocdl@langate.gsu.edu.

† Supplemental material for this article may be found at http://jb.asm.org/.

▽ Published ahead of print on 11 January 2008.

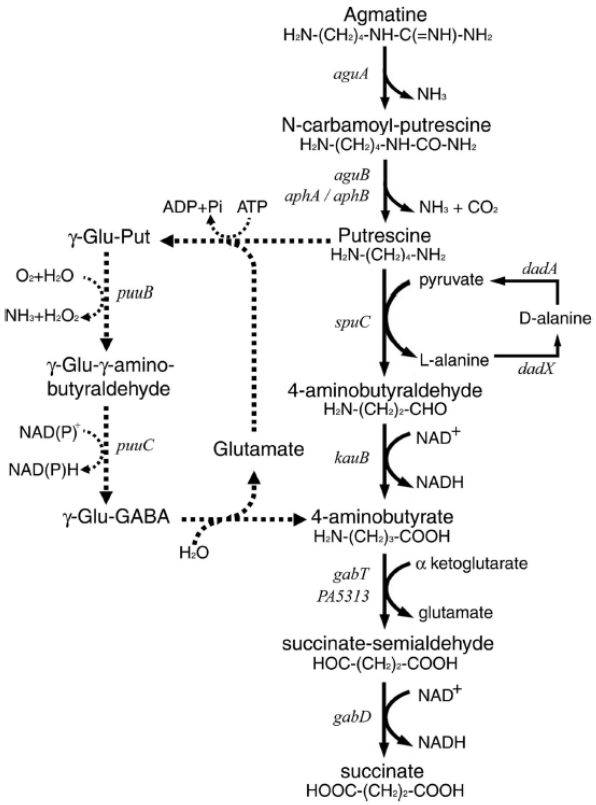

FIG. 1. Catabolic pathways of agmatine and putrescine in *P. aeruginosa* PAO1. Dashed arrows indicate the proposed γ-glutamylation pathway for putrescine catabolism in *E. coli*.

boxylic acid (TCA) cycle. The *aguBA* operon is induced by agmatine and controlled by the AguR repressor (25). While the *aguA* mutant was unable to grow on agmatine as the sole source of carbon and nitrogen, a leaky growth phenotype of the *aguB* mutant on agmatine suggested an alternative route yet to be identified.

SpuC, a putrescine-pyruvate aminotransferase that converts putrescine to 4-aminobutyraldehyde, is essential for putrescine utilization in *P. aeruginosa* (20). The subsequent dehydrogenation of 4-aminobutyraldehyde to 4-aminobutyrate (GABA) is catalyzed by a bifunctional enzyme, KauB, possessing both 4-guanidinobutyraldehyde dehydrogenase and 4-aminobutyraldehyde dehydrogenase activities (Fig. 1). The KauB activity is induced by putrescine or by agmatine (11). Conversion of GABA into succinate was proposed to require the function of two successive enzymes, succinic semialdehyde transaminase (GabT) and succinic semialdehyde dehydrogenase (GabD), respectively; however, no molecular information regarding the encoding genes *gabDT* has been reported for *P. aeruginosa*.

Putrescine catabolism involving γ-glutamylated intermediates (Fig. 1) in the conversion of putrescine into GABA was recently reported for *E. coli* (15). The *pu*trescine *u*tilization (*puu*) genes of this novel pathway were clustered in a single locus of several transcriptional units in *E. coli* (15). *P. aeruginosa* also possesses several possible homologues of the Puu proteins scattered on the chromosome (www.pseudomonas.com), but it was not clear whether these proteins participate in polyamine utilization. To exploit the catabolic capacity of *P. aeruginosa*, we conducted transcriptome analysis to identify and characterize genes that are differentially induced by exogenous agmatine and putrescine.

MATERIALS AND METHODS

Bacterial strains, plasmids, media, and growth conditions. The bacterial strains and plasmids used in this study are listed in Table 1. *E. coli* strains were grown with Luria-Bertani (LB) medium supplemented with ampicillin, 50 μg/ml; tetracycline, 12.5 μg/ml; gentamicin, 10 μg/ml; chloramphenicol, 35 μg/ml; kanamycin, 50 μg/ml; and 5-bromo-3-indolyl-β-D-galactoside (X-Gal) at 0.03% (wt/vol); and the *P. aeruginosa* strain was grown with LB medium supplemented with carbenicillin, 200 μg/ml; streptomycin, 300 μg/ml; tetracycline, 100 μg/ml; and gentamicin, 50 μg/ml. The minimal medium P (8) containing the indicated carbon and nitrogen sources at 20 mM was used for the growth of *P. aeruginosa*.

RNA preparation and DNA microarray analyses. Two independent sets of *P. aeruginosa* PAO1 cultures were grown aerobically in minimal medium P, with 350 rpm shaking at 37°C, in the presence of L-glutamate alone or with the addition of putrescine, agmatine, or GABA at 20 mM. Cells were harvested when the optical density at 600 nm reached 0.5 to 0.6 by centrifugation for 5 min at 4°C. Total RNA samples were isolated by using an RNeasy purification kit following the instructions of the manufacturer (Qiagen). Reverse transcription for cDNA synthesis, fragmentation by DNase I treatment, and cDNA probe labeling and hybridization were performed according to the instructions of GeneChip (Affymetrix). Data were processed by Microarray Suite 5.0 software, normalizing the absolute expression signal values of all chips to a target intensity of 500. GeneSpring software (Silicon Genetics) was used for the expression pattern analysis and comparison. Only genes showing consistent expression profiles in duplicates were selected for further analysis.

Construction of *lacZ* fusions. For the construction of *lacZ* fusions, the regulatory regions of interest were amplified by PCR with specific primers (see Table S1 in the supplemental material) from the genomic DNA of *P. aeruginosa* PAO1. After restriction digestion of the purified PCR products, these DNA fragments were cloned into the corresponding restriction sites of pQF50 or pQF52 (Table 1) before they were transformed into *E. coli* DH5α. The positive clones were selected on LB plates containing ampicillin and X-Gal. The nucleotide sequence of the inserts was confirmed by DNA sequencing.

Construction of mutant strains. For knockout mutants created by insertion, DNA fragments covering the genes of interest were PCR amplified (see Table S2 in the supplemental material) from PAO1 genomic DNA and cloned into the conjugation vector pRTP1 (34). The tetracycline resistance cassette was introduced by using an EZ-Tn*5* (TET-1) insertion system (Epicenter). The mutation sites were mapped by restriction endonuclease digestion and subsequently by nucleotide sequencing with a transposon-specific flanking primer. For deletion mutants, two flanking regions of a targeted gene were amplified by PCR with specific primers (see Table S2 in the supplemental material). The PCR products were purified after agarose gel electrophoresis and applied to spin columns (Qiagen). Following restriction digestions, the DNA fragments were cloned into pRTP1. A cassette carrying the gentamicin resistance gene from pGMΩ1 was purified after restriction digestion and inserted into the conjunction of the two DNA fragments, which was introduced by primer sequence designs. For gene replacement, *E. coli* SM10 served as the donor in biparental mating with PAO1-Sm (6). The desired knockout mutants were selected on LB plates containing streptomycin and either gentamicin or tetracycline, and the mutation was confirmed by PCR.

Overexpression and purification of the recombinant AphA. Recombinant His-AphA was expressed in *E. coli* Rosetta (DE3)(pLysS), following instructions of a pRSET expression system (Invitrogen Life Technologies). Logarithmically growing cells were obtained from a single-colony inoculum consisting of LB medium containing ampicillin and chloramphenicol at 20°C with shaking. The induction for protein expression was triggered by adding 1 mM of isopropylthio-galactopyranoside into the medium when the optical density at 600 nm reached 0.5. Recombinant cells were harvested after 16 h of induction by centrifugation at 4°C. The cell pellet was suspended in a 5× volume of phosphate buffer (20 mM sodium phosphate, 500 mM NaCl, 10 mM imidazole [pH 7.4]) supplemented with EDTA-free protease inhibitor cocktail (Roche). Cell extract was obtained by passage through a French pressure cell at 8,500 lb/in^2, and cell debris was removed by centrifugation at 25,000 × *g* for 30 min at 4°C. The soluble His-

TABLE 1. Strains and plasmids

Strain or plasmid	Genotype or description[a]	Source
E.coli strains		
DH5α	F$^-$ ϕ80d*lac*ΔM15 Δ(*lacZYA-argF*)*U169 deoR recA1 endA1 hsdR17* (r_K^- m_K^-) *supE44* λ$^-$ *thi-1 gyrA96 relA*	Bethesda Research Laboratories
Rosetta (DE3)pLysS	F$^-$ *ompT hsdSB* (r_B^- m_B^-) *gal dcm* (DE3)pLysSRARE (Cam^r)	EMD Bioscience
SM10	*thi-1 thr leu tonA lacY supE recA*::RP4-2-Tc::Mu (Km^r)	6
P. aeruginosa strains		
PAO1	Wild type	8
PAO1-Sm	Spontaneous Sm^r mutant strain of PAO1	26
PAO5001	*aguA*::Tc^r	25
PAO5002	*aguB*::Tc^r	25
PAO5003	*aguR*::Tc^r	25
PAO5701	*gabD*::Tc^r	This study
PAO5702	*gabD*::Tc^r/PA5313::Gm^r	This study
PAO5703	*gabT*::Tc^r	This study
PAO5704	*gabT*::Tc^r/PA5313::Gm^r	This study
PAO5008	*spuC*::Tc^r	20
PAO5706	*spuC*::Tc^r/PA5313::Gm^r	This study
PAO5707	*kauB*::Gm^r	This study
PAO5708	PA5313::Gm^r	This study
PAO5709	PA5314::Gm^r	This study
PAO5710	*dadA*::Tc^r	This study
PAO5711	*dadX*::Gm^r	This study
PAO5712	PA5303::Gm^r	This study
PAO5713	*dadR*::Gm^r	This study
PAO5714	*phoP*::Gm^r	This study
PAO5715	*phoQ*::Gm^r	This study
Plasmids		
pRTP1	Amp^r Sm^s conjugation vector	34
pUCP18	*Escherichia-Pseudomonas* shuttle vector (Amp^r)	32
pGMΩ1	Gentamicin cassette with omega loop on both ends (Amp^r)	31
pHC5302	pUCP18 derivative carrying the *dadX* gene	This study
pHC5303	pUCP18 derivative carrying the PA5303 gene	This study
pRSET	pUC-derived expression vectors; T7 promoter N-terminal six-His tag (Amp^r)	Invitrogen Life Technologies
pHE1409	pRSET derivative for six-His-tagged AphA protein expression (Amp^r)	This study
pQF50	*bla lacZ* transcriptional fusion vector (Amp^r)	3
pQF52	*bla lacZ* translational fusion vector derived from pQF50 (Amp^r)	26
pHT0322	*aphB*::*lacZ* transcriptional fusion of pQF50	This study
pHT1409	*aphA*::*lacZ* transcriptional fusion of pQF50	This study
pHT1178	*oprH*::*lacZ* translational fusion of pQF52	This study
pHT5312	*kauB*::*lacZ* transcriptional fusion of pQF50	This study
pHT5313	PA5313::*lacZ* transcriptional fusion of pQF50	This study
pHT0265	*gabD*::*lacZ* translational fusion of pQF52	This study
pGU102	*spuA*::*lacZ* translational fusion of pQF52	20
pZY6	*dadA*::*lacZ* translational fusion of pQF52	36

[a] Cam^r, chloramphenicol resistance; Km^r, kanamycin resistance; Sm^r, streptomycin resistance; Sm^s, streptomycin sensitive; Tc^r, tetracycline resistance; Gm^r, gentamicin resistance; Amp^r, ampicillin resistance.

tagged AphA protein was purified over nickel-nitrilotriacetic acid agarose resin in batch mode for native proteins, following the instructions of the manufacturer (Qiagen). The protein fraction eluted by 150 mM imidazole in phosphate buffer was subjected to anion exchange chromatography using a Mono Q FF 5/5 column (Pharmacia). Before the protein sample application, the column was equilibrated after a blank run with 20 mM Tris-HCl (pH 7.4). A linear gradient of 0 to 1 M KCl over 20 column volumes was used for protein elution. Active fractions detected by UV and sodium dodecyl sulfate-polyacrylamide gel electrophoresis were pooled together and concentrated by using an Amicon Ultra-15 centrifugal filter unit (Millipore).

Measurements of enzyme activities. The cells were grown in minimal medium P containing the carbon and nitrogen sources as indicated above. Cells in the mid-log phase were harvested by centrifugation and then passed through a French press cell at 8,500 lb/in^2 The cell debris were removed by centrifugation at 20,000 × *g* for 10 min at 4°C, and protein concentrations in the crude extracts were determined by the Bradford method (1) using bovine serum albumin as the standard.

The activity of β-galactosidase was measured at 37°C, using *o*-nitrophenyl-β-galactopyranoside as the reaction substrate, and the formation of *o*-nitrophenol was determined by spectrophotometry at 420 nm.

The succinic-semialdehyde dehydrogenase activity was assayed as described previously (29). The cell pellet was washed in 100 mM sodium phosphate buffer (pH 7.0) containing 9% glycerol, 1 mM dithiothreitol, and 1 mM phenylmethylsulfonyl fluoride. The reaction was carried out at 30°C in a mixture containing 100 mM HEPES (pH 8.0), 1.5 mM succinic semialdehyde, 0.35 mM NADP, and 5 mM 2-mercaptoethanol. The reaction was initiated by the addition of crude extract, and the activity of succinic-semialdehyde dehydrogenase was determined by monitoring the generation of NADPH at 340 nm.

To demonstrate the acetylpolyamine amidohydrolase activity of AphA, acetylputrescine was used as the substrate in the reaction mixture. Purified recombinant AphA protein was further activated by incubation with 5 mM $MnCl_2$ or $CoCl_2$ on ice for 2 h preceding the enzyme assay. The composition of the reaction mixture was as follows (0.5 ml total volume): 20 μg of purified enzyme, 20 mM acetylputrescine, l00 mM Tris-HCl (pH 7.8), 8 mM $MgSO_4$, and 60 mM KCl. After 16 h at 37°C, the reaction was stopped by boiling the samples for 10 min. Denatured proteins were precipitated and removed by centrifugation

TABLE 2. Genes induced by agmatine and putrescine in *P. aeruginosa* PAO1

Strain[a]	Gene name	Cell growth in medium supplemented with (absolute signal value)[b]:			Fold change in expression with the addition of[c]:		Description
		Glu	Glu plus Agm	Glu plus Put	Agm	Put	
PA0265[d]	*gabD*	448	6,310	6,923	14.4	15.8	Succinate-semialdehyde dehydrogenase
PA0266[d]	*gabT*	721	9,263	9,244	12.9	12.8	4-Aminobutyrate aminotransferase
PA0292	*aguA*	705	10,862	681	15.4	1.0	Agmatine deiminase
PA0293	*aguB*	74	8,564	94	115.5	1.3	*N*-CP amidohydrolase
PA0295		203	743	522	3.6	2.5	Periplasmic polyamine binding protein
PA0296	*spuI*	1,113	8,354	7,613	7.4	6.8	PA2040 homolog, glutamine synthetase
PA0297	*spuA*	275	2,451	1,663	10.3	6.8	Glutamine amidotransferase
PA0298	*spuB*	582	3,931	2,625	6.8	4.5	Glutamine synthetase
PA0299	*spuC*	1,203	7,953	6,179	6.7	5.1	Putrescine-pyruvate aminotransferase, patase
PA0321	*aphB*	37	241	16	7.1	0.5	Acetylpolyamine aminohydrolase
PA0322		55	253	40	4.9	0.9	Small molecule transporter
PA0534		26	525	683	28.4	28.7	Putative D-amino acid oxidases (deaminating)
PA0535		77	338	447	4.8	5.1	Probable transcriptional regulator
PA1178[d]	*oprH*	1,863	14,493	10,917	9.4	6.7	Outer membrane porin oprh
PA1179[d]	*phoP*	646	2,471	1,680	3.7	2.5	Two-component response regulator phop
PA1180[d]	*phoQ*	455	1,262	966	2.7	2.1	Two-component sensor kinase phoq
PA1409	*aphA*	69	1,513	32	22.1	0.6	Acetylpolyamine aminohydrolase
PA1410		99	1,563	89	16.8	0.9	Periplasmic spermidine/putrescine-binding protein
PA1540		38	271	213	7.3	5.6	Conserved hypothetical protein
PA1541		58	667	406	54.7	32.7	Drug efflux transporter
PA1742		366	2,038	2,335	5.8	6.5	Amidotransferase
PA2041		107	1,629	1,245	15.5	11.9	Amino acid permease
PA2268		60	292	647	4.9	10.8	Hypothetical protein
PA2776		194	3,655	3,674	18.5	18.6	Conserved hypothetical protein
PA3355		96	289	271	3.1	2.9	Hypothetical protein
PA3356		591	3,301	3,232	5.6	5.5	Glutamine synthetase
PA3552[d]	*pmrH*	299	1,870	794	6.2	2.5	Putative enzyme for lipopoly saccharide modification
PA3553[d]	*pmrF*	138	924	362	6.3	2.7	Putative glycosyl transferase
PA3554[d]	*pmrI*	288	1,154	626	4.0	2.3	Putative formyl transferase
PA3555[d]	*pmrJ*	77	194	118	2.8	1.5	Putative deacetylase
PA3556[d]	*pmrK, arnT*	189	672	324	7.1	2.9	Inner membrane L-Ara4N transferase arnt
PA3557[d]	*pmrL*	60	265	144	4.5	2.4	Putative membrane protein
PA3558[d]	*pmrM*	140	597	303	4.5	2.3	Putative permease
PA3559[d]	*ugd*	117	540	264	4.6	2.2	UDP-glucose dehydrogenase
PA3766		91	978	985	12.5	11.7	Aromatic amino acid transporter
PA4358[d]	*feoB*	91	462	315	5.3	3.5	Ferrous iron transport protein B
PA4359[d]	*feoA*	96	381	218	3.9	2.3	Ferrous iron transport protein A
PA5302	*dadX*	40	2,177	2,770	65.2	91.7	Alanine racemase
PA5303		105	3,657	3,934	36.7	42.6	Putative endoribonuclease
PA5304	*dadA*	165	5,126	5,682	34.6	43.5	D-Alanine dehydrogenase
PA5308	*dadR*	552	635	501	1.2	0.9	Transcriptional regulator of the AsnC family
PA5309		398	1,369	1,363	3.4	3.4	Oxidoreductase
PA5312	*kauB*	922	7,906	7,744	8.5	8.3	NAD-dependent aldehyde dehydrogenase
PA5313		144	2,847	4,226	19.9	29.4	Transaminase
PA5314		91	1,834	2,298	19.4	24.1	Hypothetical protein of unknown function
PA5521		292	873	910	3.1	3.2	Short-chain dehydrogenase
PA5522		116	585	591	4.7	5.2	Glutamine synthetase
PA5523		122	832	894	6.7	7.2	Aminotransferase

[a] PA gene numbers are annotated according to the Pseudomonas Genome Project (www.pseudomonas.com).
[b] GeneChip raw data are mean values from two independent sets of cultures. Cells were grown in minimal medium P supplemented with 20 mM of the following supplements as indicated: Glu, glutamate; Agm, agmatine; Put, putrescine.
[c] Expression change (*n*-fold) in cultures with the addition of agmatine or putrescine.
[d] Genes proposed to be regulated by magnesium limitation and by the *oprH-phoPQ* operon, according to McPhee at al. (22).

at 25,000 × *g* for 30 min at 4°C. The supernatant containing small molecules was submitted for mass spectrometry analysis to the core facilities of Georgia State University. Samples were diluted 10 times (vol/vol) in 50% methanol in water with the addition of 0.1% formic acid for positive ion analysis by electrospray ionization quadrupole-time-of-flight mass spectrometry.

Microarray data accession numbers. The raw data from GeneChip experiments have been deposited in the Gene Expression Omnibus (GEO) database at NCBI with the accession number GSE9926.

RESULTS

DNA microarrays were employed to analyze the transcriptional profiles of *P. aeruginosa* PAO1 in response to agmatine and putrescine, with an emphasis on possible catabolic routes. As shown in Table 2, cells were grown in glutamate minimal medium in the absence and presence of agmatine or pu-

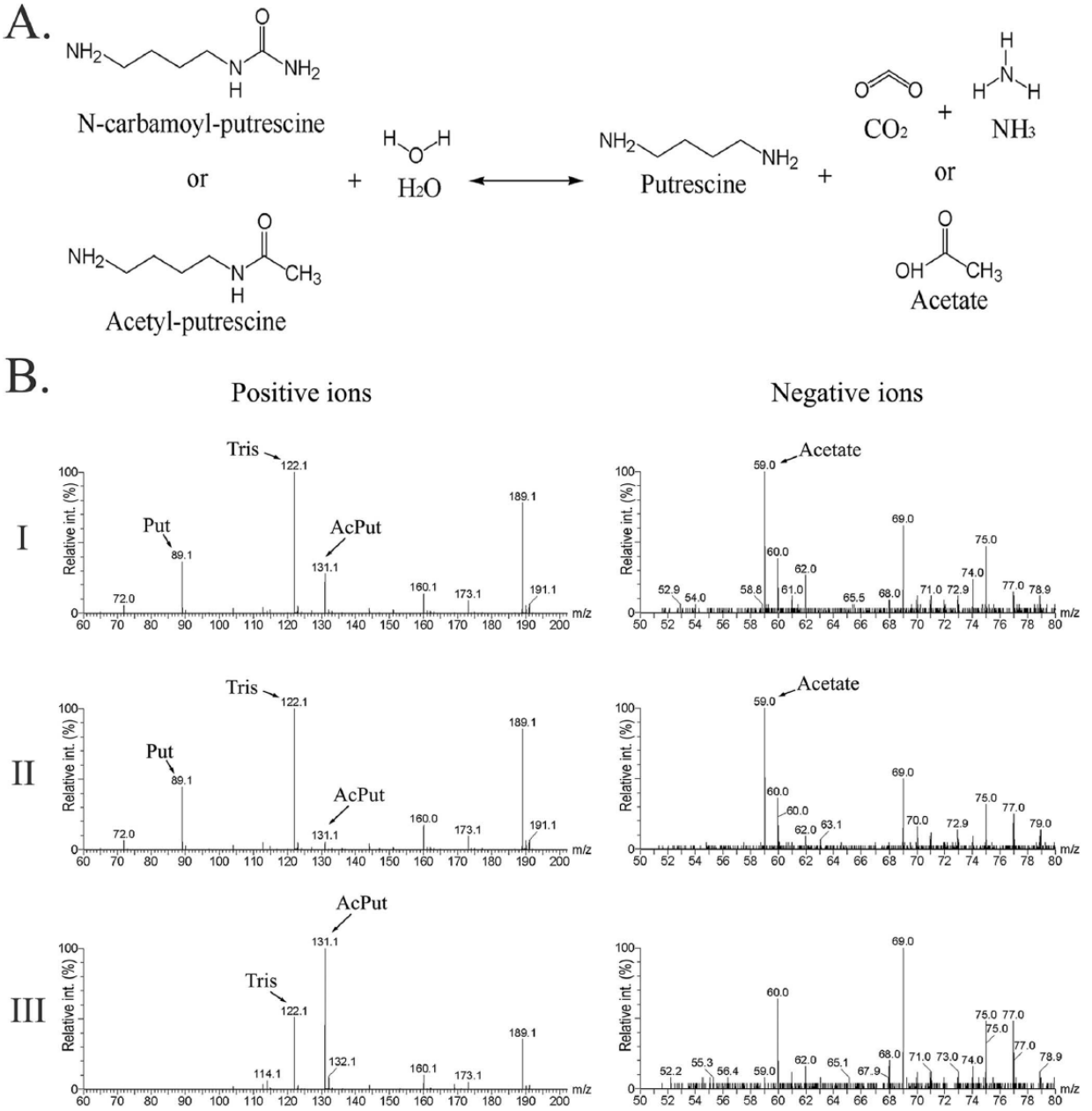

FIG. 2. Formation of putrescine by acetylpolyamine amidohydrolases. (A) Reactions catalyzed by AphA and/or AphB. Either *N*-CP or acetylputrescine can be converted into putrescine based on the similarities in chemistry. (B) Mass spectrometry analysis of AphA enzymatic activity. Purified AphA was applied to reaction mixtures containing acetylputrescine as substrate. Reaction products were subjected to electrospray ionization quadrupole-time-of-flight mass spectrometry analysis for positive and negative ions. Panel I, reactions with purified enzyme; panel II, reactions with $MnCl_2$ or $CoCl_2$ preactivated enzymes; panel III, negative control with heat-inactivated enzyme.

trescine, and genes that were induced by either of these two compounds were identified based on the criteria described in Materials and Methods. We have reported characterization of some of these genes in the following aspects: *aguBA* for agmatine catabolism (25), *spuA-I* for polyamine utilization and uptake (20), and *oprH-phoPQ* as well as PA3552 to PA3559 for polyamine-dependent antibiotic susceptibility (18). The following sections would therefore focus mainly on other genes that participate in the proposed catabolic pathway(s) of agmatine and putrescine (Fig. 1).

The agmatine-specific module. With few exceptions, the list of genes induced by the presence of agmatine overlaps completely with the list of putrescine-responsive genes. Only six genes in three possible transcriptional units were considered

TABLE 3. Expression profile of *aphA* and *aphB* promoters[a]

Strain	Genotype	Supplement	β-galactosidase activity (nmol/min/mg) induced by:	
			P_{aphA}	P_{aphB}
PAO1	WT	Glu	10	145
		Glu plus Agm	57	323
		Glu plus AcPut	736	2,262
		Glu plus Put	14	67
		Glu plus GABA	16	52
PAO5001	*aguA*	Glu	4	148
		Glu plus Agm	2	84
PAO5002	*aguB*	Glu	9	169
		Glu plus Agm	634	1,991
PAO5003	*aguR*	Glu	10	141
		Glu plus Agm	109	461

[a] Cells were grown in minimal medium P supplemented with 20 mM of the following supplements: Glu, glutamate; Agm, agmatine; AcPut, acetyl-putrescine; Put, putrescine; WT, wild type. Specific activities (nmol/min/mg) represent the averages from two measurements, with standard errors below 5%.

TABLE 4. Expression profile of the *dadA* promoter[a]

Strain	Genotype	β-galactosidase activity (nmol/min/mg) in:		
		Glu	Glu plus Put	Glu plus Ala
PAO1	WT	184	1,628	2,783
PAO5713	*dadR*	15	16	NG
PAO5008	*spuC*	99	137	3,352
PAO5706	*spuC*/PA5313	118	114	2,879
PAO5708	PA5313	249	716	1,742

[a] Cells were grown in minimal medium P supplemented with 20 mM of the following supplements: Glu, glutamate; Put, putrescine; Ala, alanine. Specific activities (nmol/min/mg) represent the averages from two measurements, with standard errors below 5%. NG, no growth. WT, wild type.

agmatine specific: the *aguBA* operon and the two putative PA1409-PA1410 and PA0322-PA0321 operons (Table 2 and Fig. 1). We have reported characterization of the *aguBA* operon and its agmatine-specific regulation by AguR (25). The other two operons were quite similar in their genetic contents; PA1409 and PA0321 encode two putative acetylpolyamine amidohydrolases, while PA1410 and PA0322 are open reading frames for a probable periplasmic binding protein and a transporter, respectively. PA1409 and PA0321 were designated *a*cetyl*p*olyamine amido*h*ydrolase *A*(*aphA*) and *aphB* based on the demonstrated enzymatic activity (see description below) and the 69% sequence identity between the encoded polypeptides.

Induction of *aphA* and *aphB* by exogenous agmatine and acetylputrescine. The *aguBA* operon encodes two enzymes with activity in the conversion of agmatine into putrescine (Fig. 1). We have reported that the *aguB* mutant exhibited a leaky growth phenotype, while the *aguA* mutant showed no growth on agmatine as the sole source of carbon and nitrogen (25). In the presence of agmatine, the *aguB* mutant was expected to accumulate *N*-CP, which has a chemical structure (Fig. 2a) similar to that of acetylputrescine, a substrate of AphA and an inducer signal of *aphA* and *aphB* (see below). We fortuitously proposed that *aphA* and *aphB* might be induced by *N*-CP (and hence agmatine) and that the leaky growth of the *aguB* mutant on agmatine was due to the conversion of *N*-CP to putrescine by the induced AphA and AphB.

To test this hypothesis, an *aphA*::*lacZ* promoter fusion was constructed and introduced into the *aguA* and *aguB* mutants and the parent strain PAO1. As shown in Table 3, the *aphA* promoter in PAO1 was only slightly induced (sixfold) by exogenous agmatine but not by putrescine. In contrast, acetylputrescine exerted a strong induction effect (74-fold). In comparison, agmatine showed no induction in the *aguA* mutant (no *N*-CP synthesis), but it exerted an enhanced level of induction in the *aguB* mutant (*N*-CP accumulation). On the other hand, agmatine induction was sustained in the *aguR* mutant strain. Similar results were also obtained when an *aphB*::*lacZ* fusion was applied in the same set of experiments. These results were consistent with the hypothesis that acetylputrescine is the authentic inducer molecule of *aphA* and *aphB* and that the agmatine induction of *aphA*/*aphB* is mediated by *N*-CP and is independent of the AguR regulatory system.

The acetylputrescine amidohydrolase activity of AphA. The AphA protein of *P. aeruginosa* PAO1 exhibits 70% sequence similarity to acetylpolyamine amidohydrolase of *Mycoplana ramosa*, which requires metals (zinc or cobalt) for its catalytic reaction on a variety of acetylpolyamines, including acetylputrescine (28). To demonstrate the proposed enzymatic activity of AphA, a recombinant form of AphA was overexpressed in *E. coli* and purified to homogeneity, as described in Materials and Methods. The recombinant AphA was applied to a reaction mixture containing acetylputrescine as substrate, and the presence of the anticipated reaction products was analyzed by mass spectrometry. As shown in Fig. 2B, a comparison of the mass spectra of the samples versus that of the control revealed the appearance of sample signals with *m*/*z* values characteristic of putrescine and acetate, the products expected for acetylputrescine hydrolysis by AphA. Although the values were not quantitative, the putrescine/acetylputrescine ratio signals were significantly higher in samples of metal-containing reactions (Fig. 2B, compare panels I and II). These results support AphA as a metalloenzyme of acetylpolyamine amidohydrolase.

The *dadRAX* locus of alanine catabolism. A three-gene locus containing the putative genes *dadA* and *dadX* in alanine catabolism and the PA5303 gene of an unknown function was induced by agmatine and putrescine (Table 2). The DadA and DadX polypeptides were annotated by the genome project as D-alanine dehydrogenase and alanine racemase, respectively, based on the highly conserved amino acid sequence similarities for bacteria. To substantiate the results of transcriptome analyses and the proposed physiological functions of *dadAX* in alanine utilization, we constructed a *dadA*::*lacZ* promoter fusion construct to study its expression profile and conducted a growth phenotype analysis of *dadA* and *dadX* mutants.

As shown in Table 4, the *dadA* promoter was induced with an order of strength of alanine that was greater than putrescine utilization in the wild-type strain PAO1 grown in glutamate minimal medium. A mutation in either *dadA* or *dadX* severely hampered alanine utilization as the sole source of carbon and nitrogen but showed only a moderate effect on agmatine/putrescine (Table 6). When the *dadX* mutant was complemented with a functional *dadX* gene expressed from multicopy plasmids, the growth of this recombinant strain on L-alanine was

TABLE 5. Expression profiles of *kauB*, PA5313, and *gabD* promoters[a]

Strain	Genotype	Promoter	β-galactosidase activity (nmol/min/mg) in:			
			Glu	Glu plus Agm	Glu plus Put	Glu plus GABA
PAO1	WT	P_{kauB}	263	907	1,013	NT
		P_{PA5313}	136	904	961	NT
		P_{GabD}	3,868	42,944	53,911	45,436

[a] Cells were grown in minimal medium P supplemented with 20 mM of the following supplements: Glu, glutamate; Agm, agmatine; Put, putrescine. NT, not tested. WT, wild type. Specific activities (nmol/min/mg) represent the averages from two measurements, with standard errors below 5%.

even enhanced in comparison to that of the wild-type PAO1. These results are consistent with the function proposed for *dadAX* in alanine utilization and support the hypothesis that the induction of *dadAX* by agmatine/putrescine is mediated by alanine as a product of a transamination reaction in the proposed catabolic pathway (Fig. 1).

Between *dadA* and *dadX*, the PA5303 gene encodes a putative endoribonuclease. Insertion of a gentamicin-omega loop cassette on PA5303 also caused a severe negative effect on alanine utilization, and this growth defect can be complemented by a recombinant plasmid carrying *dadX* but not by the one carrying PA5303. Since the omega loop structure on the flanking regions of the inserted cassette could exert a polar effect on the downstream gene, these results indicated that PA5303 may not be essential for alanine utilization and that the growth defect on alanine of the PA5303::GmΩ mutant was most likely due to a polar effect on the downstream *dadX*.

The PA5308 gene upstream of *dadA* encodes a putative transcriptional regulator of the AsnC family. Although the expression of PA5308 was not affected by agmatine or putrescine, its close proximity to *dadAX* prompted us to investigate the potential role of PA5308 in the control of *dadAX* expression. The PA5308 mutant cannot grow on L-alanine as the sole source of carbon and nitrogen (Table 6), and this mutation completely alleviated the induction effect of agmatine and putrescine on the *dadA* promoter (Table 4). On the basis of these results, PA5308 was designated *dadR* (*dadAX* *r*egulator), which is essential for the transcriptional activation of *dadAX*.

It was interesting to note that mutations of the *dadRAX* genes abolished L-alanine utilization and also that the growth of the resulting mutants on other carbon/nitrogen sources became extremely sensitive to the presence of exogenous L-alanine. For example, the growth of these mutants, but not the parent strain PAO1, in the minimal medium supplemented with either glutamate or glucose and ammonium, was severely retarded by 5 mM of L-alanine. A similar case has been reported with *Klebsiella aerogenes*, and it was proposed that this was the result of the allosteric inhibition by L-alanine on glutamine synthetase (10). We tested this hypothesis by the addition of 5 mM of glutamine in the growth medium and still found no sign of alleviation of growth inhibition by exogenous L-alanine in these mutants. These results suggest that the *dadRAX* genes are essential to maintaining alanine homeostasis and that exogenous L-alanine could exert a growth inhibition effect on targets yet to be identified in the *dad* mutants.

TABLE 6. Growth phenotype[a]

Strain	Genotype	Growth response in medium plus:					
		Glu	Agm	Put	GABA	Ala	Arg
PAO1	WT	++	++	++	++	++	++
PAO5710	*dadA*	++	+	+	+	−	NT
PAO5711	*dadX*	++	+	+	+	−	NT
PAO5713	*dadR*	++	++	++	++	−	NT
PAO5707	*kauB*	++	−	−	++	NT	NT
PAO5708	PA5313	++	++	++	++	++	NT
PAO5703	*gabT*	++	++	++	+	+	++
PAO5704	*gabT*/PA5313	++	++	++	−	+	NT
PAO5701	*gabD*	++	+	+	−	+	++
PAO5702	*gabD*/PA5313	++	+	+	−	+	NT
PAO5008	*spuC*	++	−	−	++	++	NT
PAO5706	*spuC*/PA5313	++	−	−	++	++	NT
PAO5714	*phoP*	++	++	++	++	++	++
PAO5715	*phoQ*	++	++	++	++	++	++

[a] Cell growth was tested after 24 h of incubation at 37°C in minimal medium P with 20 mM concentrations of the following supplements: Glu, glutamate; Agm, agmatine; Put, putrescine; Ala, L-alanine; Arg, L-arginine. ++, prominent growth; +, retarded growth; −, no growth; NT, not tested; WT, wild type. Consistent growth phenotypes were observed from three independent culture sets.

Linkage of alanine catabolism to putrescine utilization via a pyruvate transaminase. As described above, the *dadA* promoter was found to be inducible by putrescine (and hence agmatine). We proposed that it was due to alanine synthesis from putrescine transamination catalyzed by SpuC, which employs pyruvate as the amino acceptor (20). This hypothesis was supported by a drastic reduction of putrescine-dependent induction of the *dadA* promoter in the *spuC* mutant (Table 4). As we reported previously that the *spuC* mutants exhibited a severe defect in putrescine utilization (20), this result further supports the conclusion that SpuC is the major putrescine-pyruvate transaminase.

The *kauB*-PA5313 locus. The induction profile of the *kauB* (initially identified as an essential gene for *k*eto*a*rginine *u*tilization) and PA5313 genes was confirmed by transcriptional *lacZ* fusions. As shown in Table 5, the *kauB*-PA5313 divergent promoters were both induced by exogenous agmatine and putrescine. The *kauB* gene and the KauB protein were reported to possess an aldehyde dehydrogenase activity that can utilize 4-aminobutyraldehyde (derived from putrescine; Fig. 1) and 4-guanidinobutyraldehyde (derived from ketoarginine) as substrates (11). The results of growth phenotype analyses (Table 6) indicated that *kauB* is essential for the utilization of agmatine and putrescine but not of GABA.

Both PA5313 and its downstream gene PA5314 were induced by agmatine and putrescine (Table 2), and these two genes encode a putative pyruvate transaminase and a hypothetical protein of unknown function. The PA5313 and PA5314 mutants grew normally on either agmatine, putrescine, or GABA, but growth on spermidine was significantly retarded.

The *gabDT* locus. Conversion of GABA to succinate requires a pair of deamination and oxidation reactions (Fig. 1). In the genome annotations, PA0265 (*gabD*) and PA0266 (*gabT*) were proposed to code for succinic semialdehyde dehydrogenase (SSAD) and GABA transaminase, respectively, which exhibit high sequence similarities to GabD and GabT of

E. coli (30). In *P. aeruginosa* PAO1, the induction of *gabDT* by exogenous agmatine and putrescine was first revealed by GeneChip analyses (Table 2). This induction effect of agmatine and putrescine was confirmed by the measurements of β-galactosidase activities from PAO1 harboring pHT0265, a P*gabD*::*lacZ* fusion, as shown in Table 5. In addition, exogenous GABA also exerted a strong induction effect on the *gabD* promoter activity.

The *gabD* and *gabT* knockout mutants were constructed as described in Materials and Methods, and the growth phenotype of these mutants was tested on arginine, agmatine, putrescine, GABA, and glutamate as the sole sources of carbon and nitrogen (Table 6). These mutants did not differ from the parent strain in terms of glutamate and arginine utilization. However, the *gabD* mutant showed retarded growth on agmatine and putrescine and was unable to grow on GABA. The growth of the *gabT* mutant on GABA was also affected; the generation time of the *gabT* mutant was significantly longer than that of the wild-type PAO1 (87 min versus 42 min). These results suggested that GabD is essential for GABA utilization and the presence of at least one more GABA transaminase other than GabT.

As described above, PA5313 was proposed to encode a putative transaminase. To test whether PA5313 may serve a role in GABA utilization, a *gabT* PA5313 double mutant was constructed, and its growth on GABA as the sole source of carbon and nitrogen was completely abolished (Table 6). These results support GabT and PA5313 as two redundant transaminases in GABA catabolism.

The proposed SSAD activity of GabD was measured for a *gabD* mutant and its parent strain PAO1, grown in glutamate minimal medium in the presence or absence of GABA. In the presence of GABA, the SSAD activity was induced ninefold in PAO1 (140 versus 1,281 nmol min^{-1} mg^{-1}). In comparison, only a negligible level of SSAD activity could be detected in the *gabD* mutant in both growth conditions. These results support the idea that *gabD* encodes a GABA-inducible SSAD.

Effects of PhoP and PhoQ. As shown in Table 2, the *oprH-phoP-phoQ* operon was induced by agmatine and putrescine, which encodes an outer membrane porin OprH and the response regulator and sensor kinase of the PhoPQ two-component system (21). To investigate whether the PhoPQ system plays a role in agmatine and putrescine catabolism, we constructed the *phoP* and *phoQ* mutants and tested the growth phenotype of these two mutants on glutamate, agmatine, putrescine, and GABA as the sole sources of carbon and nitrogen. As shown in Table 6, the *phoP* and *phoQ* mutants grew well on all of these tested compounds.

Employing an *oprH*::*lacZ* fusion, exogenous putrescine exerted a 2.4-fold induction on the *oprH* promoter activities in the wild-type strain PAO1 as shown in Table 7. In the *phoP* mutant, the *oprH* promoter remained constitutively low in the presence or absence of putrescine. In comparison, the *phoQ* mutant retained a constitutively high level of *oprH* promoter activity but also showed no response to exogenous putrescine. These results supported the data from the GeneChip analysis and were consistent with the functions reported for PhoP and PhoQ on the autoregulation of the *oprH-phoP-phoQ* operon (21).

The potential effects of PhoP on putrescine-dependent induction of the *spuABCD* and *gabDT* operons was also investigated. As shown in Table 7, the expression of β-galactosidase from either the *spuA*::*lacZ* or *gabD*::*lacZ* fusion was still subjected to induction by exogenous putrescine in the *phoP* mutant. These data strongly suggested that the PhoPQ system may not play a significant role in the control of putrescine or GABA catabolism.

TABLE 7. Effects of PhoPQ on expression profiles of *oprH*, *gabD* and *spuA* promoters[a]

Strain	Promoter	Genotype	β-galactosidase activity (nmol/min/mg) in:	
			Glu	Glu plus Put
PAO1	P_{oprH}	WT	801	1,953
PAO5714		*phoP*	409	160
PAO5715		*phoQ*	4,878	3,497
PAO1	P_{spuA}	WT	154	833
PAO5714		*phoP*	139	947
PAO1	P_{gabD}	WT	3,868	53,911
PAO5714		*phoP*	3,582	39,088

[a] Cells were grown in minimal medium P supplemented with 20 mM of the following supplements as indicated: Glu, glutamate; Put, putrescine. Specific activities (nmol/min/mg) represent the averages from two measurements, with standard errors below 5%.

DISCUSSION

Participation of acetylpolyamine amidohydrolases in agmatine catabolism. In this report, we identified *aphA* and *aphB* as agmatine-inducible genes, by DNA microarrays analyses. With purified recombinant AphA proteins, a metal-dependent acetylpolyamine amidohydrolase activity of AphA was demonstrated (Fig. 2a). This enzymatic property of AphA is consistent with that reported for AphA from *Mycoplana ramosa* (28). The promoters of *aphA* and *aphB* were both induced by exogenous acetylputrescine to a much higher level than that of agmatine in the wild-type strain PAO1. However, in the *aguB* mutant, exogenous agmatine did exert a significant induction effect on the *aphA* and *aphB* promoters. *N*-CP, an intermediate in agmatine/putrescine conversion (Fig. 1), is anticipated to accumulate in the *aguB* mutant when it is fed with agmatine. Considering the fact that *N*-CP and acetylputrescine have very similar chemical structures (Fig. 2a), it is very likely that *N*-CP can serve as the signal compound of *aphA* and *aphB* induction as well as the substrate of the encoded enzymes. These fortuitous events could explain the leaky growth phenotypes of *aguB* mutants on agmatine in the previous reports (20, 25).

From human cells to many types of bacteria including *E. coli*, the acetylation of polyamines was reported as a reaction important to the conversion of excess polyamines into a physiologically inert form and hence in keeping with the homeostasis of intracellular polyamines. In *E. coli*, polyamine acetylation is catalyzed by SpeG (4, 5, 19), and acetylated polyamine is readily excreted (27). *E. coli* might not recycle acetylated polyamine, and no apparent AphA homologue can be found in this organism as revealed by a BLAST search against all available genome sequences of *E. coli* strains in the NCBI database. In contrast, *P. aeruginosa* possesses AphA and AphB, but no promising SpeG homologue can be found by sequence comparison. By taking advantage of its enormous capability of

polyamine catabolism, *P. aeruginosa* may be able to keep polyamine homeostasis through catabolic pathways instead of acetylation.

Putrescine catabolic pathways. Putrescine catabolism into GABA can be mediated by two routes in bacteria: the conventional transamination/dehydrogenation route and a recently reported γ-glutamylation route (15). In *P. aeruginosa*, the abolishment of putrescine utilization in the *spuC* and *kauB* mutants (Table 6) supports the importance of the conventional route for putrescine catabolism. When this major pathway is blocked, putrescine might be catabolized through the γ-glutamylation pathway. Alternatively, since putrescine is the precursor compound of spermidine, it may be channeled into spermidine catabolic pathways yet to be exploited.

Enzymes and the corresponding genes of the γ-glutamylation pathway were first proposed in *E. coli* as essential elements in putrescine utilization. The PuuA protein of *E. coli* catalyzes γ-glutamylation as the first step in this route. In *E. coli*, PuuA is the only member of its kind that exhibited significant similarities to GlnA, the glutamine synthetase. In comparison, there are seven PuuA homologues in *P. aeruginosa* that show up to 44% identity (SpuI, SpuB, PA1566, PA2040, PA3356, PA5508, and PA5522), and four of them (except PA2040, PA1566, and PA5508) are listed in Table 2 as putrescine-inducible genes in this study. For an unknown reason, the PA2040 gene was not included in the GeneChip analysis. However, considering the fact that SpuI and PA2040 share 96% sequence identity (nucleotide as well as protein) with an identical length of 458 amino acids and that the downstream PA2041 gene was inducible by putrescine, we proposed that PA2040 should also be included in the list. The *spuB* and *spuI* genes have been reported in our previous study (20); the *spuB* mutant exhibited a specific growth deficiency on spermidine but not on putrescine or agmatine, while the *spuI* mutant showed no apparent effect on polyamine utilization. Although γ-glutamylation seems important for spermidine catabolism, whether it plays a role in putrescine utilization was not clear due to the redundancy of these enzymes.

Another major difference between these two routes is the enzymatic reactions for putrescine deamination. The *spuC* gene encodes a putrescine-pyruvate transaminase (20), which plays a pivotal role in the putrescine-dependent induction of *dadAX* for alanine catabolism (Table 4). In the case of γ-glutamylation, the terminal amino group of glutamylputrescine was proposed to be released as ammonia by oxidoreductase (Fig. 1, PuuB), which also generates hydrogen peroxide in this reaction. Four *puuB* homologues (PA0534, PA1566, PA5309, and PA2776) were identified as putrescine-inducible genes in this study.

The KauB and SpuA proteins (Table 2) are the most prominent homologues of PuuC and PuuD, respectively, of the γ-glutamylation pathway. KauB was proposed to play an essential role in the transaminase pathway, as the *kauB* mutant lost the capability to grow on agmatine and putrescine but not on GABA (Table 6). SpuA is the only candidate of the PuuD homologue in PAO1 based on sequence comparison; however, we have reported that the *spuA* mutant grew normally on agmatine and putrescine but did exhibit a server growth defect on spermidine (20). It provides another piece of evidence to support the transaminase pathway as the major route of putrescine utilization and strongly suggests spermidine catabolism via γ-glutamylation in *P. aeruginosa*.

Apparently, the γ-glutamylation route is not energy efficient, as it takes ATP to drive the first reaction (Fig. 1). In *E. coli*, putrescine can be utilized only as a sole source of nitrogen and not of carbon, and the expression of the *puu* gene possesses a very distinct pattern of temporal induction in the early stationary phase, needs aeration (presumably for the deamination reaction by oxidoreductase), and is subject to repression by its end products succinate and ammonia. In addition, GABA catabolism, as described below, may also put another layer of restrictions to the γ-glutamylation pathway in *E. coli*. As reflected by its regulatory systems, perhaps the physiological functions of this pathway in *E. coli* are to serve mainly as a defense mechanism against any toxic effect by polyamine accumulation when the cells reach the stationary phase and secondarily as a source of nitrogen or carbon under nutrient limitation conditions. Regardless, it was very intriguing to have multiple sets of PuuA/PuuB homologues in *P. aeruginosa*. More studies are needed to elucidate the potential role of γ-glutamylation in putrescine and spermidine catabolism in *P. aeruginosa*.

Alanine catabolism. In this study, we provided genetic evidence to support the physiological function of *dadRAX* in alanine and putrescine catabolism (Table 4 and 6) and established *DadR* as a transcriptional activator of *dadAX*. For putrescine catabolism, L-alanine is generated from the transamination reaction catalyzed by SpuC. A *dadAX* operon induced in response to exogenous putrescine would ensure recycling of pyruvate to the transamination reaction and hence can optimize the metabolic flux of putrescine into the TCA cycle as well as gluconeogenesis.

GABA utilization. Conversion of GABA into succinate also requires a pair of deamination and oxidation reactions. When GABA was supplied as the sole source of carbon and nitrogen, the *gabD* mutant and the *gabT* PA5313 double mutant lost the capability to grow on this compound. The proposed succinyl semialdehyde dehydrogenase activity of GabD was induced by exogenous GABA in the wild-type PAO1 and was absent in the *gabD* mutant. The *gabT* gene encoding a GABA transaminase most likely forms an operon with the upstream *gabD* gene. As revealed by DNA microarrays analyses and *gabD*::*lacZ* fusion studies, expression of the *gabDT* operon is induced by GABA as well as by agmatine and putrescine and, presumably, by any compounds that can increase intracellular concentration of GABA.

In comparison, the *gabDT* genes of *E. coli* are part of the *csiD-ygaF-gabDTP* operon (23), which is transcribed from two σ^S promoters in response to carbon starvation and environmental stresses and one σ^{70} promoter regulated by Nac in response to nitrogen limitation (30). GabD/T-mediated GABA catabolism is considered a general stress adaptation (12, 23), and it is not inducible by exogenous GABA.

PhoPQ two-component system. It has been reported that the PhoPQ system is required for autoregulation of the *oprH-phoP-phoQ* operon under divalent cation-limiting growth conditions and is also involved in resistance to cationic antimicrobial peptides (21). Furthermore, an extensive study of microarray transcriptional profiling reported a PhoP-dependent induction of *gabDT* under Mg^{2+}-limited conditions and

suggested the presence of a putative PhoP-binding site in the promoter region of the *spuABCD* operon (22). As shown in Table 2, exogenous agmatine and putrescine induce the expression level of the *oprH-phoP-phoQ* operon, and we have demonstrated this induction effect on the *oprH* promoter activity (18). In addition, we have reported the function of the PhoPQ two-component system in antibiotic resistance triggered by exogenous agmatine, putrescine, and spermidine (18). Due to the effect of agmatine and putrescine on PhoPQ, it was not surprising to find that some genes listed in Table 2 have been reported as members of the PhoP regulon (22). However, the PhoPQ system did not seem to play a role in the catabolism of these compounds, as *phoP* and *phoQ* mutants grew normally on these nutrients as the sole sources of carbon and nitrogen (Table 6). Studies of the other putative regulatory genes in the control of putrescine and GABA utilization are in progress.

ACKNOWLEDGMENTS

We thank Siming Wang and the Georgia State University MS facility for ESI-MS analysis.

This work was supported by the National Science Foundation (MCB-0415608).

REFERENCES

1. **Bradford, M. M.** 1976. A rapid and sensitive method for the quantitation of microgram quantities of protein utilizing the principle of protein-dye binding. Anal. Biochem. **72:**248–254.
2. **Casero, R. A., Jr., and A. E. Pegg.** 1993. Spermidine/spermine N1-acetyltransferase—the turning point in polyamine metabolism. FASEB J. **7:**653–661.
3. **Farinha, M. A., and A. M. Kropinski.** 1990. Construction of broad-host-range plasmid vectors for easy visible selection and analysis of promoters. J. Bacteriol. **172:**3496–3499.
4. **Fukuchi, J., K. Kashiwagi, K. Takio, and K. Igarashi.** 1994. Properties and structure of spermidine acetyltransferase in *Escherichia coli*. J. Biol. Chem. **269:**22581–22585.
5. **Fukuchi, J., K. Kashiwagi, M. Yamagishi, A. Ishihama, and K. Igarashi.** 1995. Decrease in cell viability due to the accumulation of spermidine in spermidine acetyltransferase-deficient mutant of *Escherichia coli*. J. Biol. Chem. **270:**18831–18835.
6. **Gambello, M. J., and B. H. Iglewski.** 1991. Cloning and characterization of the *Pseudomonas aeruginosa lasR* gene, a transcriptional activator of elastase expression. J. Bacteriol. **173:**3000–3009.
7. **Ha, H. C., N. S. Sirisoma, P. Kuppusamy, J. L. Zweier, P. M. Woster, and R. A. Casero, Jr.** 1998. The natural polyamine spermine functions directly as a free radical scavenger. Proc. Natl. Acad. Sci. USA **95:**11140–11145.
8. **Haas, D., B. W. Holloway, A. Schambock, and T. Leisinger.** 1977. The genetic organization of arginine biosynthesis in *Pseudomonas aeruginosa*. Mol. Gen. Genet. **154:**7–22.
9. **Huang, S. C., C. A. Panagiotidis, and E. S. Canellakis.** 1990. Transcriptional effects of polyamines on ribosomal proteins and on polyamine-synthesizing enzymes in *Escherichia coli*. Proc. Natl. Acad. Sci. USA **87:**3464–3468.
10. **Janes, B. K., and R. A. Bender.** 1998. Alanine catabolism in *Klebsiella aerogenes*: molecular characterization of the *dadAB* operon and its regulation by the nitrogen assimilation control protein. J. Bacteriol. **180:**563–570.
11. **Jann, A., H. Matsumoto, and D. Haas.** 1988. The fourth arginine catabolic pathway of *Pseudomonas aeruginosa*. J. Gen. Microbiol. **134:**1043–1053.
12. **Joloba, M. L., K. M. Clemmer, D. D. Sledjeski, and P. N. Rather.** 2004. Activation of the *gab* operon in an RpoS-dependent manner by mutations that truncate the inner core of lipopolysaccharide in *Escherichia coli*. J. Bacteriol. **186:**8542–8546.
13. **Khan, A. U., P. Di Mascio, M. H. Medeiros, and T. Wilson.** 1992. Spermine and spermidine protection of plasmid DNA against single-strand breaks induced by singlet oxygen. Proc. Natl. Acad. Sci. USA **89:**11428–11430.
14. **Kim, I. G., and T. J. Oh.** 2000. SOS induction of the *recA* gene by UV-, gamma-irradiation and mitomycin C is mediated by polyamines in *Escherichia coli* K-12. Toxicol. Lett. **116:**143–149.
15. **Kurihara, S., S. Oda, K. Kato, H. G. Kim, T. Koyanagi, H. Kumagai, and H. Suzuki.** 2005. A novel putrescine utilization pathway involves gamma-glutamylated intermediates of *Escherichia coli* K-12. J. Biol. Chem. **280:**4602–4608.
16. **Kwon, D. H., and C. D. Lu.** 2007. Polyamine effects on antibiotic susceptibility in bacteria. Antimicrob. Agents Chemother. **51:**2070–2077.
17. **Kwon, D. H., and C. D. Lu.** 2006. Polyamines increase antibiotic susceptibility in *Pseudomonas aeruginosa*. Antimicrob. Agents Chemother. **50:**1623–1627.
18. **Kwon, D. H., and C. D. Lu.** 2006. Polyamines induce resistance to cationic peptide, aminoglycoside, and quinolone antibiotics in *Pseudomonas aeruginosa* PAO1. Antimicrob. Agents Chemother. **50:**1615–1622.
19. **Limsuwun, K., and P. G. Jones.** 2000. Spermidine acetyltransferase is required to prevent spermidine toxicity at low temperatures in *Escherichia coli*. J. Bacteriol. **182:**5373–5380.
20. **Lu, C. D., Y. Itoh, Y. Nakada, and Y. Jiang.** 2002. Functional analysis and regulation of the divergent *spuABCDEFGH-spuI* operons for polyamine uptake and utilization in *Pseudomonas aeruginosa* PAO1. J. Bacteriol. **184:**3765–3773.
21. **Macfarlane, E. L., A. Kwasnicka, M. M. Ochs, and R. E. Hancock.** 1999. PhoP-PhoQ homologues in *Pseudomonas aeruginosa* regulate expression of the outer-membrane protein OprH and polymyxin B resistance. Mol. Microbiol. **34:**305–316.
22. **McPhee, J. B., M. Bains, G. Winsor, S. Lewenza, A. Kwasnicka, M. D. Brazas, F. S. Brinkman, and R. E. Hancock.** 2006. Contribution of the PhoP-PhoQ and PmrA-PmrB two-component regulatory systems to Mg^{2+}-induced gene regulation in *Pseudomonas aeruginosa*. J. Bacteriol. **188:**3995–4006.
23. **Metzner, M., J. Germer, and R. Hengge.** 2004. Multiple stress signal integration in the regulation of the complex sigma S-dependent *csiD-ygaF-gabDTP* operon in *Escherichia coli*. Mol. Microbiol. **51:**799–811.
24. **Nakada, Y., and Y. Itoh.** 2003. Identification of the putrescine biosynthetic genes in *Pseudomonas aeruginosa* and characterization of agmatine deiminase and N-carbamoylputrescine amidohydrolase of the arginine decarboxylase pathway. Microbiology **149:**707–714.
25. **Nakada, Y., Y. Jiang, T. Nishijyo, Y. Itoh, and C. D. Lu.** 2001. Molecular characterization and regulation of the *aguBA* operon, responsible for agmatine utilization in *Pseudomonas aeruginosa* PAO1. J. Bacteriol. **183:**6517–6524.
26. **Park, S. M., C. D. Lu, and A. T. Abdelal.** 1997. Cloning and characterization of *argR*, a gene that participates in regulation of arginine biosynthesis and catabolism in *Pseudomonas aeruginosa* PAO1. J. Bacteriol. **179:**5300–5308.
27. **Parry, L., J. Lopez-Ballester, L. Wiest, and A. E. Pegg.** 1995. Effect of expression of human spermidine/spermine N1-acetyltransferase in *Escherichia coli*. Biochemistry **34:**2701–2709.
28. **Sakurada, K., T. Ohta, K. Fujishiro, M. Hasegawa, and K. Aisaka.** 1996. Acetylpolyamine amidohydrolase from *Mycoplana ramosa*: gene cloning and characterization of the metal-substituted enzyme. J. Bacteriol. **178:**5781–5786.
29. **Sanchez, M., M. A. Alvarez, R. Balana, and A. Garrido-Pertierra.** 1988. Properties and functions of two succinic-semialdehyde dehydrogenases from *Pseudomonas putida*. Biochim. Biophys. Acta **953:**249–257.
30. **Schneider, B. L., S. Ruback, A. K. Kiupakis, H. Kasbarian, C. Pybus, and L. Reitzer.** 2002. The *Escherichia coli gabDTPC* operon: specific gamma-aminobutyrate catabolism and nonspecific induction. J. Bacteriol. **184:**6976–6986.
31. **Schweizer, H. D.** 1993. Small broad-host-range gentamycin resistance gene cassettes for site-specific insertion and deletion mutagenesis. BioTechniques **15:**831–834.
32. **Schweizer, H. P.** 1991. *Escherichia-Pseudomonas* shuttle vectors derived from pUC18/19. Gene **97:**109–121.
33. **Sekowska, A., A. Danchin, and J. L. Risler.** 2000. Phylogeny of related functions: the case of polyamine biosynthetic enzymes. Microbiology **146:**1815–1828.
34. **Stibitz, S., W. Black, and S. Falkow.** 1986. The construction of a cloning vector designed for gene replacement in *Bordetella pertussis*. Gene **50:**133–140.
35. **Tabor, C. W., and H. Tabor.** 1985. Polyamines in microorganisms. Microbiol. Rev. **49:**81–99.
36. **Yang, Z., and C. D. Lu.** 2007. Functional genomics enables identification of genes of the arginine transaminase pathway in *Pseudomonas aeruginosa*. J. Bacteriol. **189:**3945–3953.

APPENDIX C

LIST OF PUBLICATIONS ON SCIENTIFIC JOURNALS

1) Cadaverine and Putrescine Catabolism through γ-Glutamylation in *Pseudomonas aeruginosa* PAO1. **Chou HT**, Wu J, and Lu CD. Article in preparation

2) Promoter Recognition and Activation by the Global Response Regulator CbrB in *Pseudomonas aeruginosa.* Abdou L, **Chou HT**, Haas D, and Lu CD. *J Bacteriol*. 2011 Apr doi:10.1128/ JB.00164-11

3) L-lysine Catabolism is Controlled by Arginine/ArgR in *Pseudomonas aeruginosa* PAO1. **Chou HT**, Hegazy M, Lu CD. *J Bacteriol*. 2010 Nov;192(22):5874-80.

4) Synthesis and evaluation of new antagonists of bacterial quorum sensing in *Vibrio harveyi.* Peng H, Cheng Y, Ni N, Li M, Choudhary G, **Chou HT**, Lu CD, Tai PC, Wang B. *ChemMedChem.* 2009 Sep;4(9):1457-68.

5) Inhibition of quorum sensing in *Vibrio harveyi* by boronic acids. Ni N, Choudhary G, Peng H, Li M, **Chou HT**, Lu CD, Gilbert ES, Wang B. *Chem Biol Drug Des*. 2009 Jul;74(1):51-6.

6) Structure-based discovery and experimental verification of novel AI-2 quorum sensing inhibitors against *Vibrio harveyi*. Li M, Ni N, **Chou HT**, Lu CD, Tai PC, Wang B. *ChemMedChem*. 2008 Aug;3(8):1242-9.

7) Identification of boronic acids as antagonists of bacterial quorum sensing in *Vibrio harveyi*. Ni N, **Chou HT**, Wang J, Li M, Lu CD, Tai PC, Wang B. *Biochem Biophys Res Commun.* 2008 May 2;369(2):590-4.

8) Transcriptome analysis of agmatine and putrescine catabolism in *Pseudomonas aeruginosa* PAO1. **Chou HT**, Kwon DH, Hegazy M, Lu CD. *J Bacteriol*. 2008 Mar;190(6):1966-75.

REFERENCES

1. **Abdou, L., H. T. Chou, D. Haas, and C. D. Lu.** 2011. Promoter recognition and activation by the global response regulator CbrB in *Pseudomonas aeruginosa*. J Bacteriol **193:**2784-2792.
2. **Arai, H., M. Hayashi, A. Kuroi, M. Ishii, and Y. Igarashi.** 2005. Transcriptional regulation of the flavohemoglobin gene for aerobic nitric oxide detoxification by the second nitric oxide-responsive regulator of *Pseudomonas aeruginosa*. J Bacteriol **187:**3960-3968.
3. **Attila, C., A. Ueda, and T. K. Wood.** 2008. PA2663 (PpyR) increases biofilm formation in *Pseudomonas aeruginosa* PAO1 through the *psl* operon and stimulates virulence and quorum-sensing phenotypes. Appl Microbiol Biotechnol **78:**293-307.
4. **Blethen, S. L., E. A. Boeker, and E. E. Snell.** 1968. Argenine decarboxylase from *Escherichia coli*. I. Purification and specificity for substrates and coenzyme. J Biol Chem **243:**1671-1677.
5. **Bradford, M. M.** 1976. A rapid and sensitive method for the quantitation of microgram quantities of protein utilizing the principle of protein-dye binding. Anal Biochem **72:**248-254.
6. **Casero, R. A., Jr., and L. J. Marton.** 2007. Targeting polyamine metabolism and function in cancer and other hyperproliferative diseases. Nat Rev Drug Discov **6:**373-390.
7. **Casero, R. A., Jr., and A. E. Pegg.** 1993. Spermidine/spermine N^1-acetyltransferase - the turning point in polyamine metabolism. Faseb J **7:**653-661.

8. **Casero, R. A., and A. E. Pegg.** 2009. Polyamine catabolism and disease. Biochem J **421:**323-338.

9. **Castanie-Cornet, M. P., T. A. Penfound, D. Smith, J. F. Elliott, and J. W. Foster.** 1999. Control of acid resistance in *Escherichia coli*. J Bacteriol **181:**3525-3535.

10. **Chang, Y. F., and E. Adams.** 1974. D-lysine catabolic pathway in *Pseudomonas putida*: interrelations with L-lysine catabolism. J Bacteriol **117:**753-764.

11. **Childs, A. C., D. J. Mehta, and E. W. Gerner.** 2003. Polyamine-dependent gene expression. Cell Mol Life Sci **60:**1394-1406.

12. **Chou, H. T., M. Hegazy, and C. D. Lu.** 2010. L-lysine catabolism is controlled by L-arginine and ArgR in *Pseudomonas aeruginosa* PAO1. J Bacteriol **192:**5874-5880.

13. **Chou, H. T., D. H. Kwon, M. Hegazy, and C. D. Lu.** 2008. Transcriptome analysis of agmatine and putrescine catabolism in *Pseudomonas aeruginosa* PAO1. J Bacteriol **190:**1966-1975.

14. **Cohen, S. S.** 1998. A Guide to the Polyamines. Oxford University Press, New York.

15. **Collier, D. N., P. W. Hager, and P. V. Phibbs, Jr.** 1996. Catabolite repression control in the Pseudomonads. Res Microbiol **147:**551-561.

16. **Cox, M., G. Gerritse, L. Dankmeyer, and W. J. Quax.** 2001. Characterization of the promoter and upstream activating sequence from the *Pseudomonas alcaligenes* lipase gene. J Biotechnol **86:**9-17.

17. **Doyle, J. S., K. L. Buising, K. A. Thursky, L. J. Worth, and M. J. Richards.** 2011. Epidemiology of infections acquired in intensive care units. Semin Respir Crit Care Med **32:**115-138.

18. **Farinha, M. A., and A. M. Kropinski.** 1990. Construction of broad-host-range plasmid vectors for easy visible selection and analysis of promoters. J Bacteriol **172:**3496-3499.

19. **Fothergill, J. C., and J. R. Guest.** 1977. Catabolism of L-lysine by *Pseudomonas aeruginosa*. J Gen Microbiol **99:**139-155.

20. **Fukuchi, J., K. Kashiwagi, M. Yamagishi, A. Ishihama, and K. Igarashi.** 1995. Decrease in cell viability due to the accumulation of spermidine in spermidine acetyltransferase-deficient mutant of *Escherichia coli*. J Biol Chem **270:**18831-18835.

21. **Gambello, M. J., and B. H. Iglewski.** 1991. Cloning and characterization of the *Pseudomonas aeruginosa lasR* gene, a transcriptional activator of elastase expression. J Bacteriol **173:**3000-3009.

22. **Ghosh, T., D. Bose, and X. Zhang.** 2010. Mechanisms for activating bacterial RNA polymerase. FEMS Microbiol Rev **34:**611-627.

23. **Gong, S., H. Richard, and J. W. Foster.** 2003. YjdE (AdiC) is the arginine:agmatine antiporter essential for arginine-dependent acid resistance in *Escherichia coli*. J Bacteriol **185:**4402-4409.

24. **Gorke, B., and J. Stulke.** 2008. Carbon catabolite repression in bacteria: many ways to make the most out of nutrients. Nat Rev Microbiol **6:**613-624.

25. **Gu, B., J. H. Lee, T. R. Hoover, D. Scholl, and B. T. Nixon.** 1994. *Rhizobium meliloti* DctD, a sigma 54-dependent transcriptional activator, may be negatively controlled by a subdomain in the C-terminal end of its two-component receiver module. Mol Microbiol **13:**51-66.

26. **Ha, H. C., N. S. Sirisoma, P. Kuppusamy, J. L. Zweier, P. M. Woster, and R. A. Casero, Jr.** 1998. The natural polyamine spermine functions directly as a free radical scavenger. Proc Natl Acad Sci U S A **95:**11140-11145.

27. **Haas, D., B. W. Holloway, A. Schambock, and T. Leisinger.** 1977. The genetic organization of arginine biosynthesis in *Pseudomonas aeruginosa*. Mol Gen Genet **154:**7-22.

28. **He, W., C. Li, and C. D. Lu.** 2011. Regulation and characterization of the *dadRAX* locus for D-amino acid catabolism in *Pseudomonas aeruginosa* PAO1. J Bacteriol **193:**2107-2115.

29. **Hegazy, M.** 2004. Characterization of the Arginine Decarboxylase Pathway in *Pseudomonas aeruginosa*. PhD Dessertation. Georgia State University, Atlanta.

30. **Hennig, A., H. Bakirci, and W. M. Nau.** 2007. Label-free continuous enzyme assays with macrocycle-fluorescent dye complexes. Nat Meth **4:**629-632.

31. **Hervas, A. B., I. Canosa, R. Little, R. Dixon, and E. Santero.** 2009. NtrC-dependent regulatory network for nitrogen assimilation in *Pseudomonas putida*. J Bacteriol **191:**6123-6135.

32. **Hoang, T. T., R. R. Karkhoff-Schweizer, A. J. Kutchma, and H. P. Schweizer.** 1998. A broad-host-range Flp-FRT recombination system for site-specific excision of chromosomally-located DNA sequences: application for isolation of unmarked *Pseudomonas aeruginosa* mutants. Gene **212:**77-86.

33. **Huang, S. C., C. A. Panagiotidis, and E. S. Canellakis.** 1990. Transcriptional effects of polyamines on ribosomal proteins and on polyamine-synthesizing enzymes in *Escherichia coli*. Proc Natl Acad Sci U S A **87:**3464-3468.

34. **Ichihara, A., S. Furiya, and M. Suda.** 1960. Metabolism of L-lysine by bacterial enzymes: III. Lysine racemase. J Biochem **48:**277-283.

35. **Itoh, Y.** 1997. Cloning and characterization of the *aru* genes encoding enzymes of the catabolic arginine succinyltransferase pathway in *Pseudomonas aeruginosa*. J Bacteriol **179:**7280-7290.

36. **Kamio, M., K. C. Ko, S. Zheng, B. Wang, S. L. Collins, G. Gadda, P. C. Tai, and C. D. Derby.** 2009. The chemistry of escapin: identification and quantification of the components in the complex mixture generated by an L-amino acid oxidase in the defensive secretion of the sea snail *Aplysia californica*. Chemistry **15:**1597-1603.

37. **Kamio, Y., and Y. Terawaki.** 1983. Purification and properties of *Selenomonas ruminantium* lysine decarboxylase. J Bacteriol **153:**658-664.

38. **Khan, A. U., P. Di Mascio, M. H. Medeiros, and T. Wilson.** 1992. Spermine and spermidine protection of plasmid DNA against single-strand breaks induced by singlet oxygen. Proc Natl Acad Sci U S A **89:**11428-11430.

39. **Kikuchi, Y., H. Kojima, T. Tanaka, Y. Takatsuka, and Y. Kamio.** 1997. Characterization of a second lysine decarboxylase isolated from *Escherichia coli*. J Bacteriol **179:**4486-4492.

40. **Ko, K. C., B. Wang, P. C. Tai, and C. D. Derby.** 2008. Identification of potent bactericidal compounds produced by escapin, an L-amino acid oxidase in the ink of the sea hare *Aplysia californica*. Antimicrob Agents Chemother **52:**4455-4462.

41. **Krzeslak, J., G. Gerritse, R. van Merkerk, R. H. Cool, and W. J. Quax.** 2008. Lipase expression in *Pseudomonas alcaligenes* is under the control of a two-component regulatory system. Appl Environ Microbiol **74:**1402-1411.

42. **Kurihara, S., K. Kato, K. Asada, H. Kumagai, and H. Suzuki.** 2010. A putrescine-inducible pathway comprising PuuE-YneI in which gamma-aminobutyrate is degraded into succinate in *Escherichia coli* K-12. J Bacteriol **192:**4582-4591.

43. **Kurihara, S., S. Oda, K. Kato, H. G. Kim, T. Koyanagi, H. Kumagai, and H. Suzuki.** 2005. A novel putrescine utilization pathway involves gamma-glutamylated intermediates of *Escherichia coli* K-12. J Biol Chem **280:**4602-4608.

44. **Kurihara, S., S. Oda, Y. Tsuboi, H. G. Kim, M. Oshida, H. Kumagai, and H. Suzuki.** 2008. Gamma-glutamylputrescine synthetase in the putrescine utilization pathway of *Escherichia coli* K-12. J Biol Chem **283:**19981-19990.

45. **Kusano, T., T. Berberich, C. Tateda, and Y. Takahashi.** 2008. Polyamines: essential factors for growth and survival. Planta **228:**367-381.

46. **Kwon, D. H., and C. D. Lu.** 2007. Polyamine effects on antibiotic susceptibility in bacteria. Antimicrob Agents Chemother **51:**2070-2077.

47. **Kwon, D. H., and C. D. Lu.** 2006. Polyamines increase antibiotic susceptibility in *Pseudomonas aeruginosa*. Antimicrob Agents Chemother **50:**1623-1627.

48. **Kwon, D. H., and C. D. Lu.** 2006. Polyamines induce resistance to cationic peptide, aminoglycoside, and quinolone antibiotics in *Pseudomonas aeruginosa* PAO1. Antimicrob Agents Chemother **50:**1615-1622.

49. **Lee, J., V. Sperandio, D. E. Frantz, J. Longgood, A. Camilli, M. A. Phillips, and A. J. Michael.** 2009. An alternative polyamine biosynthetic pathway is widespread in bacteria and essential for biofilm formation in *Vibrio cholerae*. J Biol Chem **284:**9899-9907.

50. **Lemonnier, M., and D. Lane.** 1998. Expression of the second lysine decarboxylase gene of *Escherichia coli*. Microbiology **144 (Pt 3):**751-760.

51. **Lewenza, S., R. K. Falsafi, G. Winsor, W. J. Gooderham, J. B. McPhee, F. S. Brinkman, and R. E. Hancock.** 2005. Construction of a mini-Tn5-*luxCDABE* mutant library in *Pseudomonas aeruginosa* PAO1: a tool for identifying differentially regulated genes. Genome Res **15:**583-589.

52. **Li, C., and C. D. Lu.** 2009. Arginine racemization by coupled catabolic and anabolic dehydrogenases. Proc Natl Acad Sci U S A **106:**906-911.

53. **Li, C., X. Yao, and C. D. Lu.** 2009. Regulation of the *dauBAR* operon and characterization of D-amino acid dehydrogenase DauA in arginine and lysine catabolism of *Pseudomonas aeruginosa* PAO1. Microbiology.

54. **Li, W., and C. D. Lu.** 2007. Regulation of carbon and nitrogen utilization by CbrAB and NtrBC two-component systems in *Pseudomonas aeruginosa*. J Bacteriol **189:**5413-5420.

55. **Limsuwun, K., and P. G. Jones.** 2000. Spermidine acetyltransferase is required to prevent spermidine toxicity at low temperatures in *Escherichia coli*. J Bacteriol **182:**5373-5380.

56. **Linares, J. F., R. Moreno, A. Fajardo, L. Martinez-Solano, R. Escalante, F. Rojo, and J. L. Martinez.** 2010. The global regulator Crc modulates metabolism, susceptibility to antibiotics and virulence in *Pseudomonas aeruginosa*. Environ Microbiol **12:**3196-3212.

57. **Liu, P.** 1952. Utilization of carbohydrates by *Pseudomonas aeruginosa*. J Bacteriol **64:**773-781.

58. **Lu, C. D.** 2006. Pathways and regulation of bacterial arginine metabolism and perspectives for obtaining arginine overproducing strains. Appl Microbiol Biotechnol **70:**261-272.

59. **Lu, C. D., Y. Itoh, Y. Nakada, and Y. Jiang.** 2002. Functional analysis and regulation of the divergent *spuABCDEFGH-spuI* operons for polyamine uptake and utilization in *Pseudomonas aeruginosa* PAO1. J Bacteriol **184:**3765-3773.

60. **Lu, C. D., Z. Yang, and W. Li.** 2004. Transcriptome analysis of the ArgR regulon in *Pseudomonas aeruginosa*. J Bacteriol **186:**3855-3861.

61. **Mac Faddin, J. F. (ed.).** 2000. Biochemical tests for identification of medical bacteria, Third edition ed. Lippincott Williams & Wilkins.

62. **Marton, L. J., and A. E. Pegg.** 1995. Polyamines as targets for therapeutic intervention. Annu Rev Pharmacol Toxicol **35:**55-91.

63. **Meng, S. Y., and G. N. Bennett.** 1992. Regulation of the *Escherichia coli cad* operon: location of a site required for acid induction. J Bacteriol **174:**2670-2678.

64. **Miller, J. H.** 1972. Experiments in molecular genetics / Jeffrey H. Miller. New York : Cold Spring Harbor Laboratory.

65. **Moreau, P. L.** 2007. The lysine decarboxylase CadA protects *Escherichia coli* starved of phosphate against fermentation acids. J Bacteriol **189:**2249-2261.

66. **Moreno, R., S. Marzi, P. Romby, and F. Rojo.** 2009. The Crc global regulator binds to an unpaired A-rich motif at the *Pseudomonas putida alkS* mRNA coding sequence and inhibits translation initiation. Nucleic Acids Res **37:**7678-7690.

67. **Moreno, R., and F. Rojo.** 2008. The target for the *Pseudomonas putida* Crc global regulator in the benzoate degradation pathway is the BenR transcriptional regulator. J Bacteriol **190:**1539-1545.

68. **Morris, D. R., and E. A. Boeker.** 1983. Biosynthetic and biodegradative ornithine and arginine decarboxylases from *Escherichia coli*. Methods Enzymol **94:**125-134.

69. **Morris, D. R., and A. B. Pardee.** 1966. Multiple pathways of putrescine biosynthesis in *Escherichia coli*. J Biol Chem **241:**3129-3135.

70. **Muramatsu, H., H. Mihara, R. Kakutani, M. Yasuda, M. Ueda, T. Kurihara, and N. Esaki.** 2005. The putative malate/lactate dehydrogenase from *Pseudomonas putida* is an NADPH-dependent Δ^1-piperideine-2-carboxylate/Δ^1-pyrroline-2-carboxylate reductase involved in the catabolism of D-lysine and D-proline. J Biol Chem **280:**5329-5335.

71. **Musken, M., S. Di Fiore, A. Dotsch, R. Fischer, and S. Haussler.** 2010. Genetic determinants of *Pseudomonas aeruginosa* biofilm establishment. Microbiology **156:**431-441.

72. **Nakada, Y., and Y. Itoh.** 2003. Identification of the putrescine biosynthetic genes in *Pseudomonas aeruginosa* and characterization of agmatine deiminase and N-carbamoylputrescine amidohydrolase of the arginine decarboxylase pathway. Microbiology **149:**707-714.

73. **Nakada, Y., Y. Jiang, T. Nishijyo, Y. Itoh, and C. D. Lu.** 2001. Molecular characterization and regulation of the *aguBA* operon, responsible for agmatine utilization in *Pseudomonas aeruginosa* PAO1. J Bacteriol **183:**6517-6524.

74. **Nishijyo, T., D. Haas, and Y. Itoh.** 2001. The CbrA-CbrB two-component regulatory system controls the utilization of multiple carbon and nitrogen sources in *Pseudomonas aeruginosa*. Mol Microbiol **40:**917-931.

75. **Nishijyo, T., S. M. Park, C. D. Lu, Y. Itoh, and A. T. Abdelal.** 1998. Molecular characterization and regulation of an operon encoding a system for transport of arginine and ornithine and the ArgR regulatory protein in *Pseudomonas aeruginosa*. J Bacteriol **180:**5559-5566.

76. **Park, S. M., C. D. Lu, and A. T. Abdelal.** 1997. Purification and characterization of an arginine regulatory protein, ArgR, from *Pseudomonas aeruginosa* and its interactions with the control regions for the *car*, *argF*, and *aru* operons. J Bacteriol **179:**5309-5317.

77. **Perez-Martin, J., and V. De Lorenzo.** 1995. The amino-terminal domain of the prokaryotic enhancer-binding protein XylR is a specific intramolecular repressor. Proc Natl Acad Sci U S A **92:**9392-9396.

78. **Phan, A. P., T. T. Ngo, and H. M. Lenhoff.** 1982. Spectrophotometric assay for lysine decarboxylase. Anal Biochem **120:**193-197.

79. **Pioszak, A. A., and A. J. Ninfa.** 2004. Mutations altering the N-terminal receiver domain of NRI (NtrC) That prevent dephosphorylation by the NRII-PII complex in *Escherichia coli*. J Bacteriol **186:**5730-5740.

80. **Poole, R. K., and M. N. Hughes.** 2000. New functions for the ancient globin family: bacterial responses to nitric oxide and nitrosative stress. Mol Microbiol **36:**775-783.

81. **Rahman, M., and P. H. Clarke.** 1980. Genes and enzymes of lysine catabolism in *Pseudomonas aeruginosa*. J Gen Microbiol **116:**357-369.

82. **Revelles, O., M. Espinosa-Urgel, T. Fuhrer, U. Sauer, and J. L. Ramos.** 2005. Multiple and interconnected pathways for L-lysine catabolism in *Pseudomonas putida* KT2440. J Bacteriol **187:**7500-7510.

83. **Revelles, O., M. Espinosa-Urgel, S. Molin, and J. L. Ramos.** 2004. The *davDT* operon of *Pseudomonas putida*, involved in lysine catabolism, is induced in response to the pathway intermediate δ–aminovaleric acid. J Bacteriol **186:**3439-3446.

84. **Revelles, O., R. M. Wittich, and J. L. Ramos.** 2007. Identification of the initial steps in D-lysine catabolism in *Pseudomonas putida*. J Bacteriol **189:**2787-2792.

85. **Revelles, O. a. E.-U., M (ed.).** 2004. Proline and Lysine Metabolism, vol. 3. Kluwer Academic/Plenum Publishers, New York.

86. **Rojo, F.** 2010. Carbon catabolite repression in *Pseudomonas* : optimizing metabolic versatility and interactions with the environment. FEMS Microbiol Rev **34:**658-684.

87. **Samer, Q., B. A. Cunha, P. Dua, and K.-D. Lessnau** 2009, posting date. *Pseudomonas aeruginosa* infections. http://emedicine.medscape.com/article/226748-overview. [Online.]

88. **Schweizer, H. D.** 1993. Small broad-host-range gentamicin resistance gene cassettes for site-specific insertion and deletion mutagenesis. Biotechniques **15:**831-834.

89. **Schweizer, H. P.** 1991. *Escherichia-Pseudomonas* shuttle vectors derived from pUC18/19. Gene **97:**109-121.

90. **Shah, P., and E. Swiatlo.** 2008. A multifaceted role for polyamines in bacterial pathogens. Mol Microbiol **68:**4-16.

91. **Simon, R., U. Priefer, and A. Puhler.** 1983. A broad host range mobilization system for *in vivo* genetic engineering: transposon mutagenesis in gram negative bacteria. Nat Biotech **1:**784-791.

92. **Smyth, P. F., and P. H. Clarke.** 1975. Catabolite repression of *Pseudomonas aeruginosa* amidase: the effect of carbon source on amidase synthesis. J Gen Microbiol **90:**81-90.

93. **Soksawatmaekhin, W., A. Kuraishi, K. Sakata, K. Kashiwagi, and K. Igarashi.** 2004. Excretion and uptake of cadaverine by CadB and its physiological functions in *Escherichia coli*. Mol Microbiol **51:**1401-1412.

94. **Sonnleitner, E., L. Abdou, and D. Haas.** 2009. Small RNA as global regulator of carbon catabolite repression in *Pseudomonas aeruginosa*. Proc Natl Acad Sci U S A **106:**21866-21871.

95. **Stibitz, S., W. Black, and S. Falkow.** 1986. The construction of a cloning vector designed for gene replacement in *Bordetella pertussis*. Gene **50:**133-140.

96. **Swigonova, Z., A. W. Mohsen, and J. Vockley.** 2009. Acyl-CoA dehydrogenases: Dynamic history of protein family evolution. J Mol Evol **69:**176-193.

97. **Tabor, C. W., and H. Tabor.** 1985. Polyamines in microorganisms. Microbiol Rev **49:**81-99.

98. **Tanase, S., B. M. Guirard, and E. E. Snell.** 1985. Purification and properties of a pyridoxal 5'-phosphate-dependent histidine decarboxylase from *Morganella morganii* AM-15. J Biol Chem **260:**6738-6746.

99. **Vrljic, M., H. Sahm, and L. Eggeling.** 1996. A new type of transporter with a new type of cellular function: L-lysine export from *Corynebacterium glutamicum*. Mol Microbiol **22:**815-826.

100. **Watson, N., D. S. Dunyak, E. L. Rosey, J. L. Slonczewski, and E. R. Olson.** 1992. Identification of elements involved in transcriptional regulation of the *Escherichia coli cad* operon by external pH. J Bacteriol **174:**530-540.

101. **Wertheimer, S. J., and Z. Leifer.** 1983. Putrescine and spermidine sensitivity of lysine decarboxylase in *Escherichia coli*: evidence for a constitutive enzyme and its mode of regulation. Biochem Biophys Res Commun **114:**882-888.

102. **Wortham, B. W., C. N. Patel, and M. A. Oliveira.** 2007. Polyamines in bacteria: pleiotropic effects yet specific mechanisms. Adv Exp Med Biol **603:**106-115.

103. **Yang, Z., and C. D. Lu.** 2007. Characterization of an arginine:pyruvate transaminase in arginine catabolism of *Pseudomonas aeruginosa* PAO1. J Bacteriol **189:**3954-3959.

104. **Yang, Z., and C. D. Lu.** 2007. Functional genomics enables identification of genes of the arginine transaminase pathway in *Pseudomonas aeruginosa*. J Bacteriol **189:**3945-3953.

105. **Yao, X., W. He, and C. D. Lu.** 2011. Functional characterization of seven gamma-glutamylpolyamine synthetase genes and the *bauRABCD* locus for polyamine and beta-alanine utilization in *Pseudomonas aeruginosa* PAO1. J Bacteriol **193:**3923-3930.

106. **Yeung, A. T., M. Bains, and R. E. Hancock.** 2011. The sensor kinase CbrA is a global regulator that modulates metabolism, virulence, and antibiotic resistance in *Pseudomonas aeruginosa*. J Bacteriol **193:**918-931.

107. **Zhang, X. X., and P. B. Rainey.** 2008. Dual involvement of CbrAB and NtrBC in the regulation of histidine utilization in *Pseudomonas fluorescens* SBW25. Genetics **178:**185-195.